CHAPTER

12

IMAGING TECHNIQUES

Marjorie C. McMillan

With advancing technology, diagnostic imaging techniques available for avian patients now include ultrasound, fluoroscopy, computed tomography (CT) and nuclear scintigraphy; however, routine radiography remains the most frequently performed imaging modality in birds and frequently is diagnostic without the need for more sophisticated procedures. Information obtained from radiographs will frequently complement results from other testing methods, providing for a more thorough evaluation of a disease process.

Both risk and benefit to the patient should be considered when radiography is used as a screening procedure in an apparently normal companion bird. In general, radiography should be performed only when indicated by historical information, physical examination findings and laboratory data. Indiscriminate radiographic studies create an unnecessary risk to the patient and technical staff.

Radiographic findings should always be correlated with surgical, endoscopic or necropsy findings. These comparisons will refine a clinician's ability to detect subtle radiographic changes, and improve diagnostic capabilities and therapeutic results.

Technical Considerations

The size (mainly thickness), composition (air, soft tissue and bone) and ability to arrest motion are the primary factors that influence radiographic technique. Although the skeleton is easy to visualize, specific soft tissue structures within the coelomic cavity may be difficult to differentiate, especially in smaller birds. Interpretation of the radiographs may be complicated by the blending of soft tissue structures caused by the compact viscera, rudimentary mesenteric attachments and minimal fat. Even in obese birds, contrast of the coelomic cavity is minimally improved, suggesting that, radiographically, the opacity of avian fat is similar to that of soft tissue. In the absence of pathology, the air sacs provide negative contrast throughout the thorax and abdomen that can help in differentiating structures.

Multiple factors influence the quality of a radiographic image. In radiographing the avian patient, the goal is to produce a properly positioned, detailed study with a long scale of contrast, minimal motion and the least exposure of the patient and technical personnel to radiation. In general, the image quality is controlled by:

- the production of the image—influenced by radiographic equipment, technical settings (kVp, mA and time), focal-film distance, part-film distance, focal spot size and collimation;
- the recording of the image—influenced by the type of film, cassette and screen combination; and
- the development of the image—influenced by the darkroom environment and type of processing equipment.

Attention to quality in all aspects of obtaining a radiograph will result in consistent, high quality radiographs with reduced repeat rates, increased efficiency, less patient stress, reduced radiation exposure and economic savings. A quality control program that encompasses all the factors contributing to the radiographic image is beyond the scope of this chapter and appropriate references should be reviewed.[3,5,25]

Radiographic detail depends on sharpness of the image and radiographic contrast. Sharpness, the ability to define an edge, is compromised by motion, uneven film-screen contact and a large focal spot. Radiographic contrast is controlled by subject contrast, scatter, and film contrast and fog. Detail is improved by using a small focal spot, the shortest possible exposure time (usually 0.015 seconds), adequate focus-film distance (40 inches), a collimated beam, single emulsion film and a rare earth, high-detail screen. The contact between the radiographic cassette and the patient should be even, and the area of interest should be as close as possible to the film.

There is increasing discussion of the use of mammography machines for imaging avian patients. While these machines do produce excellent quality images with extremely refined detail, the clinician should be aware that imaging requires exposure to high levels of radiation in comparison to standard radiographs. In general, mammography machines can be considered to deliver low-dose radiation therapy (levels of radiation that cause tissue destruction), and the long-term effect of exposing the body of a bird to this level of radiation is undetermined.

Radiographic Technique

The specific technical factors needed to obtain a high quality radiograph will vary with the type of radiographic equipment, film-screen combinations and various settings used for specific purposes. A technique chart for the various species can be developed.[28] As a general rule, the clinician should choose the lowest kV, a high mA and a short exposure time.[7] Usually, non-bucky techniques applicable for radiography of cats provide reasonable radiographic settings for medium to large psittacine birds.[5]

In circumstances where single emulsion, rare earth, high-detail systems are used, kVp ranging from 60 to 75 at five mAs (300mA, 1/60th of a second) usually provides an appropriate scale of contrast and eliminates motion. In small Passeriformes, such as canaries and finches, reducing the focal-film distance by one-fourth (to 30 inches) and decreasing the mAs by one-half may improve the radiographic image. Decreasing the focal-film distance can result in loss of detail due to magnification; however, with small patients, a shorter focal-film distance does not seem to compromise the radiographic image.

Although the single-emulsion film and single screen, rare earth systems result in greater detail, they do require increased exposure when compared to double emulsion film-cassette combinations. Low-absorption cassette fronts may provide comparable detailed studies with less radiation exposure.[29]

It is important to radiation safety to maintain an adequate distance from the source of radiation by using techniques that do not require personnel to restrain the patient during a radiographic study. If hospital personnel must be present during an exposure, they should wear a lead apron, lead gloves, thyroid shield, protective glasses and a film badge. No portion of a person's body should be in the primary beam, even if covered by lead. With practice, restraining methods can be developed so only the patient is exposed to radiation.

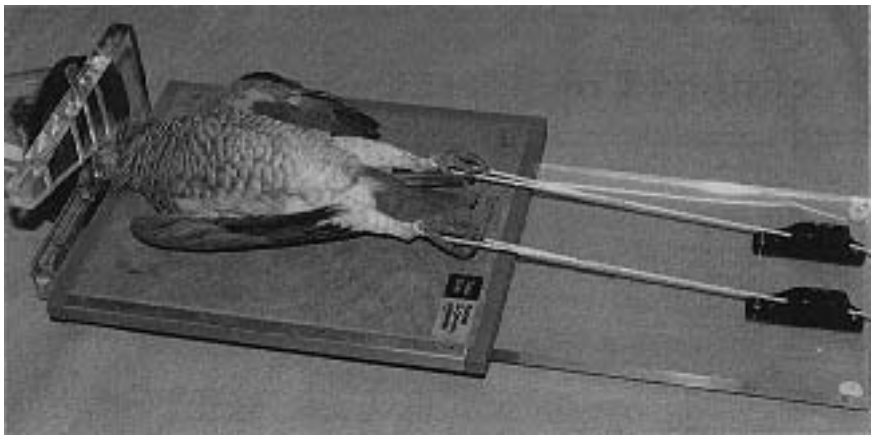

FIG 12.0 A plexiglass restraint board can be used for positioning anesthetized or unanesthetized birds for radiographs. An anesthetized bird is shown in the proper position for a VD radiograph.

Restraint and Positioning

Poor positioning is the most frequently encountered factor that compromises a radiographic study and hampers interpretation of subtle lesions. Some birds can be adequately restrained for routine views with mechanical plexiglass devices and positioning aids such as sandbags, foam blocks, lead gloves, velcro, pipe cleaners and plastic and paper tape.[10,18] Other patients will require isoflurane anesthesia to obtain the most diagnostic radiographs; however, it should be noted that anesthesia or chemical restraint for radiographic examination will decrease normal gastrointestinal motility and as such is generally contraindicated in studies to evaluate the function of this organ system. Anesthesia should be considered mandatory when radiographing strong, powerful birds or patients that are fractious, highly stressed, experiencing significant respiratory distress or those that have an injury that may be exacerbated by struggling. If anesthesia is required, appropriate evaluation of the patient prior to anesthesia is indicated (see Chapter 39). With experience, a complete set of diagnostic, high quality radiographs can be obtained in an anesthetized bird in less than five minutes.

If heavy metal intoxication is suspected in a critically ill bird, a quick radiographic screening for metal densities can be obtained by placing the bird in a bag and taking a DV radiograph. A horizontal beam radiograph can also be taken through the bag to provide a lateral view. This technique is useful only to demonstrate radiographically detectable metal particles (Harrison GJ, unpublished).

The most frequently performed radiographic studies in companion birds are ventrodorsal (VD) and left-to-right lateral (LeRtL) whole body projections. To use a plexiglass restraint board, the neck of the bird just below the angle of the mandible is secured in the stock-like, contoured portion of a restrainer while the body is still wrapped in a towel. For the VD view, the head is restrained and the wings are extended 90 degrees from the body and secured with sandbags, velcro straps or tape. The wings should be restrained close to the body to prevent iatrogenic fractures. The legs are pulled caudally and parallel to the body and secured at the tarsometatarsus with tape or velcro straps (Figure 12.0).

For the LeRtL view, the wing and leg restraints are loosened while the head and body are rotated into right lateral recumbency. The dependent wing is extended 90 degrees to the body and secured. A foam block or other soft material is placed between the wings, and the left wing is extended and restrained slightly caudally to the right. Placing a block of foam between the wings helps to prevent overextension and potential injury. Both legs are extended caudally with slight tension and secured individually at the tarsometatarsus. The dependent leg is positioned slightly cranially. Securing the legs individually helps to reduce rotation of the body, which is common if the legs are fastened together. The beam should be collimated to the patient size to reduce scatter, and radiopaque right or left markers should be appropriately positioned.

In a symmetrically positioned VD view, the spine and sternum will be superimposed, and the scapulae, acetabula and femurs will be parallel (Figure 12.1).

In LeRtL projection, the ribs, coracoid, acetabula and kidneys will be superimposed, if the positioning is accurate (Figure 12.3).

While in the VD position, collimation may be used to obtain radiographs of the pelvis, craniocaudal projection of the legs and mediolateral view of the wings (Figure 12.9, 12.10). The orthogonal view of the wing in the caudocranial projection requires horizontal beam radiography. In the lateral position, views of the pelvis, spine and legs can be achieved (Figure 12.11, 12.12).

Radiography of the skull requires general anesthesia to ensure accurate positioning and to minimize motion. Complete evaluation of the skull requires LeRtL, RtLeL, VD, dorsoventral (DV) and rostrocaudal (RCd, frontal sinus) views (Figure 12.5 to 12.8). In evaluating skull trauma, left and right 75° ventrodorsal oblique views are recommended.[7]

Radiographic Interpretation

If radiographic films are manually processed, an initial assessment of positioning and technique can be made during a "wet" reading; however, final interpretation should be reserved until the film is completely dry. The environment in which interpretation occurs is important. A dimly lighted area with minimal disturbance and an evenly illuminated viewing box at eye level improves viewing conditions. Personal preference determines whether an organ-by-organ approach or concentric circle system is used to evaluate the radiograph. Whichever method is chosen, it is important that the entire radiograph is studied, and that the observer does not just focus on the lesion. Minifying and magnifying lenses may improve interpretation by enhancing detail or magnifying structures, especially in smaller avian patients. It is advantageous to use a standardized form when recording radiographic findings.

Neonatal Radiography

Stress should be minimized when radiographing neonatal birds. The surface of the cassette should be warmed with a towel to avoid placing a young bird on a cold surface. Paper tape should be used for restraint to avoid damage to the numerous blood feathers. In some circumstances, proper positioning may be sacrificed in the best interest of the patient. Pressure must not be placed on a full crop to prevent regurgitation and subsequent aspiration.

The abdomen of neonates appears pendulous because the gastrointestinal tract is dilated, fluid-filled and blends with the other soft tissue organs (see Figure 30.7). This results in a homogenous appearance to the coelomic cavity. The air sacs are relatively indistinguishable. The skeleton is incompletely mineralized and will have a reduced density, and fractures may be difficult to detect (Figure 12.76).

Musculoskeletal System

Radiographic Anatomy

The cranium of birds contains numerous connections to the sinuses, which are reflected radiographically. The osseous scleral ring is clearly visible radiographically, while the interorbital septum that lies between the eyes is barely visible (Figures 12.5,12.6).

The articulation between the clavicle and sternum in birds is membranous rather than bony. The distal ends of the clavicle are fused, forming the furcula (wishbone) (Figures 12.1 to 12.4). The coracoid articulates with the cranial portion of the sternum and the shoulder joint. Only the radial and ulnar carpal bones are present. The distal carpal bones are fused with each other and with the proximal ends of the metacarpal bones. This area is referred to as the carpometacarpus. The digits are traditionally numbered I (alular), II (major) and III (minor). Developed feathers are hollow, and the rachis will have an air density center. Developing feathers contain blood to the level of the pulp cavity and will appear as soft tissue densities (Figure 12.9).

The spine is separated into cervical, thoracic, synsacral (fused thoracic, lumbar, sacral and caudal), free-caudal and fused caudal (pygostyle) sections. The number of cervical vertebrae varies with the species (budgerigars = 11, Amazon parrots = 12). In Galliformes, the last cervical vertebra is fused to the first three thoracic vertebrae. The number of thoracic vertebrae varies from three to ten depending on the species.

Ribs are present on the cervical and thoracic vertebrae. The cervical ribs have short, ventrally oriented spines that are fused to the cervical vertebrae. The thoracic ribs are complete (number varies with the species) and are divided into two portions; the dorsal

portion articulates with the vertebra and the ventral portion articulates with the sternum (Figure 12.1). It should be noted that not all ribs have a sternal portion. The sternal rib is equivalent to the mammalian costal cartilage. Uncinate processes that anchor the caudal edge of several vertebral ribs to the cranial edge of the subsequent rib may be present on some ribs (see Anatomy Overlay).

There are 10 to 23 synsacral vertebrae and 5 to 8 free caudal vertebrae. The ilium and ischium are fused and are also fused to the synsacrum. The pubic bones are long, thin and unfused (except in ratites), presumably as an adaptation for egg laying (Figure 12.1).

No separate tarsal bones occur. The proximal tarsal bones are fused with the tibia; this structure is termed the tibiotarsus. The digital tarsal bones are fused with the metatarsal bones resulting in a tarsometatarsus. In parrots, each digit has one more phalange than the number of the digit. For example, digit III is composed of four phalanges (Figures 12.11, 12.12).

Various portions of the skeletal system may be perfused by air sacs in some avian species. The cervical vertebrae may be perfused by the cervical air sac; the thoracic vertebrae, ribs and humerus may be perfused by the interclavicular air sac; and the synsacrum and femur may be perfused by the abdominal air sacs (see Anatomy Overlay).

Avian long bones are characterized by thin cortices. The ossification of long bones is different in birds than in mammals, which should not be misinterpreted as pathology (see Chapter 42).

Radiographic Evidence of Skeletal Disorders

Categorizing abnormalities aids in reducing the differential diagnoses and allows some judgement as to the aggressiveness and chronicity of a lesion.[15,24]

The species and age of a bird influence the type of musculoskeletal pathology that will be encountered. In companion birds, bone changes associated with metabolic bone disease and pathologic fractures are more common than traumatic injury or infection. Congenital bone abnormalities are uncommon; however, developmental changes associated with poor husbandry and improper nutrition occur frequently. Hypovitaminosis D_3 and calcium and phosphorus imbalances result in changes in the size, shape and length of bones that are characterized by generalized osteopenia and folding fractures secondary to osteomalacia (see Figure 31.10).

Valgus deformity of the tibiotarsi (bow leg), kyphosis, scoliosis, lordosis and sternal compression may occur secondary to osteomalacia (see Figure 33.8). If the spinal or sternal abnormalities are severe, compromise of the thoracic cavity may occur that causes displacement of the heart and respiratory distress. "Splay leg" may be complicated by osteomalacia as well as contracture of tendons and muscles, causing clenching of the feet and rotation at the stifle joint. Hypervitaminosis D_3 can cause diffuse metastatic mineralization within soft tissues, particularly the kidneys (see Figure 21.3).[7]

Skeletal trauma may result in fractures, sprain injuries and concussions (see Chapter 16). Luxations are infrequent and usually involve the digits, stifle or coxofemoral joint, and often occur due to dangling from leg bands, inappropriate toys and unsafe enclosures (Figure 12.78). The important considerations in the radiographic evaluation of fractures include location, articular involvement, bone density, periosteal reaction, soft tissue involvement and whether the fracture is simple or comminuted and open or closed (see Chapter 42).

In companion birds, head trauma most often results in concussion and soft tissue injury. In birds, fractures of the cranium are infrequently discussed, possibly because of the necessity of taking multiple radiographic views to delineate between normally superimposed structures of the head and fracture lines. Detection of non-displaced fractures generally requires a CT scan. Fractures of the jugal arch, pterygoid bone and displacement of the quadrate bone have been reported (Figure 12.37).[18] Penetrating skull injuries occur in big bird-little bird encounters and cat attacks.

Fractures of the cervical spine are infrequent, but may be incorrectly diagnosed due to the normal sigmoid curve in this region. Accurate radiographs of the cervical spine require extension of the head and

CLINICAL APPLICATIONS

A general approach to interpretation of skeletal disorders includes the evaluation of:

- Change in bone density (osteopenia or osteosclerosis)
- Distribution of lesions (diffuse, monostotic or polyostotic)
- Architecture of the bone (cortical changes, disruption in continuity, size and shape, trabecular pattern)
- Periosteal change (smooth or coarse, lamellar or irregular)
- Margination (sharp, well-defined or poorly defined)
- Soft tissue changes

neck without rotation of the skull or body. When vertebral fractures occur, they are often located in the caudal thoracic region or the synsacrum.[7]

Diaphyseal fractures of the extremities are the most common traumatic injury. Acute fractures are characterized by sharp, well-defined margins, absence of periosteal response and concurrent soft tissue swelling (see Figure 16.16). Chronic fractures are characterized by rounding, flaring and indistinct fracture ends, periosteal change and minimal soft tissue involvement or atrophy. Fracture repair depends on the bone involved, location, type of fracture and chronicity. Avian fractures heal in a manner similar to that described for mammals, except the endosteal component is more pronounced.[2] Healing is usually complete within three to eight weeks. Lack of visualization of the fracture lines and smooth, well-defined callus bridging all cortices indicate complete healing (see Figure 42.2).

Osteolysis is the predominant radiographic change with infectious or neoplastic processes, and differentiation between these etiologies will require biopsy (see Figure 25.8). Osteomyelitis and septic arthritis may occur secondary to open fractures, penetrating wounds, iatrogenic contamination, hematogenous sources, extension from air sac disease or pododermatitis. Acute infection may show bone destruction with minimal periosteal reaction. Periosteal change is usually present with chronic infections (see Figure 33.7).

Fungal osteomyelitis may cause pronounced periosteal reaction or increased medullary opacity due to granuloma formation. *Mycobacterium* spp. may also cause medullary granulomas as well as septic arthritis and bone lysis. Infection is most common in the extremities, and vertebral osteomyelitis is rare. Osteomyelitis in the calvarium is usually due to extension from chronic rhinitis, sinusitis or periorbital lesions, and aspergillosis and mycobacteriosis may be involved. When infection occurs in association with fractures, there is often delayed union, and chronicity is characterized by regions of sclerosis and lysis. Fragments of increased density suggest compromised vascular supply and potential sequestra formation.

With acute septic arthritis, joint effusion due to synovitis may be the only radiographic change, and arthrocentesis is necessary for diagnosis (Figure 12.77). Bacteria, mycoplasma, mycobacteria and parasites may be causative agents. As an infection progresses, destruction of articular cartilage results in loss of joint space, and osteolysis and periosteal changes may occur in the epiphysis and metaphysis. Distal joints are most commonly affected, especially when the infection is secondary to septic pododermatitis. Occasionally, luxation of the affected joint may occur. Effusion and diminished joint space may occur also with degenerative joint disease, but they are usually accompanied by chronic changes such as periarticular lipping, sclerosis of subchondral bone and osteophytes (see Figure 42.11).

Primary bone neoplasia such as osteosarcoma is uncommon but has been reported in the proximal humerus, maxilla and wing tips. Bone neoplasia is frequently characterized by osteolysis with minimal periosteal change; however, osteoblastic tumors with marked periosteal reaction do occur. Most tumors involving bone occur secondary to soft tissue neoplasia (see Figure 25.2). These tumors are frequently associated with soft tissue swelling, bone destruction and pathologic fractures, and biopsies are necessary to differentiate between tumors and osteomyelitis. Metastatic bone lesions are rare.

Normal pre-ovulatory hens will have an increased medullary bone density (polyostotic hyperostosis). Prolonged, abnormally elevated estrogen levels cause a diffuse, increased medullary bone density.[14] The bones have a "marble" or mottled appearance, depending on whether bone deposition is uniform or patchy (Figure 12.65). Discrete, nodular regions of bone resembling osteomas occasionally occur on the ribs, vertebrae or pubic bones. Polyostotic hyperostosis has also been reported in hens with oviductal tumors and in cocks with sertoli cell tumors.[21,23]

Hypertrophic osteopathy is rare, but has been reported in association with pericardial effusion.[4] Radiographic lesions were characterized by extensive, fine, brush-like periosteal reaction involving most of the long bones. In other species, hypertrophic osteopathy is associated with pulmonary disease and neoplasia involving the lungs, bladder or liver.

Cardiovascular System

Radiographic Anatomy

In general, the base of the heart is angled craniodorsally and lies at the second rib. The apex is directed in a caudoventral direction and lies between the fifth and sixth ribs (varies with species) (Figure 12.1 to 12.4, 12.15, 12.16). The size and shape of the cardiac

silhouette will vary with the phase of respiration, cardiac cycle and species.

In mammals, various formulas for measuring the cardiac size from radiographs have proved inaccurate, and currently echocardiography is the most reliable method for assessing cardiac size and function. In the VD view of a normal Amazon parrot, the cardiac silhouette as measured across the heart base at the level of the atria is about 50% of the width of the coelomic cavity measured at the fifth thoracic vertebra (Figure 12.1). The lateral margins of a normal heart and liver in psittacine birds create an hourglass shape (Figure 12.1). In macaws, there is normally a ventrally directed kink between the heart and liver in the lateral view (Figure 12.35).

Radiographic Evidence of Cardiac Disease

Primary cardiac disease is rare, although congenital defects are occasionally detected on postmortem examination. Congenital and viral diseases should be considered in juvenile birds with cardiac murmurs, exercise intolerance and cardiomegaly. The latter is usually accompanied by other systemic changes. Secondary cardiac disease is more common. Pericardial effusion is recognized radiographically as a symmetrical, globoid enlargement of the cardiac silhouette and may occur in birds with chlamydiosis, polyomavirus, tuberculosis and neoplasia (Figure 12.63).

With cardiomegaly, heart enlargement is usually asymmetrical. Cardiomegaly may be caused by cardiomyopathy secondary to poxvirus (reported in macaws[12]), myxomatous valvular degeneration, endocarditis (particularly secondary to pododermatitis), hemochromatosis, chronic anemia and compression from extrinsic masses (see Chapter 27). Elongation of the heart shadow, loss of the caudal and cranial waists, loss of indentation at the junction between the heart and liver lobes and an increase in transatrial dimensions indicate an increase in cardiac size.

Microcardia is associated with hypovolemia due to acute volume loss or endotoxic shock (see Figure 21.2). There is retraction of the heart from between the liver lobes, a more angular appearance to the cardiac shape and decreased transatrial size. Whatever the etiology, microcardia suggests a critical state, and appropriate volume replacement should be instituted immediately.

Atherosclerosis with mineralization will result in prominence of the great vessels and may cause an increased density of the caudal lung field. Although seen most often in older birds on high-fat diets, severe vascular changes may occur in young birds. Acute myocardial infarcts, syncope and seizures (perhaps due to hypoxemia) have been described in birds with atherosclerosis in the absence of radiographic lesions.

TABLE 12.1 Radiographic Lesions of the Respiratory System

Differential Diagnosis	Radiographic Interpretation
Parabronchial infiltrates	Blotchy pulmonary pattern
Caseous exudate, hemorrhages or edema	Non-distinguishable parabronchi
Tumor, fungal granuloma or abscess	Abnormal pulmonary pattern (anatomy)
Air sac disease	Fixed full inspiration, barrel shape to cranial body cavity
Bacterial and fungal infection, hypovitaminosis A	Consolidating air sacculitis
Trauma, infraorbital sinus infection	Subcutaneous emphysema
Abscess or granuloma	Pulmonary masses

Respiratory System

Radiographic Anatomy

The radiographic changes associated with respiratory disease are often subtle, and high quality radiographs are necessary to detect these lesions (Table 12.1). The trachea in toucans and mynah birds deviates ventrally at the level of the thoracic inlet (see Figure 47.3). Radiographically, the normal syrinx is difficult to visualize but lies between the second and third thoracic vertebrae in most birds (Figure 12.3). The heart covers much of the lung field in the VD view and only the caudal edge of the lungs can be visualized (Figure 12.35). In normal birds, the borders of the air sacs cannot be distinguished.

Lung parenchyma appears as a honeycombed structure with the majority of the air densities representing an end-on view of parabronchi (Figure 12.35). The bronchioles can be visualized as transverse, indistinct, linear structures on the ventrodorsal radiograph. Air bronchograms and atelectasis, which occur in mammals with pulmonary disease, do not occur in birds because of their unique lung anatomy (a network of inter-connecting tubules with the lungs adhered to the thoracic wall).[12] Bacterial or fungal infections are the most common cause of pathologic abnormalities involving the respiratory tract. Chronic nasal discharge, periorbital swelling and soft tissue masses are indications for radiographs of the nasal cavity and infraorbital sinus.

Radiographic Evidence of Respiratory Disorders

Hypovitaminosis A may cause an accumulation of caseous exudate that appears as a soft tissue opacity within the sinus without bone destruction. Soft tissue swelling with osteolysis of the calvarium is often associated with osteomyelitis due to aspergillosis or mycobacteriosis. Air-filled swellings from distention of the cervicocephalic air sacs may be caused by infection, granulomas or idiopathic obstruction and should be differentiated from subcutaneous emphysema, which is more diffuse.[27]

Changes in tracheal diameter may be caused by intrinsic or extrinsic masses, stricture or stenosis. Intraluminal soft tissue masses or undulating soft tissue plaques may be caused by bacteria, hypovitaminosis A, parasites, fungi, foreign body or neoplasm. A solitary mass in the syrinx may cause severe obstructive, open-mouthed dyspnea with no obvious radiographic changes. Superimposition of the great vessels, ribs and soft tissue over the syrinx compromises interpretation. A subtle increase in soft tissue in this region or fluid accumulation in the distal trachea suggests obstruction. Although contrast tracheography may help delineate some masses, tracheoscopy is less stressful to the patient and more definitive (Figure 12.47).

Soft tissue surrounding the distal trachea is usually apparent. Tracheal strictures secondary to trauma from fight-induced injuries or cuffed endotracheal tubes occasionally occur. Tracheal stenosis and deformity of the tracheal rings are uncommon. Peritracheal masses may occur in the thoracic inlet due to thyroid enlargement secondary to goiter or neoplasm (Figure 12.45). Thyroid masses are usually well defined with smooth margins. *Aspergillus* sp. granuloma encasement of the syrinx often causes a hoarseness in vocalization and slow, progressive respiratory distress (Figure 12.46).

With pulmonary disease, the normal honeycombed pulmonary parenchyma may be enhanced by parabronchial infiltration causing prominent ring shadows obliterated by filling of the parabronchial lumen with fluid or caseous exudate or replaced by neoplastic or granulomatous infiltrates (see Table 12.1). Pneumonia often causes a prominent parabronchial pattern in the hilum and mid-portion of the lungs (Figure 12.47). As pneumonia progresses, the air-filled parabronchial lumen is replaced with caseous exudate, causing a blotchy mottled appearance to the lungs. This change is common at the caudal aspects of the lungs and is best detected on VD radiographs. Pulmonary edema and hemorrhage have a more diffuse appearance (Figure 12.50). Discrete, well defined masses are usually abscesses, granulomas or tumors (Figure 12.49).

The size of the air sacs will vary between inspiration (increased) and expiration (decreased). Additionally, the lung architecture will be more apparent on inspiration. Air sac disease may cause a barrel-shaped appearance to the thorax (Figure 12.51). Consolidated or thickened air sacs are not as compliant as normal air sacs, causing the inspired air to be deposited in a relatively fixed cavity.

Radiographic changes indicative of inflamed air sacs include diffuse thickening, nodular infiltration or consolidation. Fine lines across the air sacs with mild increased opacity indicate thickening and are best detected on the lateral radiograph (Figure 12.52). The loss of visualization of abdominal viscera, blending of the air sacs, blending of the interfaces between air and soft tissue and a hazy heterogeneous appearance to the air sacs are suggestive of consolidation (Figures 12.53, 12.54). Hyperinflation of the air sacs in combination with a radiolucent appearance suggest air trapping due to obstructed flow or abnormal compliance.

Subcutaneous emphysema may result from traumatic rupture of an air sac or as a complication of endoscopy (see Chapter 22). Fractures of the coracoid or ribs may penetrate the air sacs, causing emphysema.

Coelomic Cavity and Gastrointestinal System

Radiographic Anatomy

The crop is present in the right lateral thoracic inlet area on the VD view. It may extend to varying degrees across the midline depending on the presence of ingesta and the species of bird (Figure 12.71, 12.74). The thoracic portion of the esophagus can usually be differentiated on the VD and lateral radiographs. The cervical portion of the esophagus cannot be distinguished without contrast media.

The proventriculus lies dorsal to the liver on the lateral view (Figure 12.35). The left lateral border of the proventriculus may be difficult to distinguish from the left lateral edge of the liver on the VD view. If the liver is of normal size, the proventriculus shadow will lie slightly lateral to the liver on the VD view. If the ventriculus contains radiodense material, it can generally be viewed on both the VD and lateral

radiographs in its normal location, caudal and ventral to the proventriculus.

The position of the intestinal tract is widely variable but it generally occupies the caudal, dorsal abdominal cavity (Figure 12.72). The cloaca may or may not be visualized, depending on its contents. The summation between the liver and proventriculus on the VD view should not be misinterpreted as pathology (Figure 12.35). The duodenal loops lie to the right of the ventriculus in the VD view (Figure 12.72).

Spleen

If detectable on the VD radiograph, the spleen will be noted as a slightly oblong, rounded structure to the right of midline between the proventriculus and ventriculus. On the lateral view, the spleen, if visible, overlaps the caudal end of the proventriculus and may be slightly dorsal to it (Figure 12.35). Suggested normal spleen sizes include: budgerigar = 1 mm, African Grey Parrot or Amazon parrot = 6 mm, Umbrella Cockatoo = 8 mm. The spleen of a pigeon is elongated or bean-shaped. In many other species it is spherical. Splenomegaly may be caused by infectious, neoplastic or metabolic diseases (Figure 12.62), (Table 12.2).

Liver

The liver does not normally extend beyond the sternum on the lateral radiograph (Figure 12.35). In psittacine birds, the liver should not extend laterally past a line drawn from the coracoid to the acetabulum. The size of the hepatic silhouette can best be determined by making measurements of a VD radiograph taken on inspiration. The distance is measured in millimeters from the mid-sternum to the lateral-most aspect of the ribs at the base of the heart. This measurement is referred to as the sternal/rib distance (SR). This distance is divided by one-half and should be equal to the width of the right liver as measured at the base of the heart. The size of the right liver is determined by measuring from the mid-sternum to the edge of the liver at the base of the heart. If the actual measurement of the liver is greater than its anticipated size as determined by the SR value, then the liver is considered enlarged. If the actual measurement of the right liver is less than its anticipated size as determined by the SR value, then the liver is considered to be reduced in size (Harrison GJ, unpublished).

The liver in macaws and cockatoos frequently appears to be reduced in size (Figure 12.58). The importance of this finding remains undetermined; however, many birds with microhepatia are being fed seed diets that may or may not be supplemented with fruits and vegetables. Many affected birds have abnormally low populations of gram-negative bacteria, low bile acids levels and elevated LDH, AST and GGT activities. The CPK may be normal or elevated (Harrison GJ, unpublished). The pesticide residues that are present in most commercially available foods may play a role in the high incidence of hepatopathies in companion birds and should be addressed in birds with microhepatia. In obese pigeons, the liver will appear enlarged, which will resolve when the birds are fasted.

TABLE 12.2 Differential Diagnosis for Hepatomegaly, Splenomegaly and Nephromegaly

Hepatomegaly	Etiologies
Infectious	Chlamydial, viral (eg, Pacheco's disease virus, reovirus, polyomavirus), bacterial, mycobacterial and fungal
Neoplastic	Primary (biliary adenocarcinoma, hepatocellular carcinoma, fibrosarcoma, hemangiosarcoma, hepatoma and lymphoma) and Metastatic (adenocarcinoma, fibrosarcoma and melanoma)
Parasitic	Toxoplasmosis (mynahs), *Sarcocystis* sp., flukes (cockatoos) and *Plasmodium* sp.
Metabolic	Lipidosis, fatty degeneration, hemochromatosis (mynahs and toucans) and gout
Splenomegaly	**Etiologies**
Infectious	Chlamydial, viral, bacterial and mycobacterial
Neoplastic	Lymphoma, hemangiosarcoma, fibrosarcoma and leiomyosarcoma
Metabolic	Lipidosis and hemochromatosis
Nephromegaly	**Etiologies**
Infectious	Bacterial, chlamydial
Neoplastic	Adenocarcinoma, embryonal nephroma
Metabolic	Dehydration, lipidosis, gout
Cystic	Occluded ureters, congenital
Toxic	Heavy metals

(modified from McMillan[13])

The liver is frequently involved in systemic disease, and hepatomegaly is a common radiographic finding. Symmetrical enlargement of the liver lobes is most common and is usually associated with infectious and metabolic processes (Table 12.2). Neoplasms and granulomatous diseases can cause asymmetrical enlargement of the liver.

Radiographic changes associated with liver enlargement are loss of hourglass waist in the VD view, rounding of liver lobe margins, compression of abdominal air sacs, extension of the liver lobes beyond the scapula/coracoid line, cranial displacement of the

heart, dorsal elevation of the proventriculus and caudodorsal displacement of the ventriculus (Figure 12.1, 12.60).[13] A dilated, fluid-filled proventriculus may appear radiographically similar to hepatomegaly, and a careful assessment of the VD view can be used to differentiate between these lesions.

Pancreas

Radiographic changes involving the pancreas are rare, although diminished contrast in the right cranial abdomen due to sanguineous exudate from acute necrotizing pancreatitis has been reported. Pancreatic masses are uncommon; however, space-occupying lesions in the right cranioventral abdomen may involve the pancreas, and large pancreatic cysts do occur.

Gastrointestinal Tract

The specific areas of the gastrointestinal tract are best visualized through barium contrast examination. The presence of gas, change in position and abnormal distention suggest a disease process. Altered gastrointestinal motility causing uniform or segmental dilatation can be due to functional or mechanical ileus.

Birds do not normally have gas in the intestinal tract, and any gas should be considered abnormal. Aerophagia can occur secondary to severe respiratory disease or is frequently seen as an artifact of gas anesthesia (Figure 12.69). Distended, fluid-filled bowel loops should be considered abnormal except in mynah birds and toucans.

Inflammation, infection, foreign bodies, parasites, intussusception, stricture, granuloma and neoplasia may cause intraluminal obstruction and segmental increases in the diameter of the gastrointestinal tract lumen secondary to excess gas and fluid accumulation. Extraluminal masses such as neoplasm, abscesses, eggs and cysts may compress the gastrointestinal tract and cause changes similar to intraluminal obstruction.

Uniform distention of the gastrointestinal tract is most commonly associated with functional ileus due to viral or bacterial infections, toxicity (eg, heavy metals), septicemia, hypoxemia, peritonitis or anesthesia. Distention of the ingluvies, proventriculus or ventriculus may be due to a localized process or obstruction within the intestines. A barium contrast study is indicated for complete evaluation of the intestinal tract.

The cloaca may be distended from a retained soft-shelled egg, papilloma, cloacalith, neoplasm or idiopathic atonic dilatation (Figure 12.70). Atonic distension of the cloaca may occur with spinal trauma and infiltrative neoplasms involving the sacral nerves.

Abdominal masses usually cause a change in the location of the gastrointestinal tract. Hepatomegaly usually causes dorsal displacement of the proventriculus and caudodorsal displacement of the ventriculus. Splenic, testicular, ovarian and renal masses compress the gastrointestinal tract ventrally and either cranially or caudally. Adhesions due to inflammatory or septic peritonitis from ruptured eggs or perforation can also result in displacement of the gastrointestinal tract (Figure 12.67).

Abdominal effusion is associated with liver disease, neoplasia, metabolic disorders, sepsis, inflammation and cardiac failure. Fluid results in a homogeneous appearance to the intestinal peritoneal cavity (IPC) and obscures visualization of specific organs (Figure 12.67). Consolidating air sacculitis can appear radiographically similar to fluid in the IPC in the lateral view, but differentiation is possible in the VD radiograph. If a pathologic process is occurring within the air sacs, specific organs within the intestinal peritoneal cavity will be definable in the VD view. If the fluid is within the IPC, there will still be a homogeneous appearance to the region of the viscera, and the air sacs will be compressed (Figure 12.67). Fluid accumulation in the IPC may compress the liver ventrally and displace the proventriculus and ventriculus cranially.

Urogenital System

The anatomy and physiology of the avian kidneys prevent the radiopacity that is characteristic of mammalian kidneys. The kidneys are attached to the synsacrum, are flattened dorsoventrally and have smoothly rounded cranial and caudal divisions (Figure 12.35).

The kidneys are best visualized in the lateral view. Because the renal silhouettes are superimposed, lateral oblique views may be necessary to distinguish each kidney. The cranial division of the kidney protrudes from the pelvic brim, and the caudal division may also be visualized on the lateral view. The kidneys are generally not visible on the VD view, although the rostral edge of the cranial division can occasionally be seen. If the kidneys are enlarged or

increased in opacity, they may be more readily visualized in the VD position. The length of a normal African Grey Parrot kidney is about 3 cm on the lateral view. In the Umbrella Cockatoo, the suggested normal kidney size is 3 cm x 0.7 cm. The kidneys are normally surrounded by air, and loss of the air shadow indicates renal enlargement, dorsal displacement of abdominal organs or the presence of abdominal fat or fluid (Figure 12.56).

Bilateral symmetrical nephromegaly results in a diminished abdominal air sac space surrounding the kidneys and occurs with infection, metabolic disease, dehydration, post-renal obstruction and lymphoreticular neoplasia. Dehydration may also be associated with increased renal density (see Figure 21.2). A localized enlargement with irregular borders is most commonly associated with a neoplasm, although abscesses may appear radiographically similar (Figure 12.57).

Most renal tumors are locally invasive and usually do not metastasize. A solitary mass with smooth, well defined margins is suggestive of a cyst; however, biopsy is the only definitive way to differentiate cysts, neoplasms and abscesses. Intravenous excretory urography is necessary to confirm renal disease when severe nephromegaly obliterates the air space and creates a positive silhouette sign with other viscera.

Masses involving the spleen, oviduct, testicles, ovary and intestines may occupy space in the caudodorsal abdomen and mimic renal lesions (Figure 12.62). The testes of a reproductively active male are easily distinguishable and should not be misinterpreted as renal enlargement.

Testicular abnormalities causing radiographic signs are uncommon. Occasionally tumors cause testicular enlargement, and functional sertoli cell tumors may cause polyostotic hyperostosis. Orchitis is most easily diagnosed through laparoscopy, and radiographically cannot be distinguished from physiologic hypertrophy.

In a hen, an active ovary resembling a bunch of grapes may be apparent cranial to the kidneys, and an increased soft tissue opacity in the caudodorsal abdomen just ventral to the kidneys represents the oviduct (Figure 12.64). The most common radiographically detectable abnormalities involving the female genital tract are retained eggs, cystic oviduct and egg-related peritonitis.

Mineralized eggs are easily visualized and often located in the terminal oviduct. Multiple eggs may be present, and eggs may be free in the coelomic cavity due to reverse peristalsis or oviductal rupture. Soft-shelled eggs are difficult to differentiate from other abdominal masses, and ultrasound may aid in the diagnosis (Figure 12.66).

Hyperestrogen syndrome is common in budgerigars and is characterized by an enlarged, distended oviduct, medullary hyperostosis, diminished abdominal detail, visceral displacement, abnormal attempts at egg formation and abdominal hernia (Figure 12.65).[14] Egg-related peritonitis can be difficult to discern from other causes of abdominal effusion. Cessation of egg laying, weight loss and abdominal distention in a hen with a history of chronic egg laying are suggestive of egg-related peritonitis. Abdominocentesis and ultrasound can be used to differentiate between causes of abdominal fluid (Figure 12.67).

Contrast Procedures

Administration of contrast agents can be used to enhance visualization of intraluminal abnormalities involving the gastrointestinal tract, respiratory system, cardiovascular system and subarachnoid space, and provides a qualitative assessment of function. Contrast agents used in mammals are considered safe in birds, although limited studies have been performed to assess specific contrast media reactions.[6,14]

The presence of concurrent disease and a patient's age, size and state of hydration should all be considered prior to initiating a contrast study. Severely debilitated and seriously ill birds should be stabilized and any fluid and electrolyte imbalances corrected prior to the study. Contrast studies are often stressful because of the number of radiographs required, and sedation is contraindicated in studies involving the gastrointestinal tract because of its effect on gastrointestinal motility. If anesthesia is used, it will slow the passage of contrast media, which should not be misinterpreted as a pathologically induced decrease in transit time.

Gastrointestinal Positive and Double Contrast Procedures

Gastrointestinal studies are the most frequently performed contrast procedures in birds. They are useful in delineating the position, structure and function of the gastrointestinal tract and associated organs.

Indications for barium follow-through examination are acute or chronic vomiting or diarrhea that is nonresponsive to treatment, abnormal survey radiographic findings suggestive of an obstructive pattern, unexplained organ displacement, loss of abdominal detail suggesting perforation, hemorrhagic diarrhea, history of ingestion of foreign material and chronic unexplained weight loss.[11] Dehydrated birds should be rehydrated before administration of contrast media to prevent the material from forming concretions within the gastrointestinal tract.

Gastrointestinal motility may be altered by pathologic conditions, stress and medications. Any drugs that may alter motility such as tranquilizers, anesthetics and anticholinergics should be discontinued for twenty-four hours prior to the gastrointestinal contrast study. The age, size, diet and condition of the patient will all affect gastrointestinal transit time. Faster transit times occur in small birds on soft diets. Passage is slowed in large seed-eating birds, obese birds, in neonates on soft diets and in anesthetized birds.

Obtaining survey radiographs prior to beginning a procedure will ensure proper technique as well as provide a method of re-evaluating any changes in the radiographic pattern that may influence the study. The best contrast study can be performed when the gastrointestinal tract is empty. Excess fluid in the ingluvies should be removed with a gavage tube prior to the administration of contrast media. The presence of ingesta or fluid interferes with the quality of the study and may obscure lesions. Usually, a four-hour fast is adequate for emptying of the gastrointestinal tract without placing undue stress on smaller avian species. The gastrointestinal tract may be empty at the time of presentation in birds that are regurgitating.

Commercial barium sulfate suspensions provide the best studies. Chemical grade barium is difficult to mix properly and may flocculate. If perforation of the gastrointestinal tract is suspected, an organic iodine is recommended; however, these preparations are hypertonic and can cause dehydration, especially in small patients. Additionally, organic iodines are hydroscopic and are rapidly absorbed from the gastrointestinal tract. Dilution of the contrast medium with intraluminal fluid may compromise the study and interfere with defining the region of perforation. These agents do not coat the mucosa like barium does and are not recommended for routine gastrointestinal examinations.

In juvenile birds, barium should be warmed prior to administration. This is not necessary with adult birds. To administer barium, the head and neck are extended and a soft, flexible feeding tube is passed into the crop (see Figure 15.6). Small species do not require a speculum for passage of the tube; however, larger species need the beak held open either with a speculum or gauze. Measuring the distance from the beak to the crop and marking the tube helps ensure that the tube is within the crop and not accidentally passed into the tracheal lumen. The tube should be palpated within the crop prior to the administration of contrast material.

The dose of barium sulfate varies depending on the species and presence or absence of a crop, and ranges from 0.025-0.05 ml/g body weight, with the lower dose range used in larger species. Lesions in the mucosa are best identified by using a higher dose, and a lower dose can be used if the intention is to simply identify borders of the gastrointestinal tract.

The contrast media should be administered slowly until the crop is comfortably distended. Placing a finger over the distal portion of the cervical esophagus may help prevent reflux of barium sulfate while it is being administered. Placing excessive pressure on the full crop may induce regurgitation. Slow removal of the tube may also help reduce reflux. If any regurgitation occurs, the administration of contrast media should cease in order to reduce the risk of

CLINICAL APPLICATIONS

Radiographic abnormalities that may be defined by gastrointestinal contrast studies include:

- Change in location, size or shape of abdominal organs
- Differentiation between the gastrointestinal tract and other organs
- Altered motility (increased or decreased)
- Increased or decreased luminal diameter
- Mucosal irregularities
- Filling defects
- Changes in wall thickness
- Extravasation of contrast media
- Dilution of contrast with mucus or fluid

pulmonary aspiration (see Chapter 22). Barium has been used for bronchography in non-avian species because it is less irritating than other contrast agents.[25] It is the volume of barium inhaled into the respiratory tract and not the agent itself that may cause problems.

Radiographic sequence may vary depending on the species and condition under investigation; however, in general, radiographs should be taken immediately after administration of contrast media and at 0.5-, 1-, 2-, 4-, 8- and 24-hour intervals (Table 12.3). The temporal sequence may vary if a lesion is identified during the study.

If the crop is the only area of concern, a double contrast ingluviography may be performed in association with a barium follow-through study or as a separate procedure. Double contrast studies allow enhanced visualization of the crop wall for irregularities such as thickening, mucosal defects, masses and the detection of foreign bodies that may be obscured by a single-phase contrast study. The total volume of contrast to be administrated (0.025 ml/g) is determined. Half of the total volume is given as air and the rest as barium. The air should be administered first to prevent air bubbles from forming within the contrast media. Although double contrast cloacography can also be performed, direct visualization with endoscopic equipment or an otoscope is preferable (Figure 12.70).

Contrast Study Findings

Delayed transit time may be caused by functional or mechanical ileus. Mechanical ileus, depending on the level of obstruction and degree of luminal compromise, usually causes segmental dilation of the gastrointestinal tract. Functional ileus usually causes a uniform distention of the gastrointestinal tract (see Figure 32.22). Mechanical obstruction occurs with intraluminal or extraluminal masses, foreign body ingestion, helminthiasis and stricture. Intraluminal masses such as neoplasm, abscess, granuloma, intussusception and papilloma will cause filling defects within the contrast column (see Figure 25.15). Mucosal irregularity and ulceration may aid in differentiating neoplasia from more benign processes, but fungal disease and neoplasia can be difficult to distinguish radiographically, and biopsy is the only definitive method to differentiate these diseases. Extraluminal masses involving the thyroid gland, spleen, gonads, oviduct or kidney may compress the lumen of the gastrointestinal tract and cause altered motility or obstruction.

Functional ileus occurs most frequently with neuropathic gastric dilatation and most often involves the proventriculus and ventriculus, although portions of the intestines may also be involved (see Figure 32.24).[11] Neurotoxins such as lead, inflammatory processes involving the coelomic cavity, severe enteritis and anesthetics may cause functional ileus.

Displacement of the gastrointestinal tract may occur with organomegaly, accumulations of fluid in the intestinal peritoneal cavity, adhesions or hernia. Hepatomegaly causes dorsal elevation of the proventriculus and caudal movement of the ventriculus. Splenic, gonadal and renal lesions may displace the intestines ventrally. Masses originating from the cranial division of the left kidney may push the ventriculus cranially. Adhesions associated with egg-related peritonitis may result in abnormal positioning of portions of the gastrointestinal tract, with a fixed appearance and changes in luminal diameter. Hernias, usually in hens, cause caudoventral displacement of the gastrointestinal tract.

A change in luminal diameter and wall thickness most often occurs with obstruction or functional ileus. Fungal diseases and neoplasia can cause narrowing of the lumen due to mural infiltration. Inflammatory changes can also increase wall thickness and influence motility (see Figure 36.31). Mucosal defects are most pronounced with aggressive diseases such as neoplasia or fungal infections. Spiculation of the contrast column due to a hyperemic mucosa, stringing out of barium from mixing with mucus, diminished bowel distensibility and increased transit times occur with inflammation (see Figure 19.12).

TABLE 12.3 Barium Sulfate Transit Times*

	Stomach	Small Intestines	Large Intestines	Cloaca
African Grey Parrot	10-30	30-60	60-120	120-130
Budgerigar	5-30	30-60	60-120	120-240
Racing pigeon	5-10	10-30	30-120	120-240
Indian Hill mynah	5	10-15	15-30	30-90
Hawk	5-15	15-30	30-90	90-360
Amazon parrot	10-60	60-120	120-150	150-240
Canary	5	10-15	15-30	30-90
Pheasant	10-45	45-120	120-150	150-240

*Time in minutes for barium sulfate administered by crop gavage to reach and fill various portions of the GI tract.

Extravasation of contrast media occurs most often with foreign body perforation, although metal feeding tubes or inflexible catheters can result in iatrogenic perforation of the gastrointestinal tract if improperly used. Mural erosion in association with neoplasm, abscess or granuloma are less frequent causes of perforation (see Figure 25.14). If a perforation is suspected, an organic iodine contrast agent is recommended to prevent contamination of the coelomic cavity with barium.

Repeatability of a lesion on multiple views is important when attempting to identify intraluminal masses. Gas bubbles and ingesta can create artifacts that mimic mucosal defects and can lead to an incorrect diagnosis. Tailoring the study to the individual patient and obtaining additional views during the study will aid in accurate interpretation.

Intravenous Excretory Urography

In birds, the absence of a urethra, bladder, renal pelvis or division between the medulla and cortex, as well as the glomerular filtration rate, tubular resorption and the renal portal system make contrast urography of limited value. The primary indication for intravenous excretory urography is in defining mass lesions associated with the urinary tract or delineating the size and shape of the kidneys if they cannot be adequately visualized on routine radiographs (Figure 12.55).[14] Excretory urography may also have some application for diagnosing functional disorders. Excretory urography should not be attempted in patients with dehydration or debilitation or if renal function is severely compromised.

Sodium diatrizoate (680 mg of iodine/kg), iothalamate sodium (800 mg of iodine/kg) or meglumine diatrizoate (800 mg of iodine/kg) have been used for urography in birds with no observable adverse effects.[6,14] These organic iodines should be warmed prior to administration through the ulnar, jugular or medial metatarsal veins. Radiographs are taken immediately after contrast administration and at one-, two-, five-, ten- and twenty-minute intervals using the same technique developed for the survey radiograph.

Most diagnostic information is obtained within the first five minutes of the study (Figure 12.55). The aorta, heart and pulmonary artery will be visualized within ten seconds; kidneys and ureters in 30 to 60 seconds; and cloaca in three to five minutes after administering the contrast media (Figure 12.55).[7] In the nephrographic phases of the study, there is an immediate, uniform opacification of the kidneys highlighting their size, shape and contour. In the normal kidney, the three divisions are readily discernible. There is no pyelographic phase.

Mass lesions such as renal tumors and cysts cause changes in the size, shape and contour of the kidneys and are distinguishable from gonadal lesions because of the contrast enhancement. Tumors are usually solitary mass lesions with irregular margins and are best visualized in the lateral view. Cysts tend to have smooth, well defined borders. Biopsy is necessary to definitively differentiate between tumors and cysts. Abnormalities of the ureters are rare, but they may be compressed in birds with egg binding and cloacal or abdominal masses.[1] Occasionally, cloacal lesions may be outlined during urography.

Radiographic changes in the excretory urogram are most striking when the renal disease is unilateral because the unaffected kidney is usually hypertrophied. In contrast, obstruction of a ureter may increase the radiodensity of the ipsilateral kidney by delaying the washout from the kidney. If urine containing contrast medium is discharged into a pool of urine containing no contrast media, the opacification will be delayed and reduced. Because a large pool of urine may be retained in a hydroureter and with hydronephrosis, late films should be taken when no contrast media is noted on early radiographs.

If one kidney appears to be non-functioning, it is important to consider the urinary protein concentration, cytologic features of sediment and the size of the contralateral kidney. In acute renal failure, the excretory function is rapidly and severely, but often reversibly, compromised. If the contralateral kidney is hypertrophied, the absence of function on the opposite side is probably chronic in nature (urolithiasis) and may even indicate agenesis of that kidney (see Figure 21.4).

Positive Contrast Rhinosinography

Contrast studies of the nasal cavity and sinuses may aid in evaluation of the upper respiratory tract; however, CT has replaced these procedures in other species (Figure 12.38 to 12.40). A 15 to 20% organic iodine agent can be injected into the sinus, and the same views recommended under skull radiography are taken for evaluation. Reactions to the contrast agent include edema and periorbital swelling. At the end of the procedure, the media can be flushed out of the sinuses with sterile saline to decrease the amount

of local irritation. Space-occupying masses such as neoplasms, abscesses or granulomas may cause an obstruction to the flow of contrast media (Figures 12.42, 12.43). In normal psittacine birds, there should be communication between the infraorbital sinus, nasal cavity, opposite sinus, periorbital region and tympanic region (Figures 12.39, 12.40).[12] In some Passeriformes, the sinuses do not communicate (Figure 12.41).

Positive Contrast Tracheography and Bronchography

Contrast studies of the lower respiratory tract should be considered high risk because patients requiring these procedures are usually experiencing serious respiratory compromise. Tracheoscopy is preferable in patients of sufficient size (300 g). Focal lesions in the terminal trachea or at the tracheobronchial bifurcation that are difficult to visualize on survey radiographs may be defined by contrast tracheography (Figure 12.47).[12]

Patients should be stabilized with oxygen therapy and a tube placed in an abdominal sac to provide oxygen and anesthesia. Birds should be anesthetized for these studies. Contrast media is administered via a tube placed in the trachea. Small aliquots (approximately 0.1 ml) of a non-ionic agent or propyliodone should be given at a time, and radiographs taken to determine tracheal filling. A minimal amount of contrast media will be needed if fluoroscopy can be used to identify a foreign body.

Non-selective Angiography

Cardiac disease requiring definition by contrast studies is rare. Diseases such as cardiomyopathy, some congenital shunts and valvular disease may be defined by angiography in some larger birds; however, ultrasonography is being utilized with greater frequency in other species. Non-selective angiography has been used for defining the normal cardiac silhouette and major vessels. The same agents used for urography can be injected as a single, rapid, intravenous bolus in the jugular or ulnar veins to enhance visualization of the heart and great vessels. A rapid film changer, cinefluoroscopy or videotaping is necessary to record the image.

Myelography

Assessment of back trauma or congenital defects may require myelography. Patients must be anesthetized for this procedure. The bird is placed in lateral recumbency and a 25 ga needle or smaller is carefully inserted into the subarachnoid space. Cerebral spinal fluid will flow into the needle, and several drops can be collected for cytology. A non-ionic contrast media (0.25 ml/kg) is slowly injected into the cerebellar medullary cistern. Routine radiographs of the spine are taken.

Alternative Imaging

Fluoroscopy

A fluoroscope can be connected via an image intensifier to a video camera that can be used to make real-time recordings of organ movement. In birds, fluoroscopy is the best way to monitor the motility of the gastrointestinal tract. Patients can be placed in a darkened box to perform fluoroscopy. This technique may be particularly useful for detecting hernias, neoplasms, proventricular dilatation, hypermotility, ileus and gastric ulceration. In a normal parrot given a bolus of barium sulfate by crop tube, the barium will fill the proventriculus and ventriculus in five to ten minutes. The barium will reach the intestines in 15 minutes. These findings suggest that unrestrained (reduced stress) birds have a faster gastrointestinal motility time than is routinely reported using standard radiographic techniques.[22]

Ultrasound

Ultrasonography is an imaging technique that makes use of high frequency sound waves transmitted by a transducer that is in contact with the skin. The waves are transmitted through the tissues in the abdomen and the echoes are recorded by the receiving transducer unit. The resistance to sound waves depends on the molecular structure of the tissue that is being penetrated. If the sound waves encounter bone, most of the waves are absorbed and not reflected. If the sound waves are transmitted through air, most are reflected and not absorbed. In both of these cases, organs that lie behind these structures will not be detected.

Ultrasound studies in birds are somewhat limited by patient size and conformation and the presence of air sacs; however, in larger avian patients with abdomi-

Continued on page 325

Radiographic Anatomy and Abnormalities

Radiography is an extremely valuable diagnostic tool in avian patients. Every avian clinician should be comfortable with radiographic techniques and interpretation of radiographic findings. One of the challenges of identifying subtle changes in radiographs of birds is the wide species variability in normal anatomic structures. Radiographs and xeroradiographs of the Orange-winged Amazon Parrot, cockatiel, Bobwhite Quail and Mallard Duck are provided to assist the clinician in developing a more complete understanding of the unique anatomic structures encountered in varying genera of birds. These radiographs were provided by Bonnie J. Smith and Stephen A. Smith and are reprinted with permission from Veterinary Radiology 31:114-124, 1990; 32:87-95, 1991; 31:226-234, 1990; 32:127-134, 1991.

Following the initial radiographs that address normal radiographic anatomy are case presentations demonstrating characteristic radiographic changes associated with pathology in various organ systems. The reader is encouraged to compare the radiographic findings in these cases with the normal radiographs and xeroradiographs presented in the first section. Additionally, radiographs detailing changes associated with specific organ systems can be found in respective sections throughout the book.

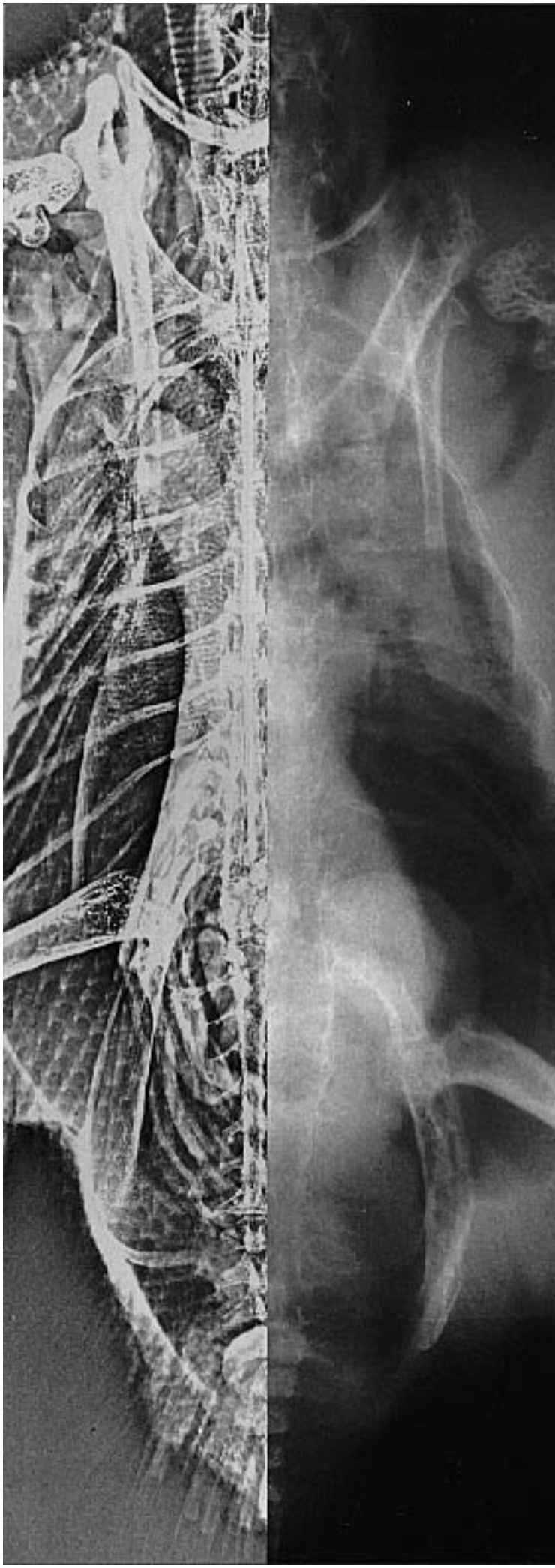

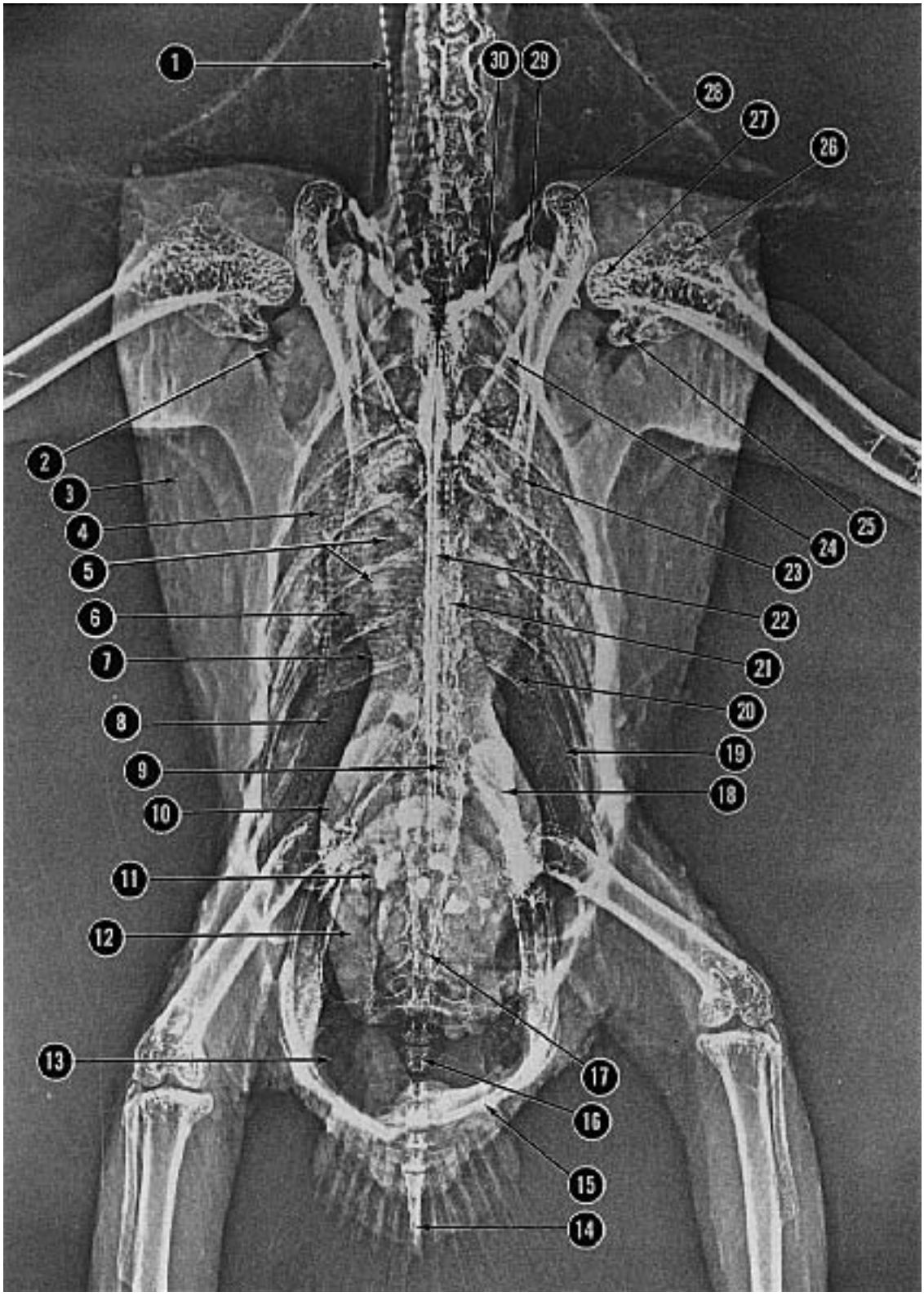

1) trachea
2) clavicular air sac
3) pectoral muscle
4) lung
5) great vessels
6) heart
7) normal hourglass constriction ("waist") of heart-liver shadow
8) area of overlap of caudal thoracic and abdominal air sacs
9) area of spleen
10) liver
11) ventriculus with grit
12) intestines
13) abdominal air sacs
14) pygostyle
15) pubis
16) free caudal vertebra
17) synsacrum
18) periacetabular portion of ilium
19) sternal rib
20) vertebral rib
21) notarium
22) sternum, ventral extremity of carina
23) caudal extremity of scapula
24) medial border of coracoid
25) ventral tubercle of humerus
26) dorsal tubercle of humerus
27) head of humerus
28) should extremity of coracoid
29) head of scapula
30) clavicle

FIG 12.1 Ventrodorsal xeroradiograph of a normal Orange-winged Amazon Parrot (courtesy of Bonnie J. Smith and Stephen A. Smith).

FIG 12.2 Ventrodorsal radiograph of a normal Orange-winged Amazon Parrot (courtesy of Bonnie J. Smith and Stephen A. Smith).

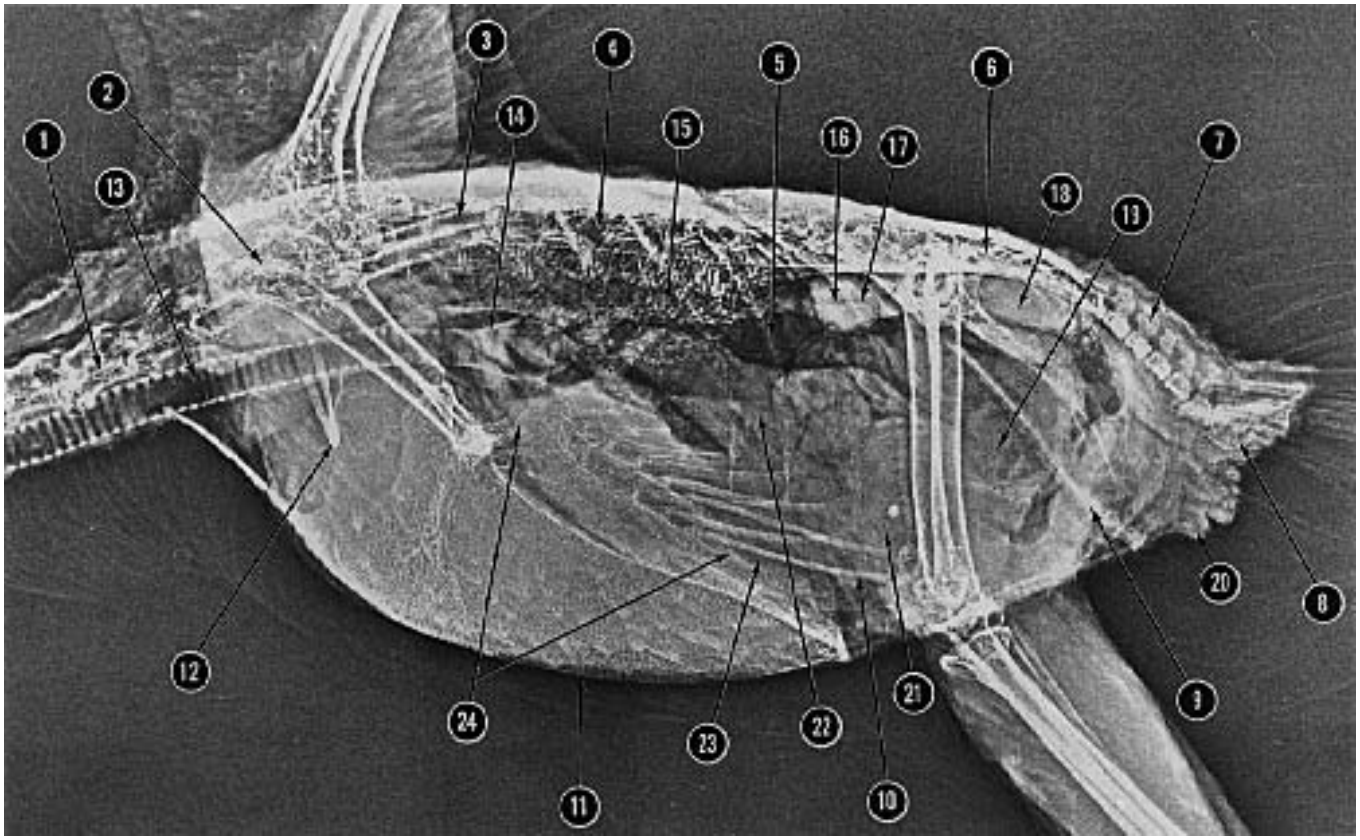

1) cervical vertebra
2) coracoid
3) scapula
4) area of notarium
5) vertebral rib
6) synsacrum
7) free caudal vertebrae
8) pygostyle
9) pubis
10) sternal rib
11) kell of sternum
12) clavicles (at point of fusion into furcula)
13) trachea
14) syrinx
15) lung (note characteristic "stipled" appearance)
16) area of gonad
17) kidney (cranial division)
18) kidney (caudal division)
19) intestines
20) vent
21) ventriculus
22) proventriculus
23) liver
24) heart (apex and base)

FIG 12.3 Lateral xeroradiograph of a normal Orange-winged Amazon Parrot (courtesy of Bonnie J. Smith and Stephen A. Smith).

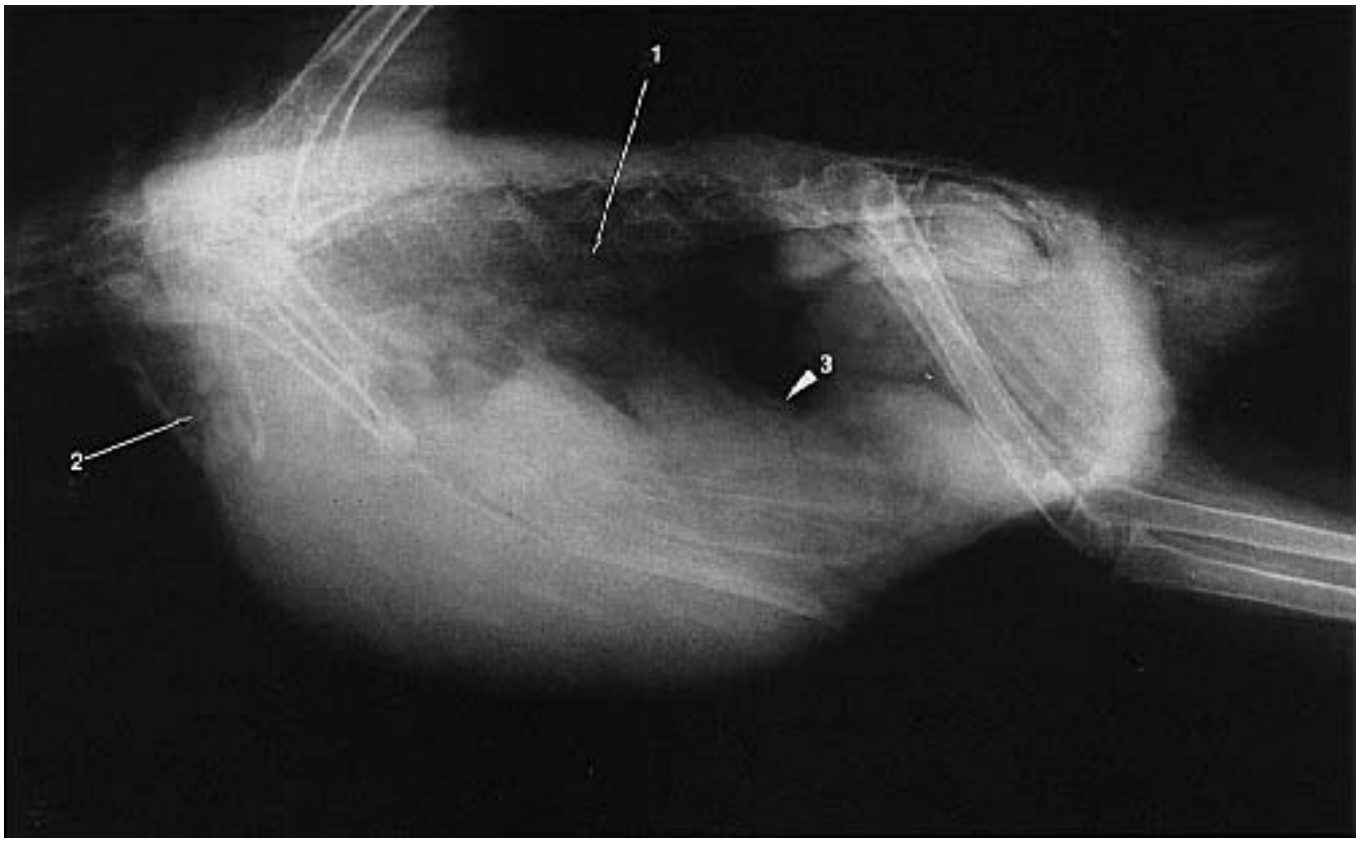

FIG 12.4 Lateral radiograph of a normal Orange-winged Amazon Parrot. 1) mesobronchus en route to abdominal air sac 2) crop containing ingesta 3) spleen (courtesy of Bonnie J. Smith and Stephen A. Smith).

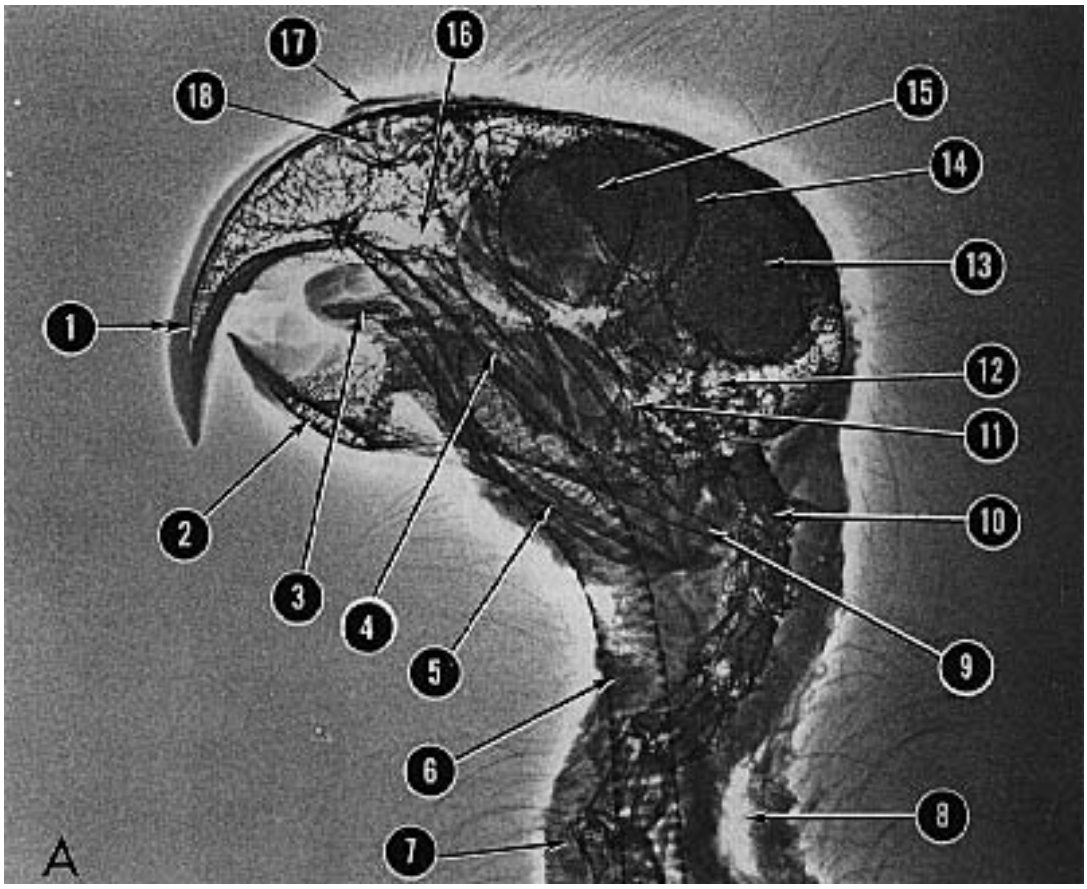

FIG 12.5 Lateral xeroradiograph and radiograph of the head of a normal Orange-winged Amazon Parrot (courtesy of Bonnie J. Smith and Stephen A. Smith).

1) rhinotheca (superficial portion of arrow) covering premaxilla (lower portion of arrow)
2) mandibular symphysis
3) entoglossal bone of hypobranchial apparatus (hyoid) within the tongue
4) jugal arch (zygomatic arch)
5) ceratobranchial bone of hyoid
6) trachea
7) cervical rib
8) cervicocephalic air sac
9) retroarticular process of mandible
10) cervical vertebra
11) quadrate bone
12) tympanic area
13) cranial cavity
14) caudal edge of orbit
15) scleral ossicle
16) rostral part of infraorbital sinus
17) cere
18) nasal aperture

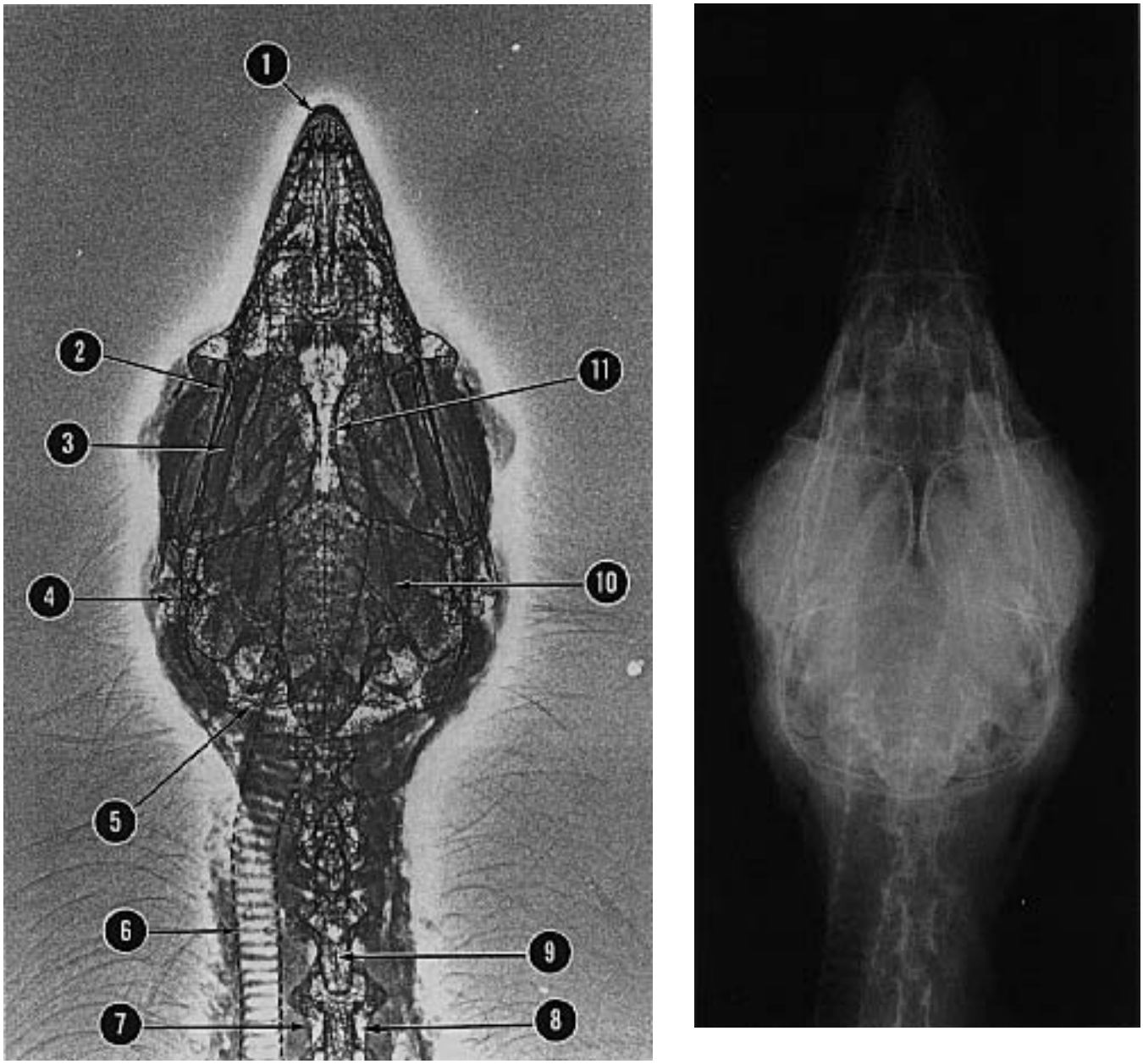

1) rhinotheca covering premaxilla
2) jugal arch (zygomatic arch)
3) mandible
4) area of quadratomandibular joint (analogous to temporomandibular joint)
5) caudal edge of cranium
6) trachea
7) cervical rib
8) cervicocephalic air sac
9) cervical vertebra
10) ceratobranchial bone (hyoid apparatus)
11) medial border of the left orbit

FIG 12.6 Ventrodorsal xeroradiograph and radiograph of the head of a normal Orange-winged Amazon Parrot (courtesy of Bonnie J. Smith and Stephen A. Smith).

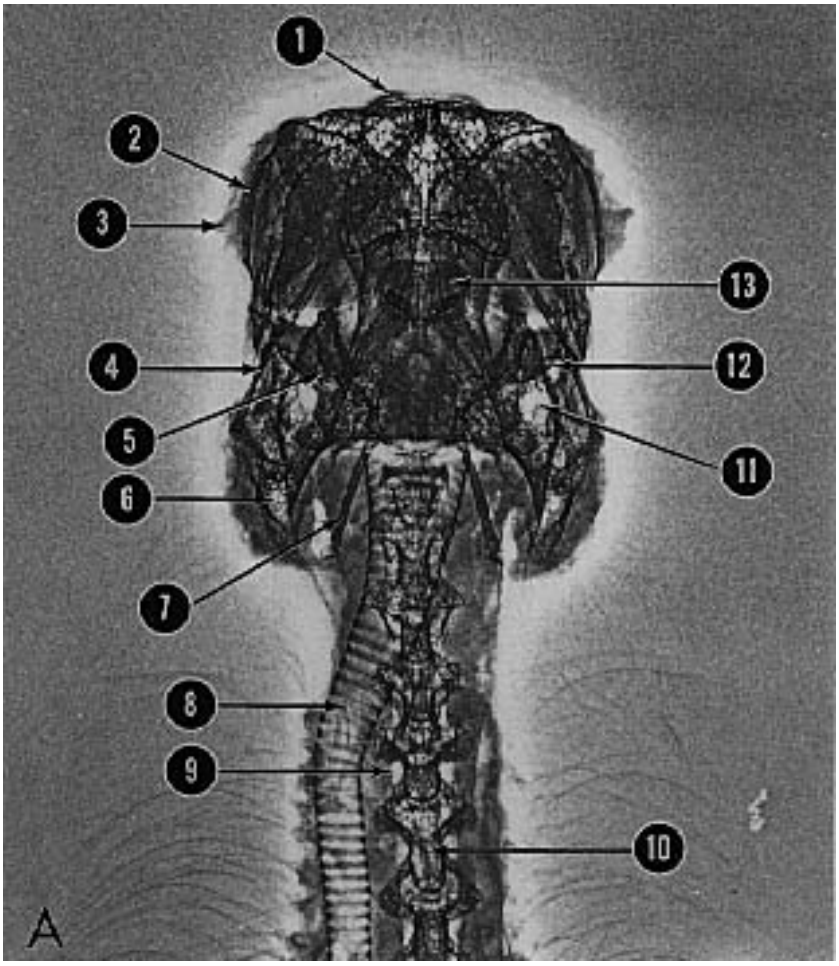

FIG 12.7 Rostrocaudal xeroradiograph and radiograph of the head of a normal Orange-winged Amazon Parrot (courtesy of Bonnie J. Smith and Stephen A. Smith).

1) cere
2) scleral ossicle
3) eyelid
4) jugal arch (zygomatic arch)
5) tympanic area
6) mandible
7) ceratobranchial bone of hyoid
8) trachea
9) cervicocephalic air sac
10) cervical vertebra
11) infraorbital sinus
12) edge of cranium
13) tongue (note paired entoglossum of hyoid)

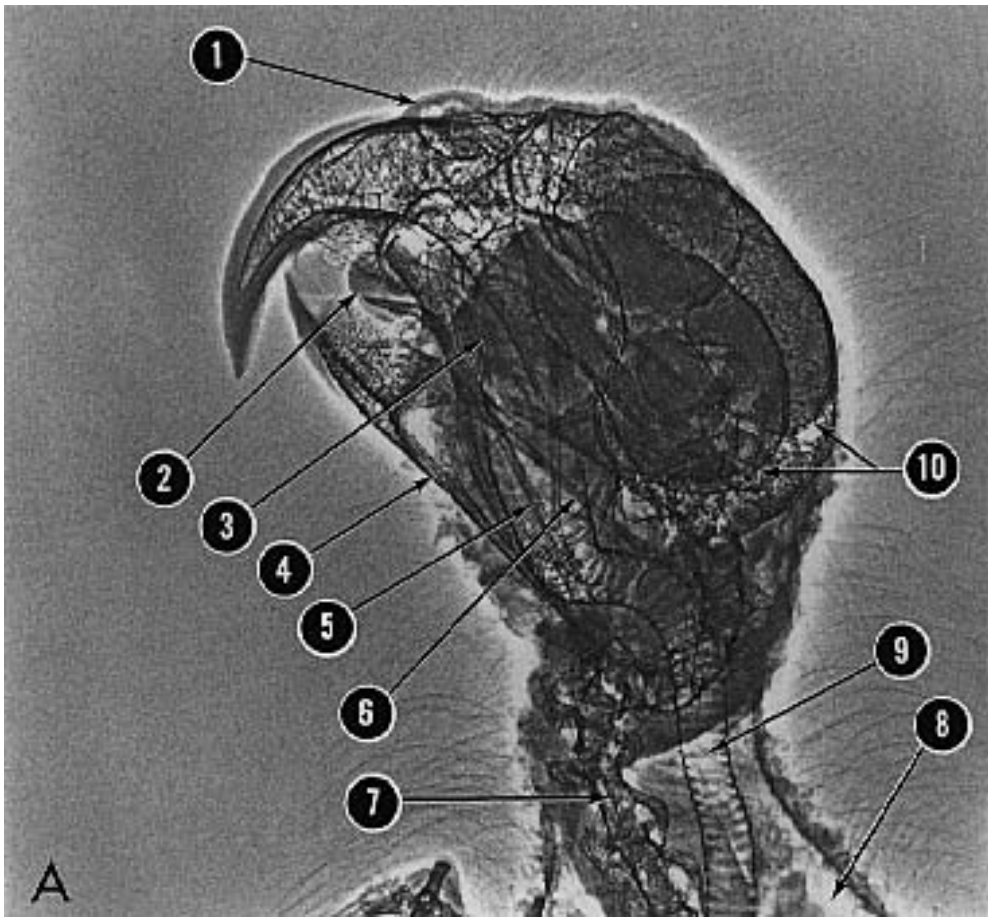

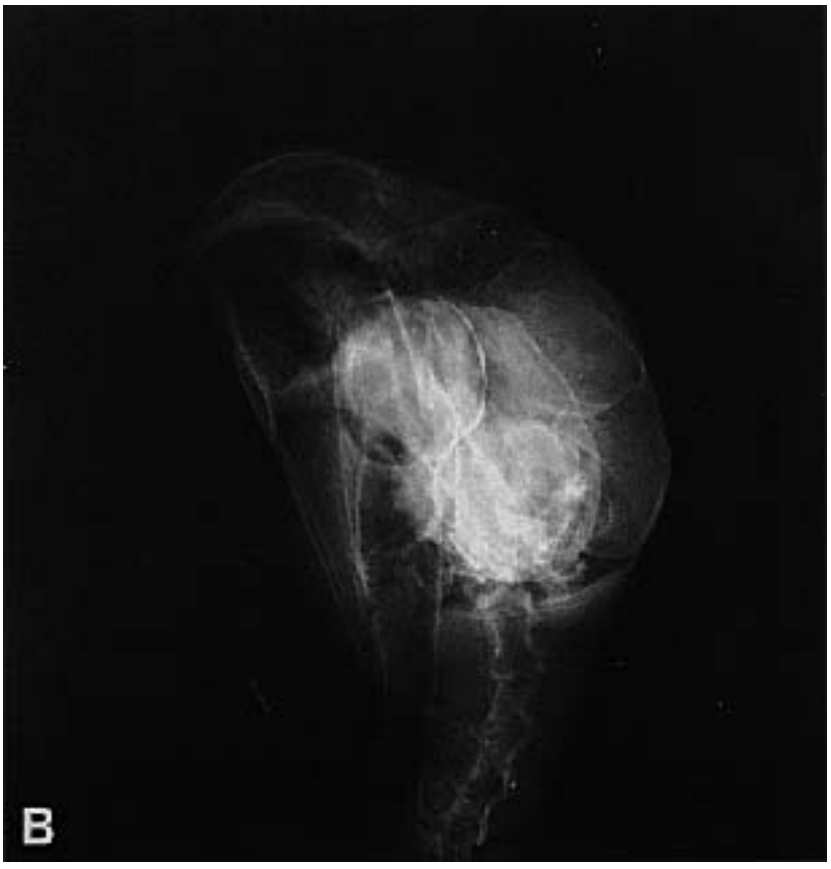

FIG 12.8 Oblique xeroradiograph and radiograph of the head of a normal Orange-winged Amazon Parrot (courtesy of Bonnie J. Smith and Stephen A. Smith).

1) cere
2) tongue containing entoglossum of hyoid
3) scleral ossicle
4) ramus of mandible
5) ceratobranchial bone of hyoid
6) jugal arch (zygomatic arch)
7) cervical vertebra
8) cervicocephalic air sac
9) trachea
10) edge of cranium

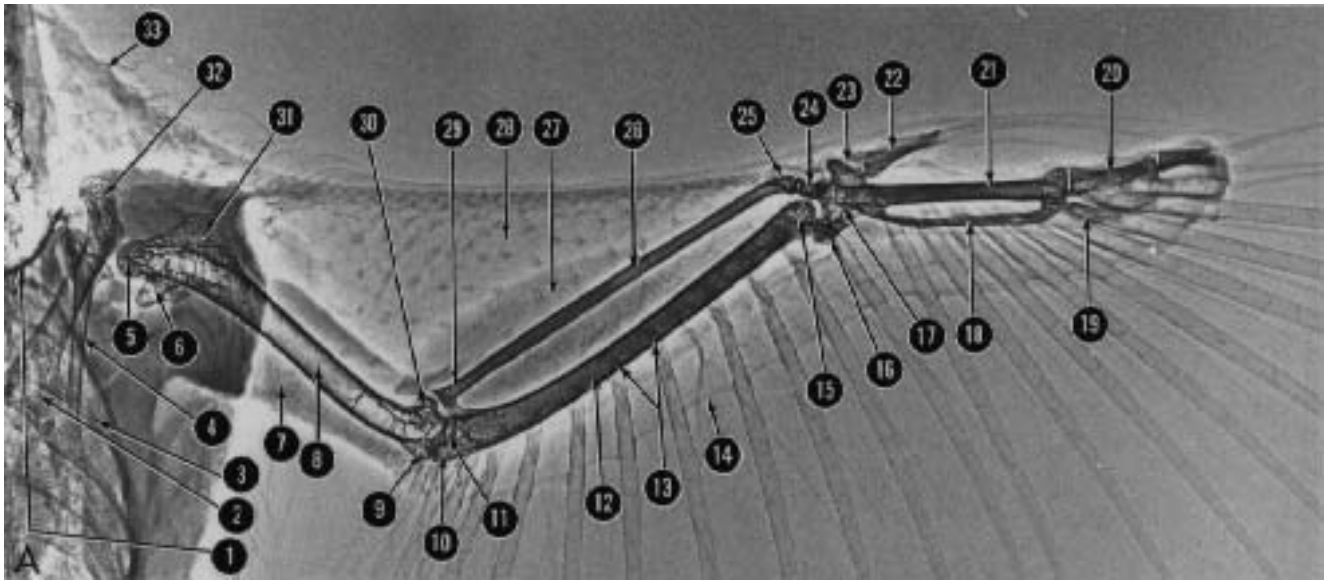

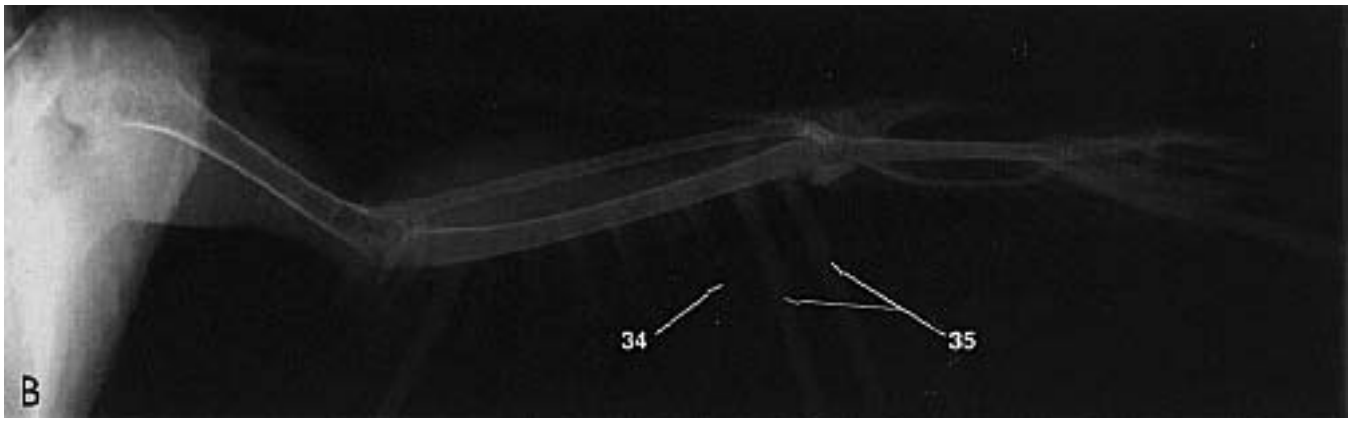

1) clavicle
2) sternal extremity of coracoid
3) rib
4) scapula
5) head of humerus
6) ventral tubercle of humerus
7) extensor muscles of elbow
8) humerus
9) ventral condyle of humerus
10) olecranon
11) cotyles of ulna
12) ulna
13) attachment of secondary flight feathers ot periosteum of ulna
14) post-patagial membrane
15) condyles of ulna
16) ulnar carpal bones
17) intercarpal joint
18) minor metacarpal bone (MC III)
19) minor digit (digit III) composed of one phalanx
20) major digit (digit II, composed of two phalanges)
21) major metacarpal bone (MC III)
22) alular digit (digit I)
23) alular metacarpal bone (MC I)
24) radial carpal bone
25) distal extremity of radius
26) radius
27) extensor muscles of carpus and digit
28) propatagium (note feather follicles)
29) head of radius
30) dorsal condyle of humerus
31) minor tubercle of humerus
32) should extremity of coracoid
33) cervical patagium
34) mature feather with radiolucent core
35) immature feather with vascular core (blood feather)

FIG 12.9 Ventrodorsal xeroradiograph and radiograph of the wing of a normal Orange-winged Amazon Parrot (courtesy of Bonnie J. Smith and Stephen A. Smith).

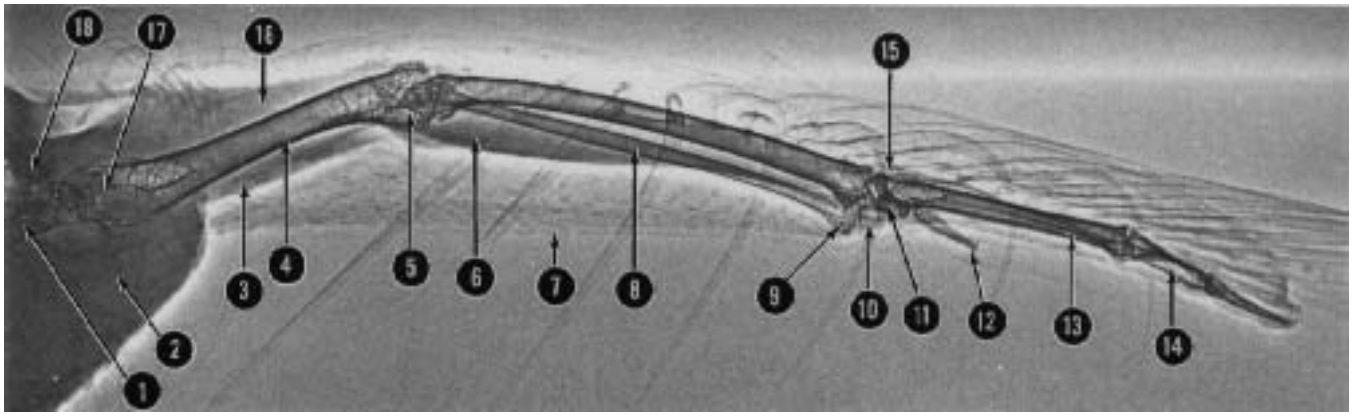

1) coracoid
2) pectoral muscle
3) flexor muscles to elbow
4) humerus
5) elbow joint, superimposition of radial head, olecranon and distal humerus
6) extensor muscles of carpus and digits
7) propatagium
8) radius
9) distal extremity of radius
10) radial carpal bone
11) area of carpometacarpus
12) alular digit (digit I)
13) major and minor metacarpals (superimposed MC III and MC II)
14) major and minor digits (super imposed digit III and II)
15) intercarpal joint
16) extensor muscles of elbow
17) shoulder joint
18) head of scapula

FIG 12.10 Craniocaudal xeroradiograph of a wing of a normal Orange-winged Amazon Parrot. The wing has been slightly rotated to separate the image, of the radius, ulna and alular digit (courtesy of Bonnie J. Smith and Stephen A. Smith).

1) ilium
2) greater trochanter of femur superimposed over femoral head
3) femur
4) patella
5) femoral condyles
6) proximal extremity of tibiotarsus
7) body of tibiotarsus
8) condyles of tibiotarsus
9) cotyles of tarsometatarsus
10) tarsometatarsus
11) metatarsal I
12) digit III (consists of four phalanges)
13) digit II (consists of three phalanges)
14) digital pad
15) digit IV (consists of five phalanges)
16) digit I (consists of two phalanges)
17) podotheca (note abrupt change in skin from delicate and feathered to thick and scaled)
18) calcaneus
19) intertarsal joint
20) fibula
21) sternal rib
22) pubis
23) ischium

FIG 12.11 Lateral xeroradiograph and radiograph of the pelvic limb of a normal Orange-winged Amazon Parrot (courtesy of Bonnie J. Smith and Stephen A. Smith).

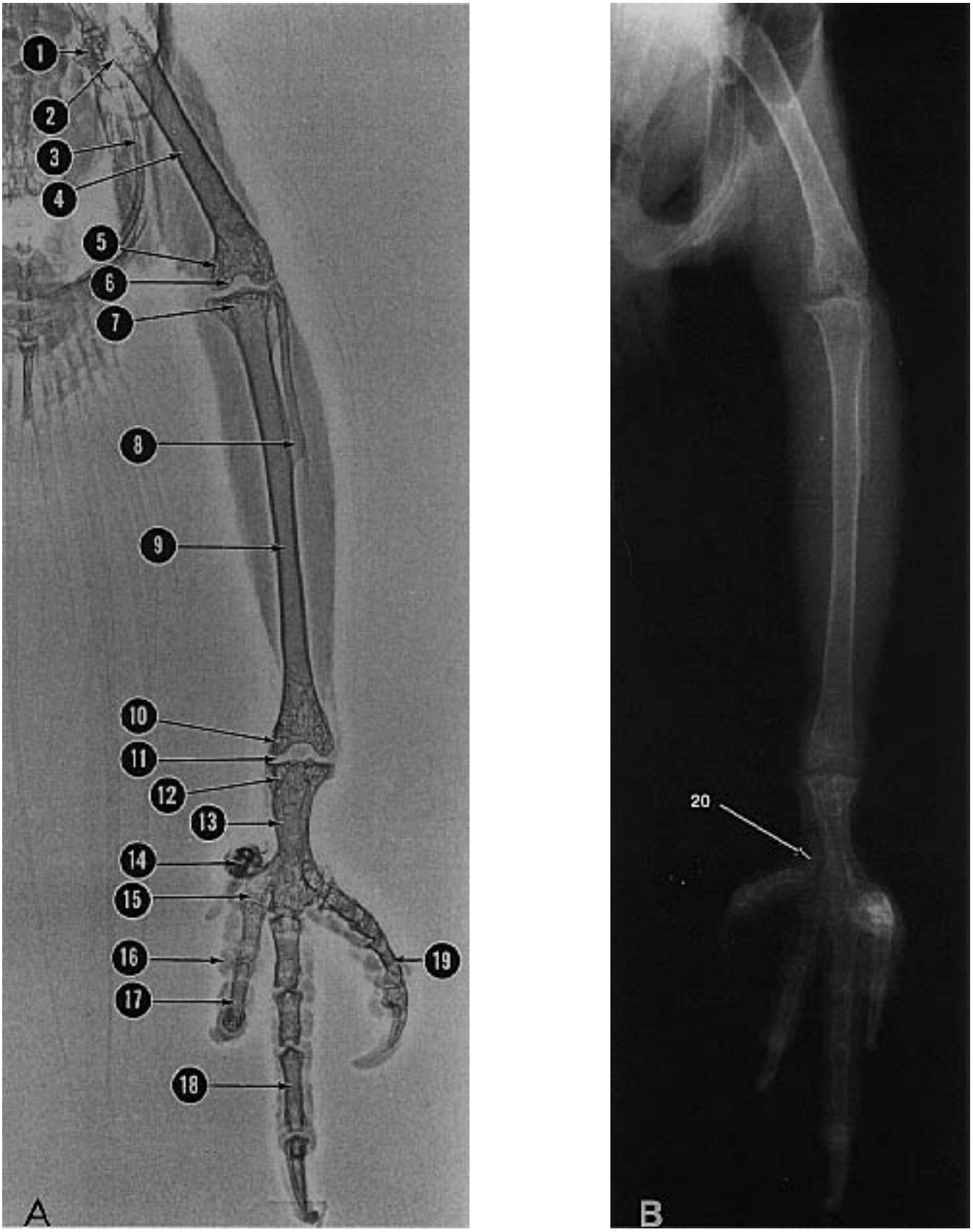

1) neck of femur
2) head of femur within acetabulum
3) pubis
4) femur
5) medial femoral condyle
6) intercondylar sulcus
7) proximal extremity of ti biotarsus
8) fibula
9) tibiotarsus
10) condyles of tibiotarsus
11) intertarsal joint
12) cotyles of tarsometa-tarsus
13) tarsometatarsus
14) digit I
15) tarsometatarsal trochlea for digit II
16) digital pad
17) digit II
18) digit III (four phalanges)
19) digit IV
20) metatarsal I

FIG 12.12 Craniocaudal xeroradiograph and radiograph of the pelvic limb in a normal Orange-winged Amazon Parrot (courtesy of Bonnie J. Smith and Stephen A. Smith).

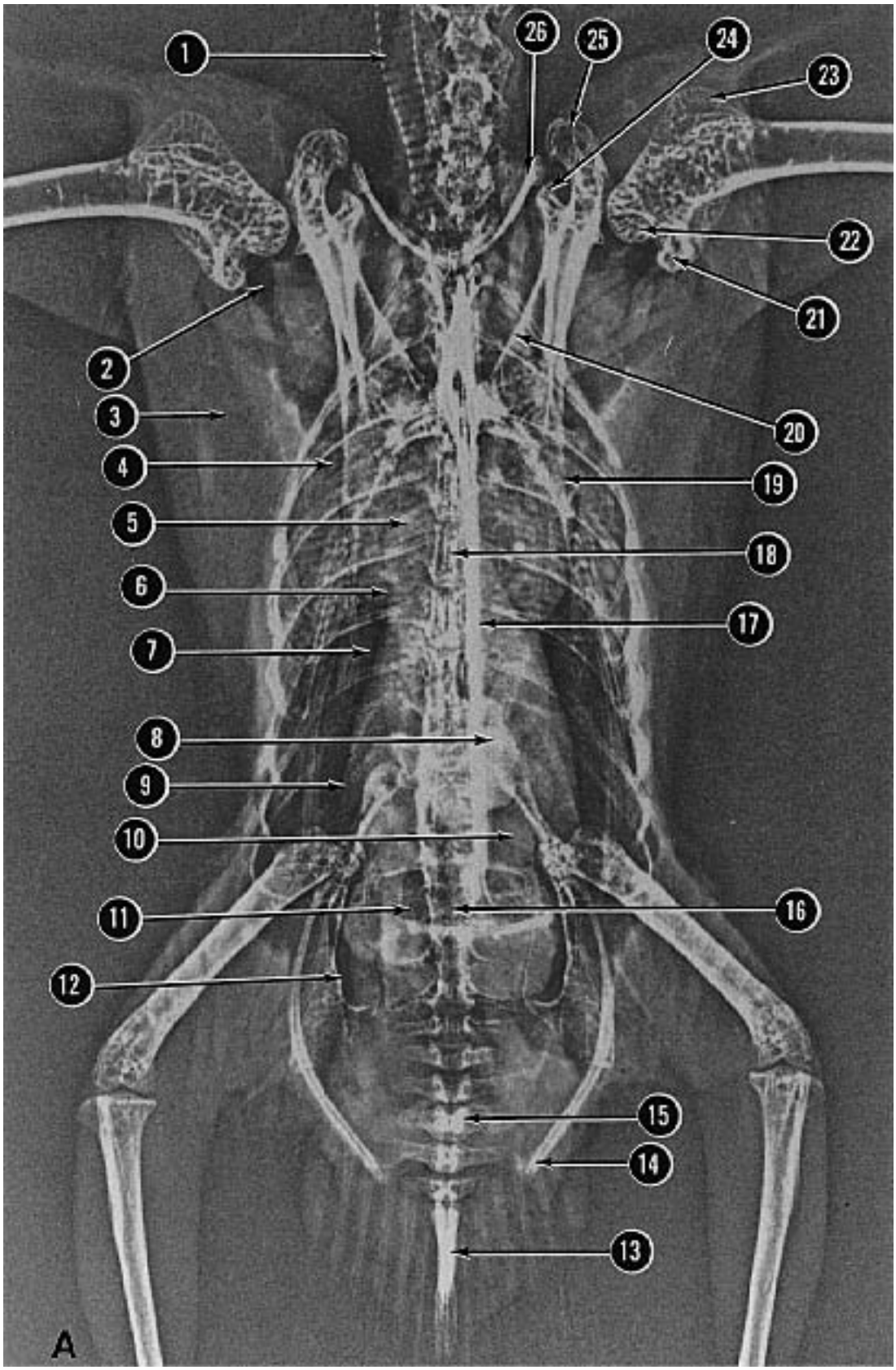

1) trachea
2) clavicular air sac
3) pectoral muscle
4) lung
5) heart
6) normal hour-glass constriction ("waist") of the heart-liver shadow
7) area of overlap of caudal thoracic and abdominal air sacs
8) spleen
9) liver
10) ventriculus
11) intestines
12) abdominal air sac
13) pygostyle
14) pubis
15) free caudal vertebra
16) synsacrum
17) sternum, ventral extremity of carina
18) notarium
19) caudal extremity of scapula
20) medial border of coracoid
21) ventral tubercle of humerus
22) head of humerus
23) dorsal tubercle of humerus
24) head of scapula
25) shoulder extremity of coracoid
26) clavicle

FIG 12.13 Ventrodorsal xeroradiograph (facing page) and radiograph of a normal cockatiel (courtesy of Bonnie J. Smith and Stephen A. Smith).

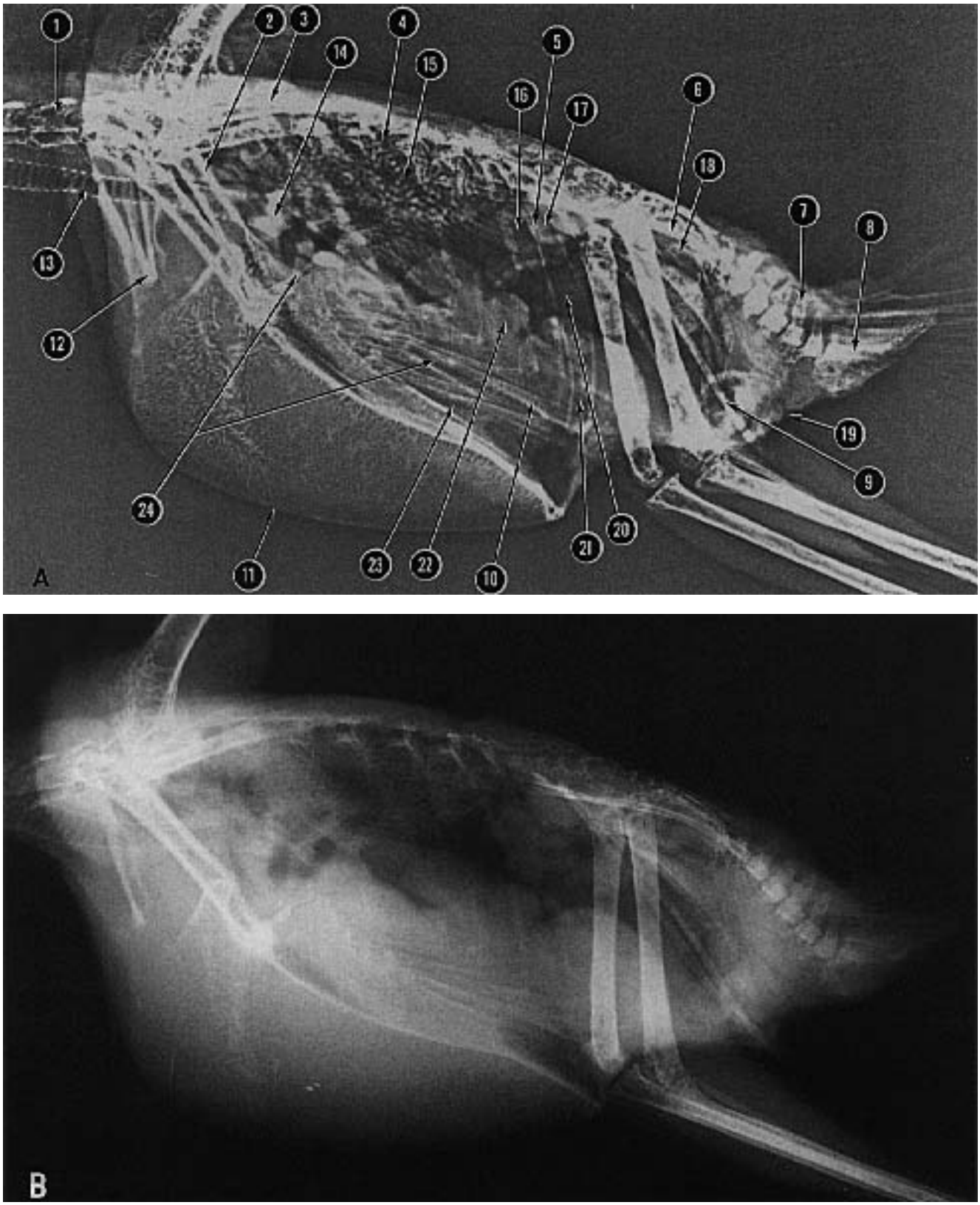

1) cervical vertebra
2) coracoid
3) scapula
4) area of notarium
5) vertebral rib
6) synsacrum
7) free caudal vertebra
8) pygostyle
9) pubis
10) sternal rib
11) keel of sternum
12) clavicle
13) trachea
14) area of syrinx
15) lung
16) area of gonad
17) cranial division of kidney
18) caudal division of kidney
19) vent
20) intestines
21) ventriculus
22) proventriculus
23) liver
24) heart

FIG 12.14 Lateral xeroradiograph and radiograph of a normal cockatiel (courtesy of Bonnie J. Smith and Stephen A. Smith).

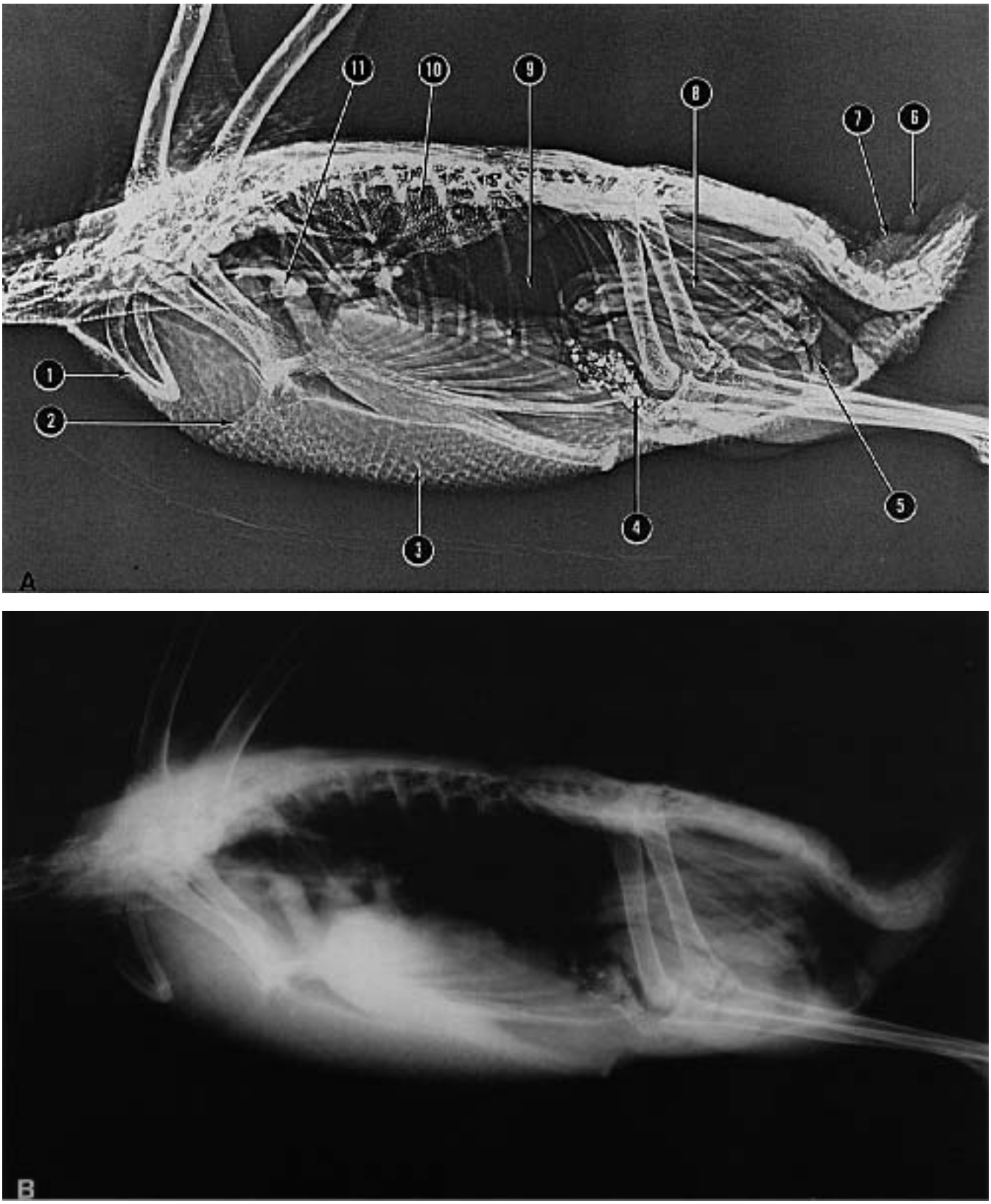

1) clavicle
2) cranial margin of keel of sternum (note absence of concave curvature)
3) feather follicles (note prominence characteristic of Anseriformes)
4) ventriculus containing grit
5) pubis
6) papilla of uropygial gland
7) uropygial gland (note large size)
8) intestines
9) abdominal air sac
10) lung
11) area of syrinx (note absence of bulla in the hen)

FIG 12.15 Lateral xeroradiograph and radiograph of a normal Mallard Duck (courtesy of Bonnie J. Smith and Stephen A. Smith).

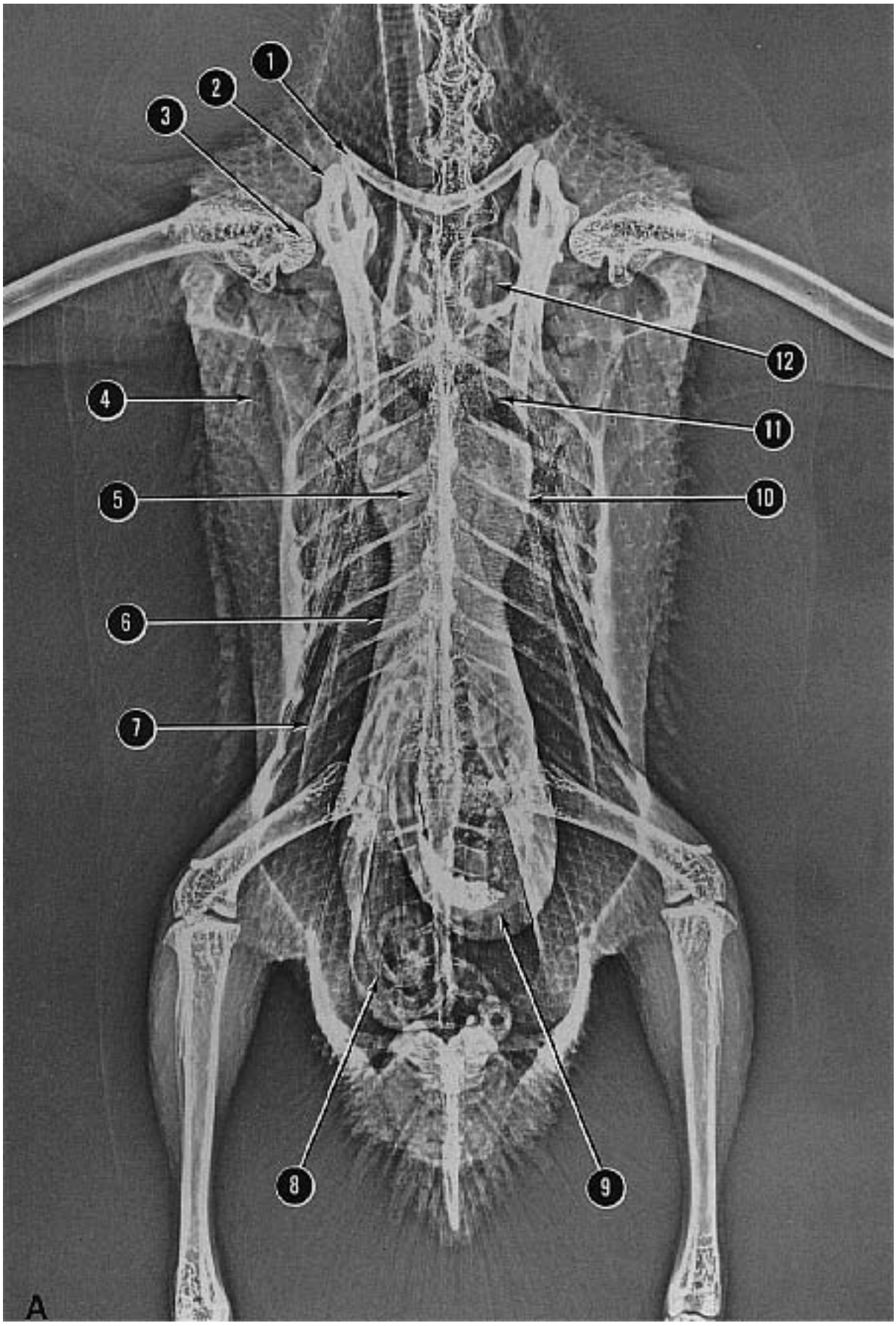

1) clavicle
2) shoulder extremity of coracoid base
3) head of humerus
4) feather follicle
5) heart
6) liver
7) lateral caudal process of sternum
8) intestines
9) ventriculus containing grit
10) caudal extremity of scapula
11) left brachiocephalic trunk
12) cavity of syringeal bulla

FIG 12.16 Ventrodorsal xeroradiograph (facing page) and radiograph of a normal male Mallard Duck (courtesy of Bonnie J. Smith and Stephen A. Smith).

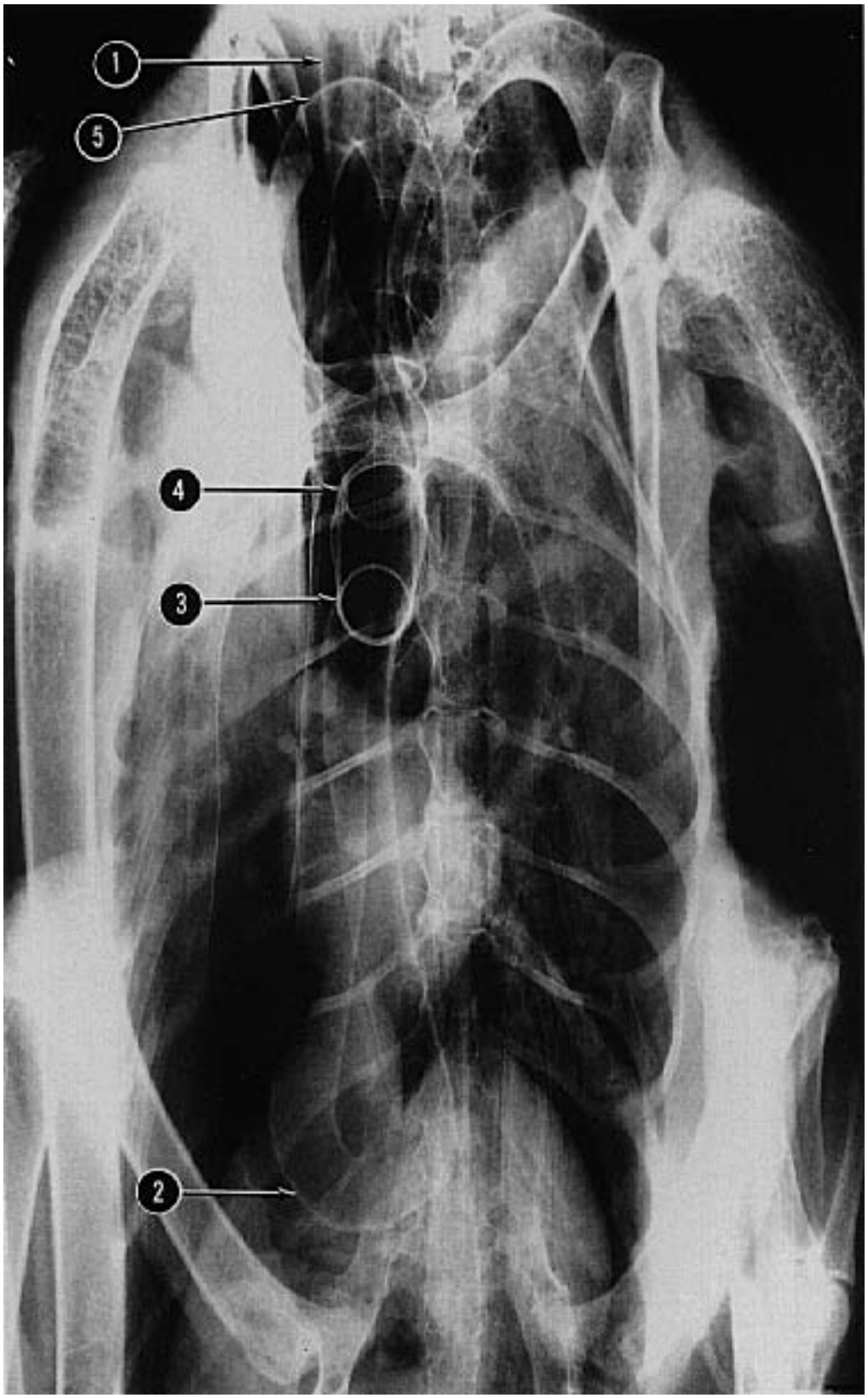

FIG 12.17 Ventrodorsal radiograph of a clinically normal Trumpeter Swan. In this species, the trachea is lengthened and is permanently curved within an excavation in the sternum. The 1) trachea enters the thoracic inlet, 2) courses caudally within the sternal excavation and re-curves cranially near the caudal end of the sternum. 3,4) A small loop is formed within the sternal excavation, which is visible as an end-on tubular view, and the trachea then courses 5) cranially to the thoracic inlet, where it re-curves and enters the syrinx (courtesy of Bonnie J. Smith and Stephen A. Smith).

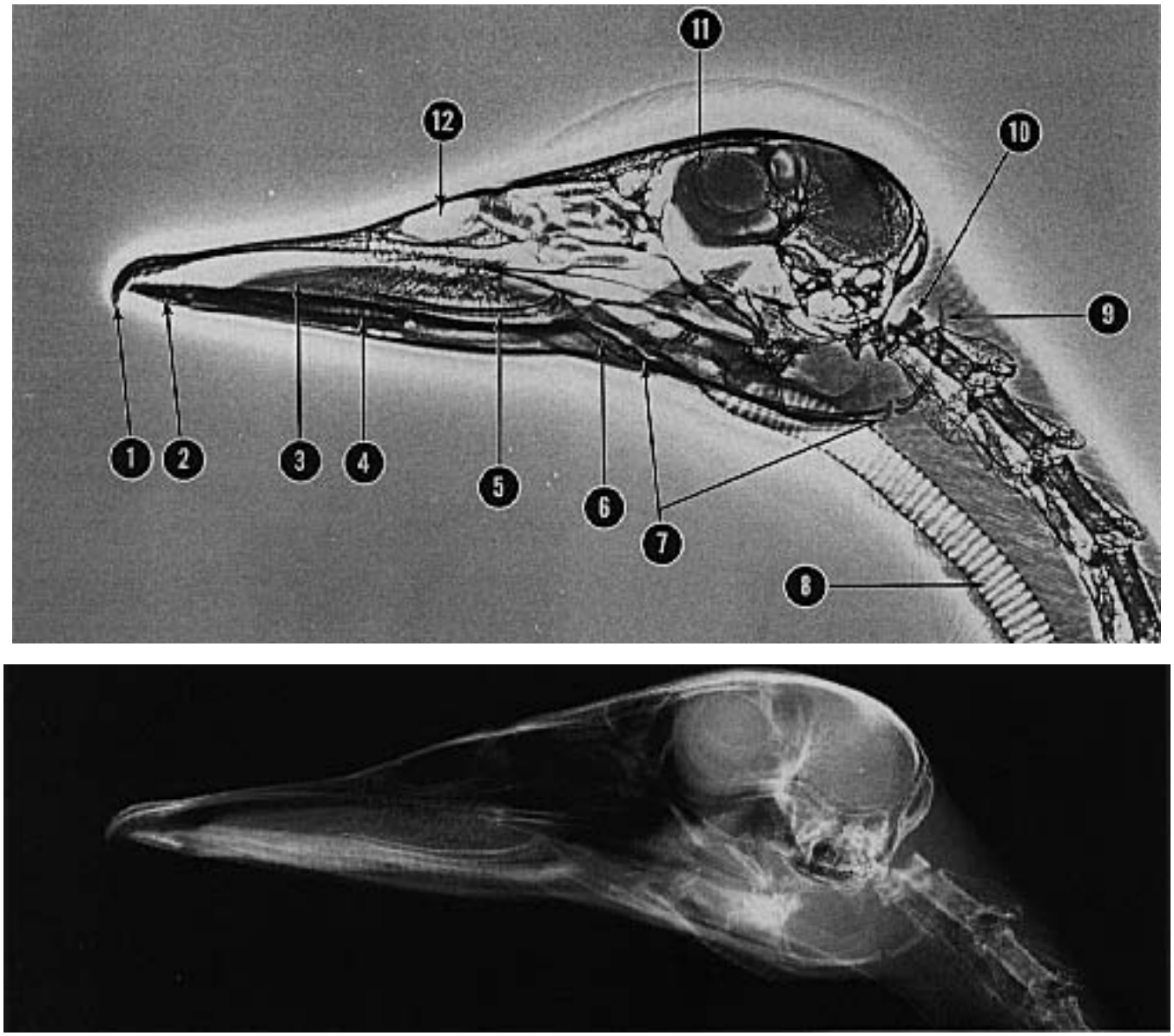

1) nail
2) mandibular symphysis
3) tongue
4) lamellae of bill
5) entoglossum of hyoid apparatus (note large size to support well developed tongue)
6) rostral basibranchial bone of hyoid apparatus
7) ceratobranchial bone of hyoid apparatus
8) trachea
9) epibranchial bone of hyoid apparatus
10) atlas
11) scleral ring
12) nasal aperture

FIG 12.18 Lateral xeroradiograph and radiograph of a normal Mallard Duck (courtesy of Bonnie J. Smith and Stephen A. Smith).

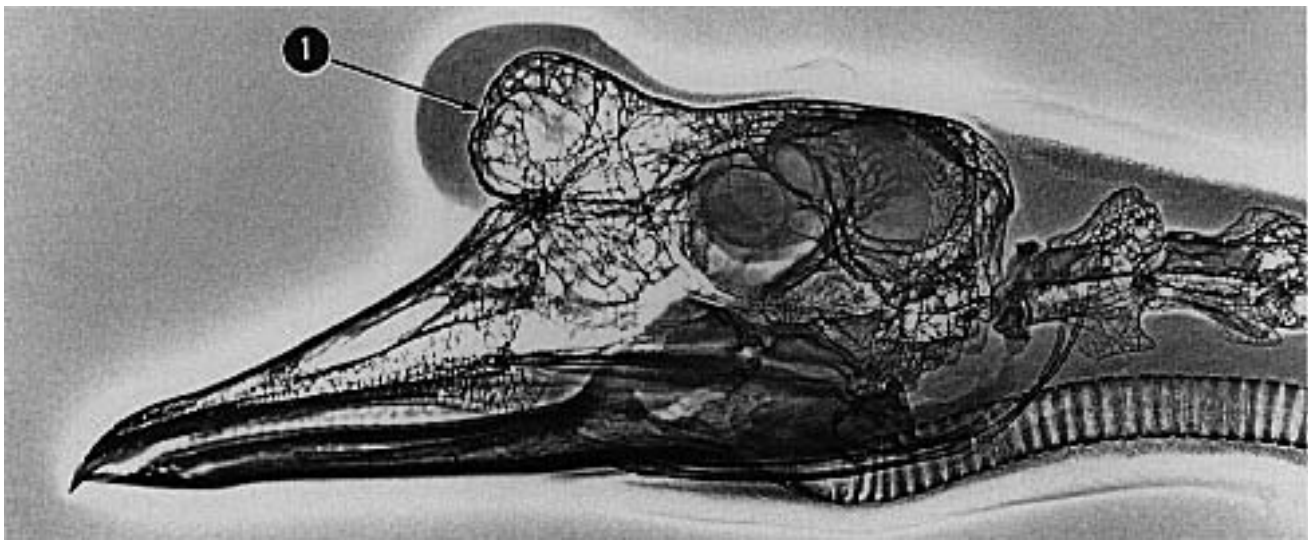

FIG 12.19 Lateral xeroradiograph of the Chinese Goose demonstrating the 1) frontal knob. Note the bony core of this structure and its well-developed soft tissue covering (courtesy of Bonnie J. Smith and Stephen A. Smith).

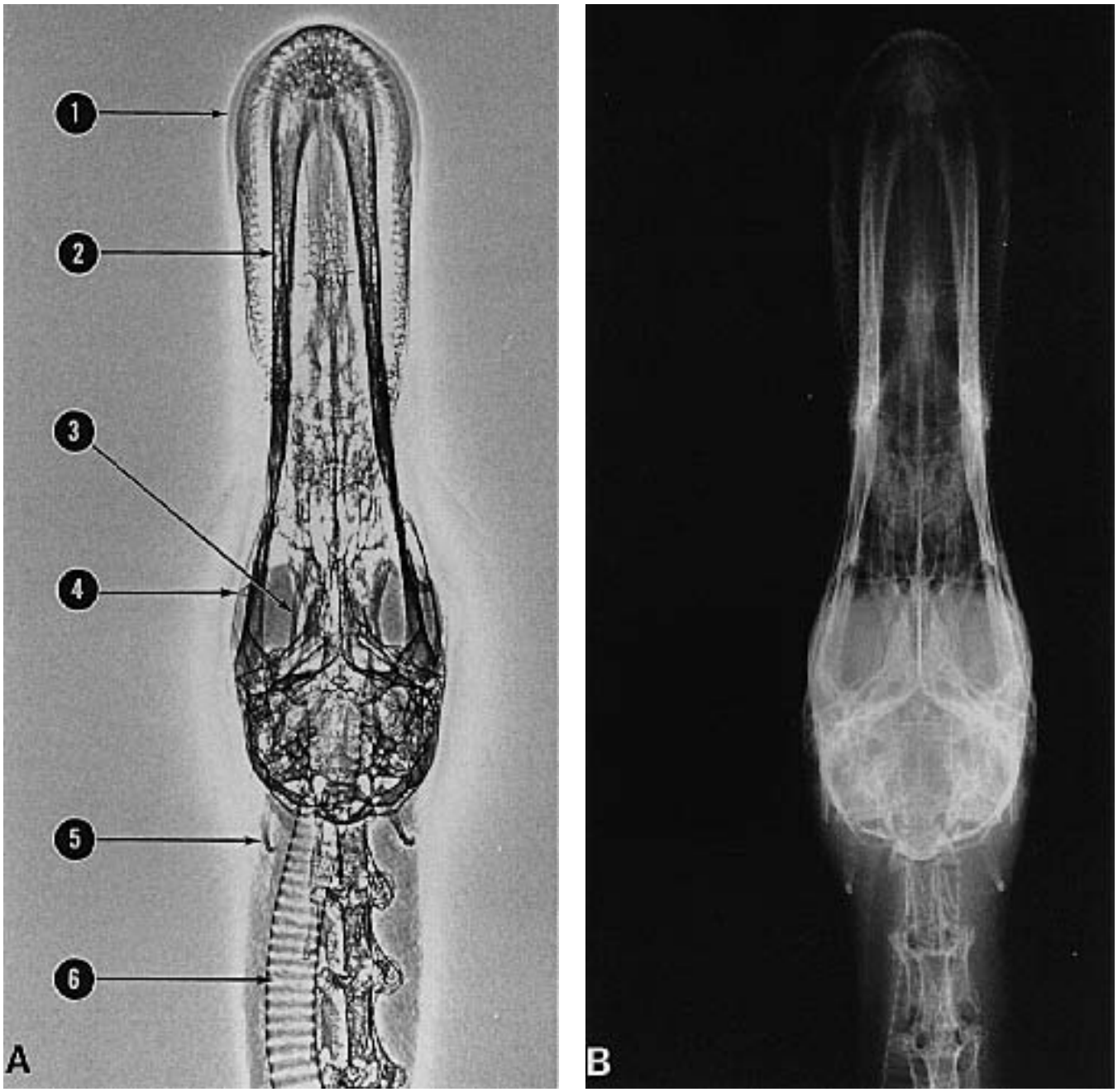

FIG 12.20 Ventrodorsal xeroradiograph and radiograph of the head of a normal Mallard Duck. 1) upper bill covering premaxilla 2) mandible 3) ceratobranchial bone of hyoid apparatus 4) scleral ring 5) epibranchial bone of hyoid apparatus 6) trachea (courtesy of Bonnie J. Smith and Stephen A. Smith).

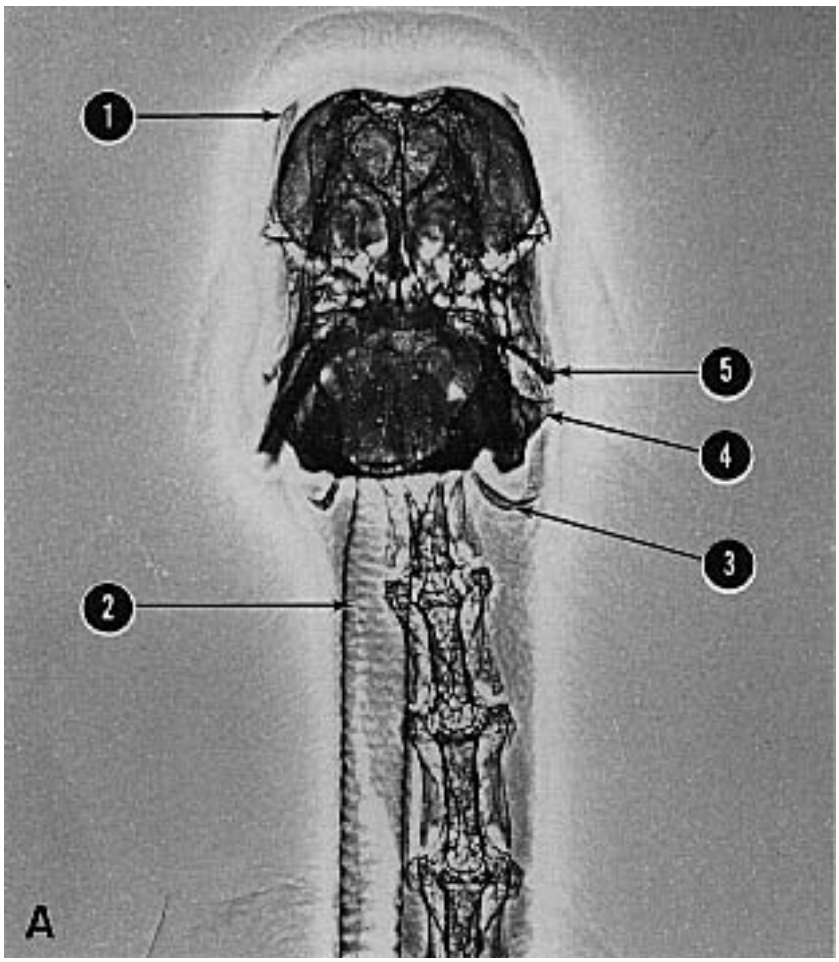

FIG 12.21 Rostrocaudal view of xeroradiograph and radiograph of a normal Mallard Duck. 1) scleral ring 2) trachea 3) ceratobranchial bone of hyoid apparatus 4) mandible 5) jugal arch (zygomatic arch) (courtesy of Bonnie J. Smith and Stephen A. Smith).

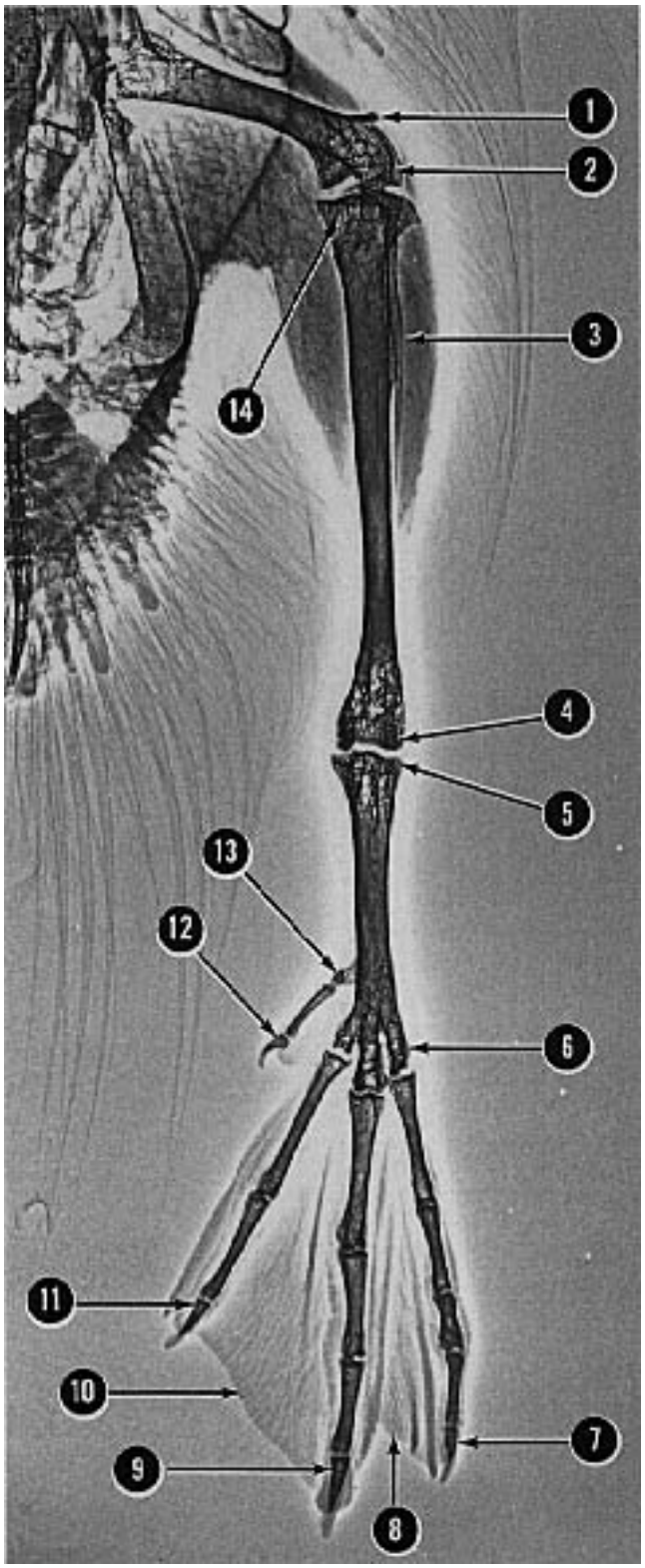

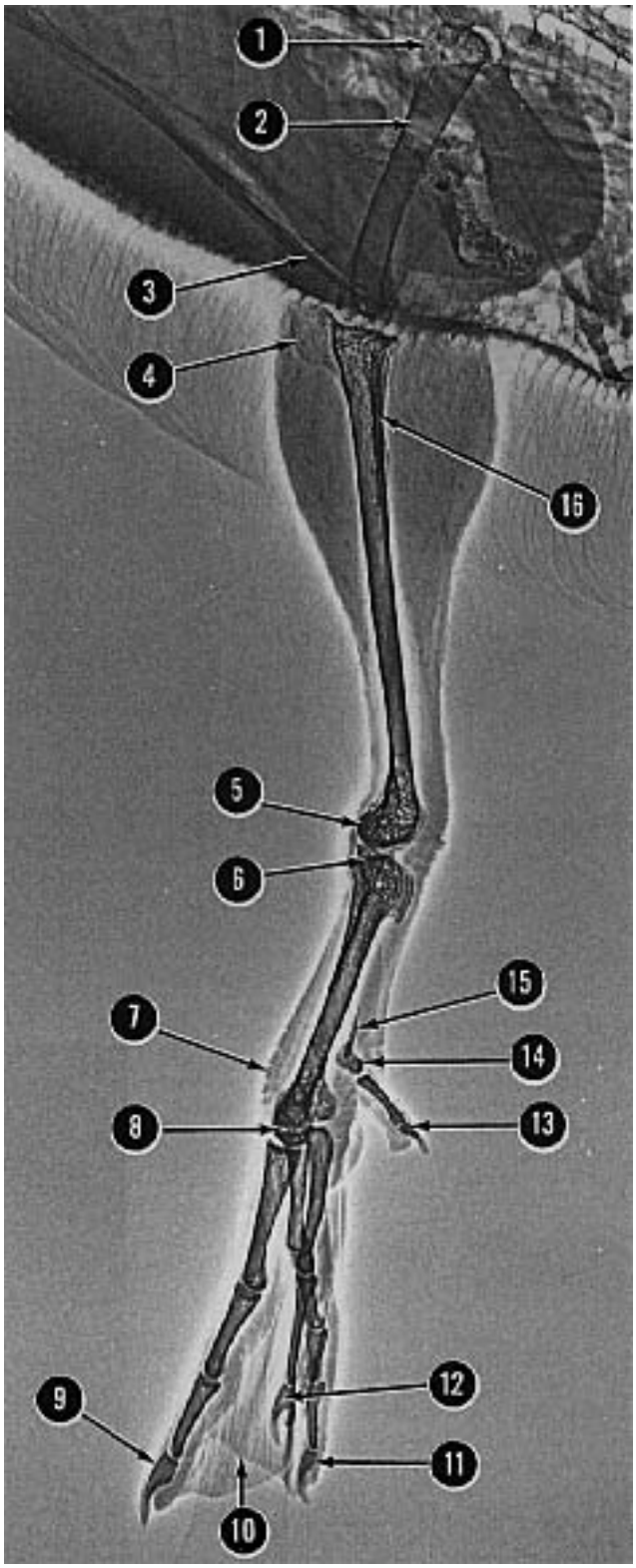

1) patella
2) condyles of femur
3) fibula
4) condyle of tibiotarsus
5) cotyle of tarsometatarsus
6) tarsometatarsal trochlea for digit IV
7) distal phalanx of digit IV
8) lateral interdigital web
9) distal phalanx of digit III
10) intermediate interdigital web
11) distal phalanx of digit II
12) distal phalanx of digit I
13) metatarsal bone I
14) proximal tibiotarsus

1) greater trochanter of femur
2) femur
3) patella, superimposed over keel
4) cnemial crest of tibiotarsus
5) condyles of tibiotarsus
6) cotyles of tarsometatarsus
7) podotheca (unfeathered skin covering pes)
8) trochlea of tarsometatarsus
9) distal (fourth phalanx) of digit III (note horny nail covering bony core)
10) interdigital web
11) distal (fifth) phalanx of digit IV
12) distal (third) phalanx of digit II
13) distal (second) phalanx of digit I
14) metatarsal bone I
15) ossification within digital tendon
16) fibula, superimposed with body of tibiotarsus

FIG 12.22 Craniocaudal xeroradiograph (left) and mediolateral xeroradiograph (right) of the pelvic limb of a normal Mallard Duck (courtesy of Bonnie J. Smith and Stephen A. Smith).

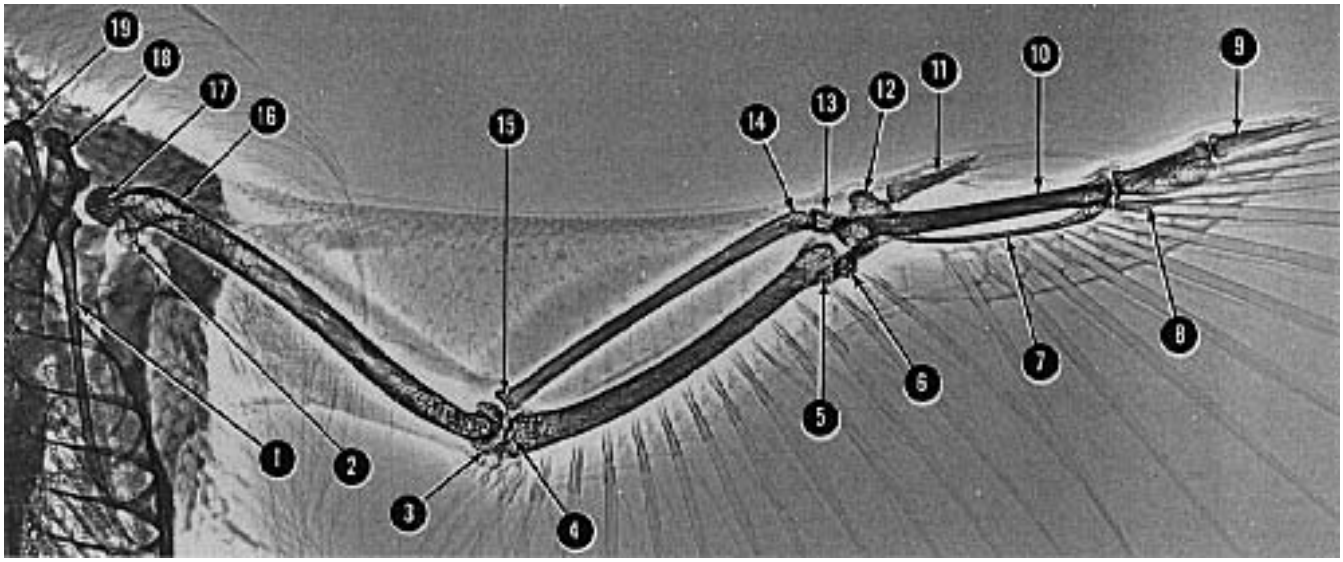

1) body of scapula
2) ventral tubercle of humerus
3) condyles of humerus
4) olecranon of ulna
5) condyles of ulna
6) ulnar carpal bones
7) minor metacarpal bone
8) minor digit (consisting of one phalanx)
9) major digit (consisting of two phalanges)
10) major metacarpal bone
11) alular digit
12) extensor of alular metacarpal bone
13) radial carpal bone
14) distal extremity of radius
15) head of radius
16) pectoral crest of humerus
17) head of humerus
18) should extremity of coracoid bone
19) clavicle

FIG 12.23 Ventrodorsal xeroradiograph of the wing of a normal Mallard Duck (courtesy of Bonnie J. Smith and Stephen A. Smith).

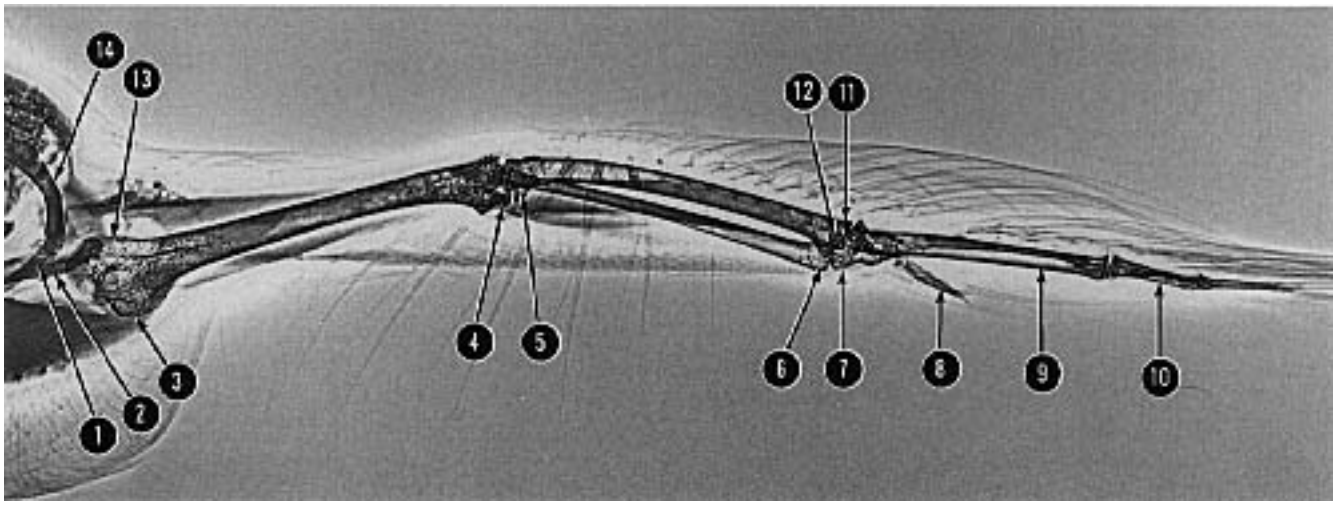

1) clavicle
2) coracoid bone
3) pectoral crest of humerus
4) condyles of humerus
5) superimposed proximal radius and ulna
6) distal extremity of radius
7) radial carpal bone
8) alular digit
9) superimposed major and minor metacarpal bones
10) superimposed major and minor digits
11) distal extremity of ulna
12) ulnar carpal bone superimposed over other carpal structures
13) scapula

FIG 12.24 Craniocaudal xeroradiograph of the wing of a normal Mallard Duck (courtesy of Bonnie J. Smith and Stephen A. Smith).

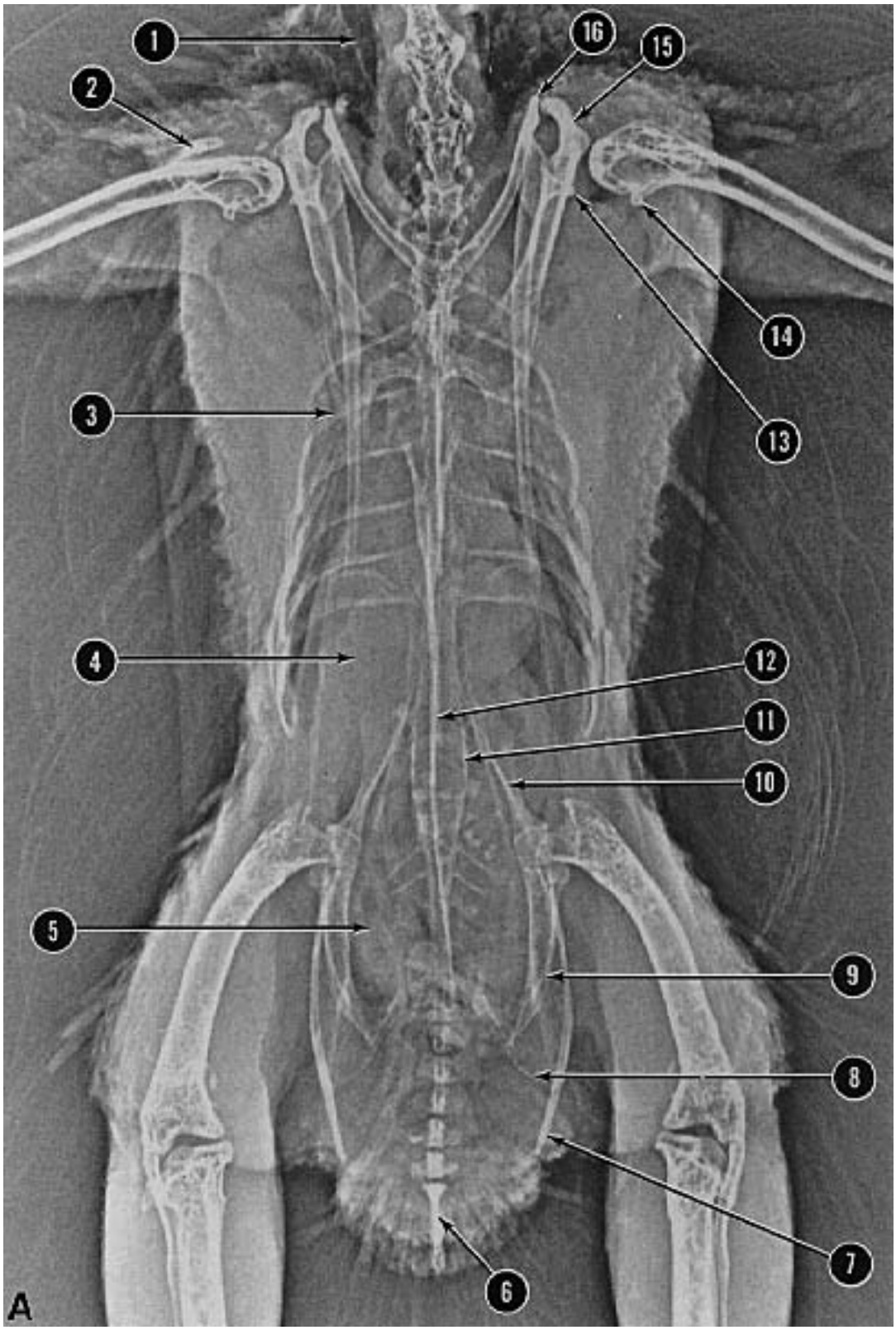

1) trachea
2) feather shaft (rachis)
3) vertebral rib)
4) liver
5) intestines
6) pygostyle
7) pubis
8) terminal process of ischium
9) postacetabular portion of ilium
10) preacetabular portion of ilium
11) synsacrum
12) ventral extremity of carina (keel)
13) head of scapula
14) ventral tubercle of humerus
15) shoulder extremity of coracoid
16) shoulder extremity of oviduct
17) egg within magnum of oviduct

FIG 12.25 Ventrodorsal xeroradiograph (previous page) and radiograph of a normal female Bobwhite Quail (courtesy of Bonnie J. Smith and Stephen A. Smith).

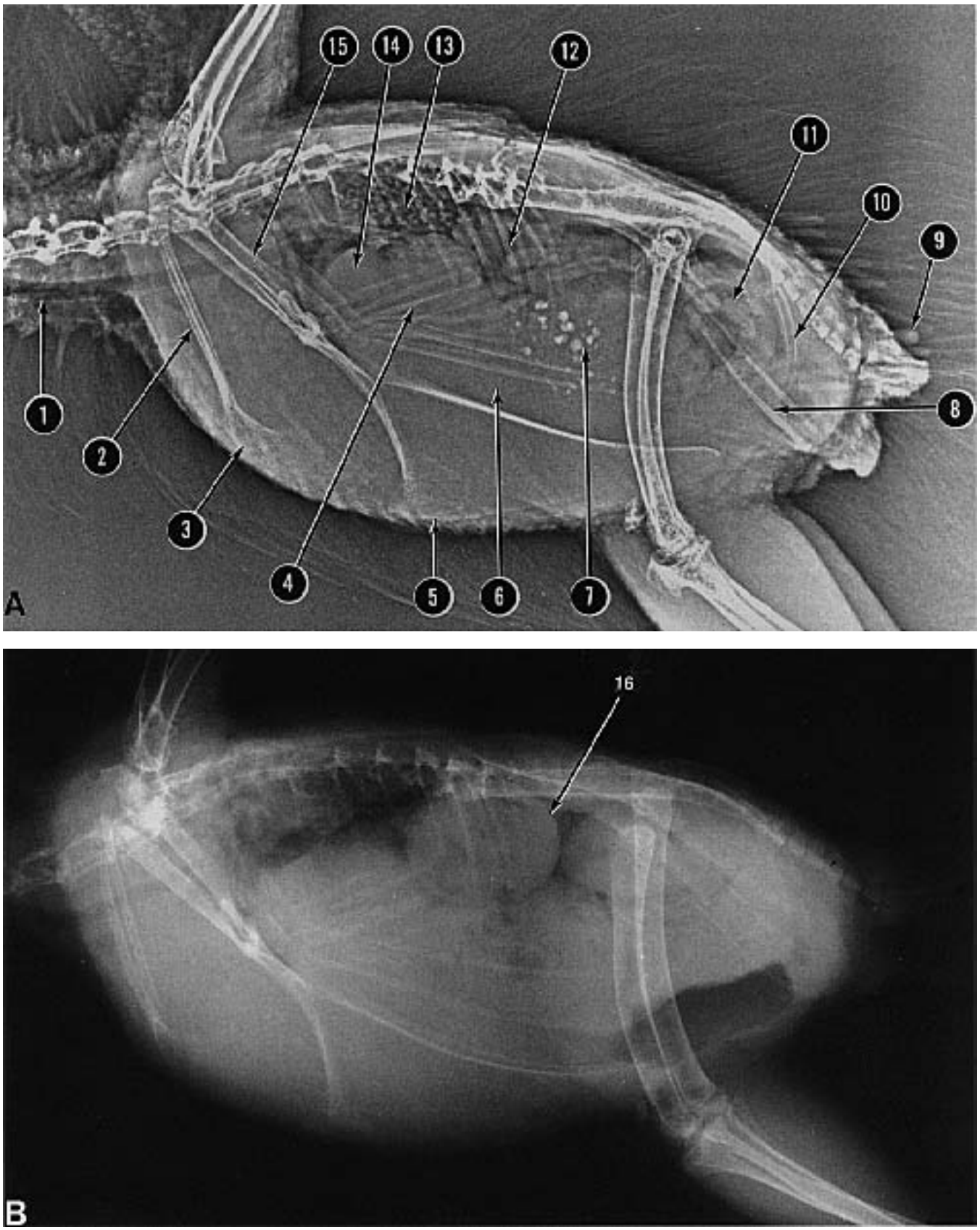

1) trachea
2) clavicle
3) clavicle at point of fusion into furcula (note hooked shape)
4) sternal rib
5) carina (keel)
6) area of liver
7) ventriculus containing grit
8) pubis
9) papilla of uropygial gland
10) terminal process of ischium
11) intestines
12) vertebral rib
13) lung
14) heart
15) coracoid
16) follicle on ovary

FIG 12.26 Lateral xeroradiograph and radiograph of a normal female Bobwhite Quail. Note the short, heavy muscled, rotund body and compact viscera. Differentiation between the heart and the liver is difficult (courtesy of Bonnie J. Smith and Stephen A. Smith).

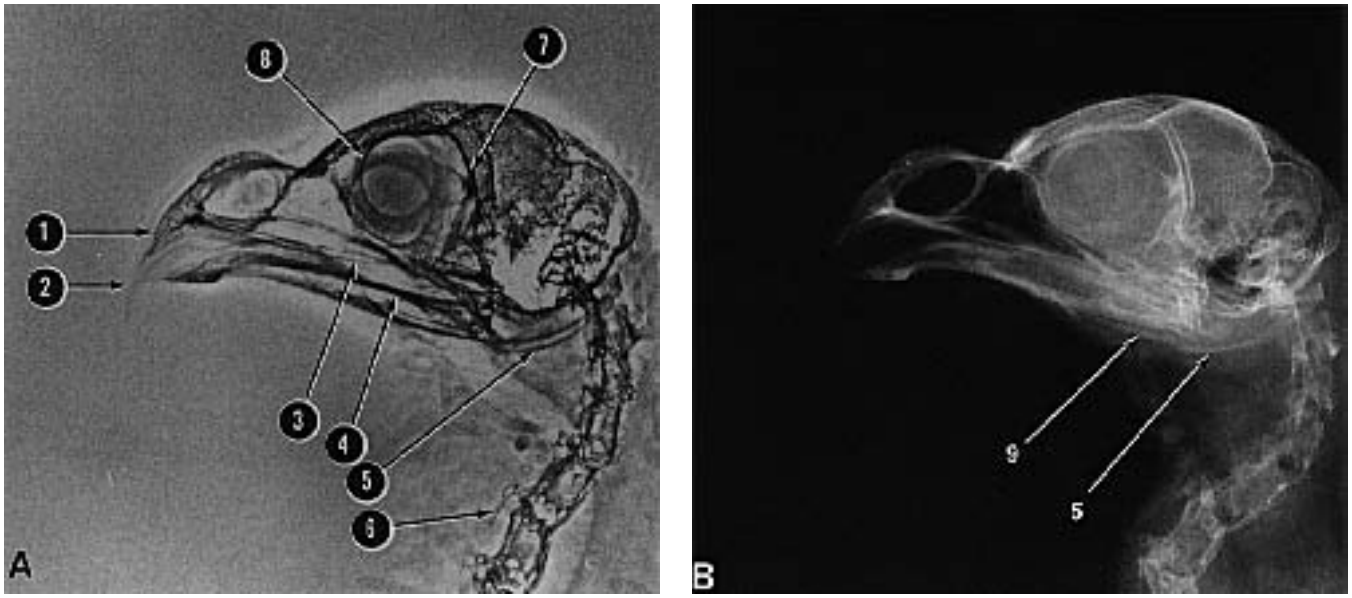

FIG 12.27 Lateral xeroradiograph and radiograph of the head of a normal Bobwhite Quail. 1) premaxilla 2) rhinotheca covering premaxilla 3) jugal arch (zygomatic arch) 4) mandible 5) ceratobranchial bone of hyoid apparatus 6) cervical rib on cervical vertebra 7) caudal edge of orbit 8) scleral ring 9) rostral basibranchial bone of hyoid apparatus (courtesy of Bonnie J. Smith and Stephen A. Smith).

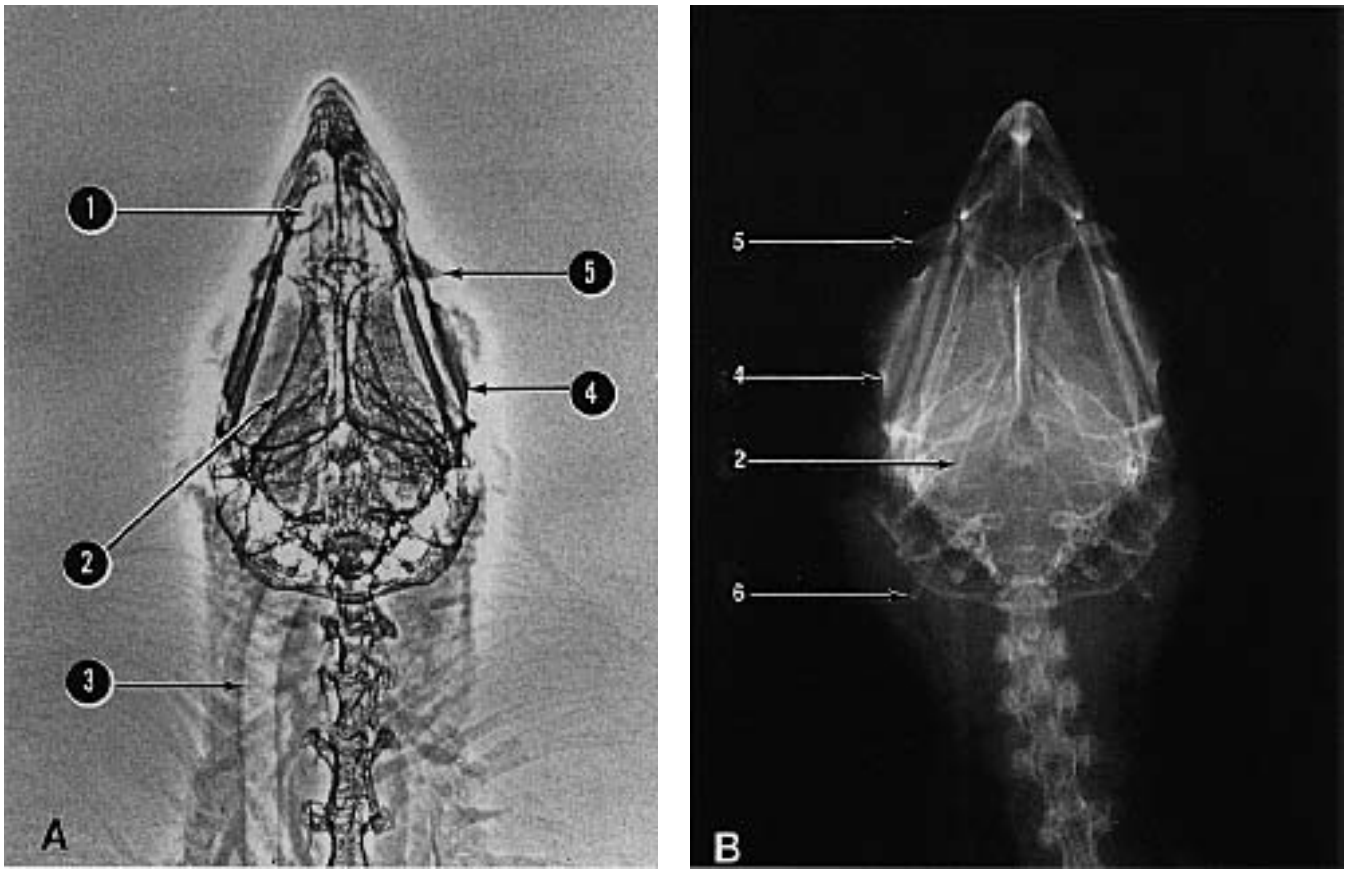

FIG 12.28 Ventrodorsal xeroradiograph and radiograph of the head of a normal Bobwhite Quail. 1) nares 2) ceratobranchial bone of hyoid apparatus 3) trachea 4) scleral ring 5) lacrimal bone 6) epibranchial bone of hyoid apparatus (courtesy of Bonnie J. Smith and Stephen A. Smith).

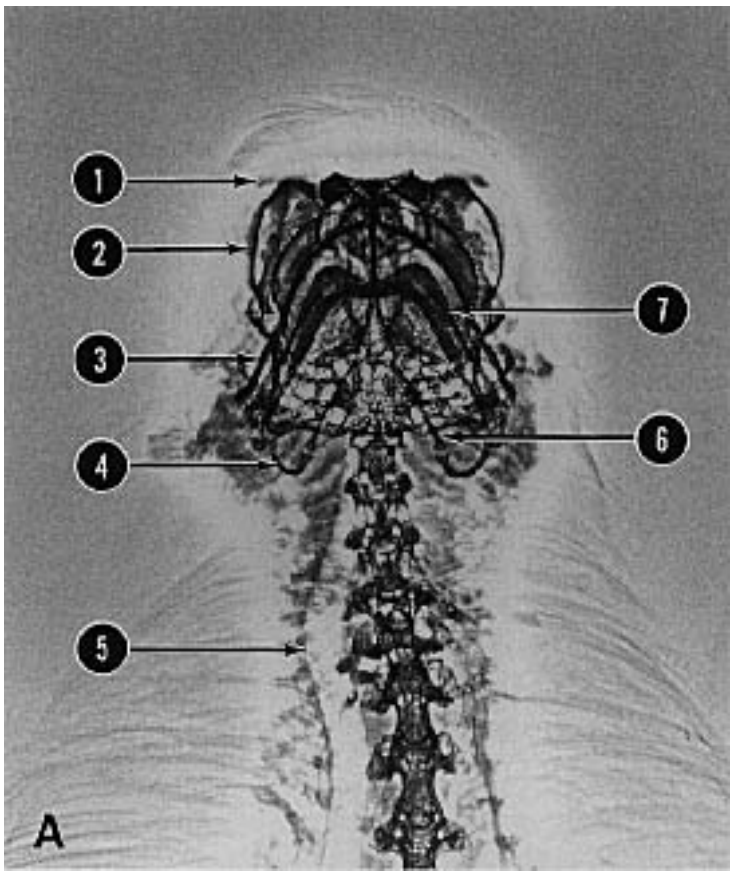

FIG 12.29 Rostrocaudal xeroradiograph and radiograph of the head of a normal Bobwhite Quail. 1) lacrimal bone 2) scleral ring 3) jugal arch (zygomatic arch) 4) epibranchial bone of hyoid apparatus 5) trachea 6) ceratobranchial bone of hyoid apparatus 7) mandible (courtesy of Bonnie J. Smith and Stephen A. Smith).

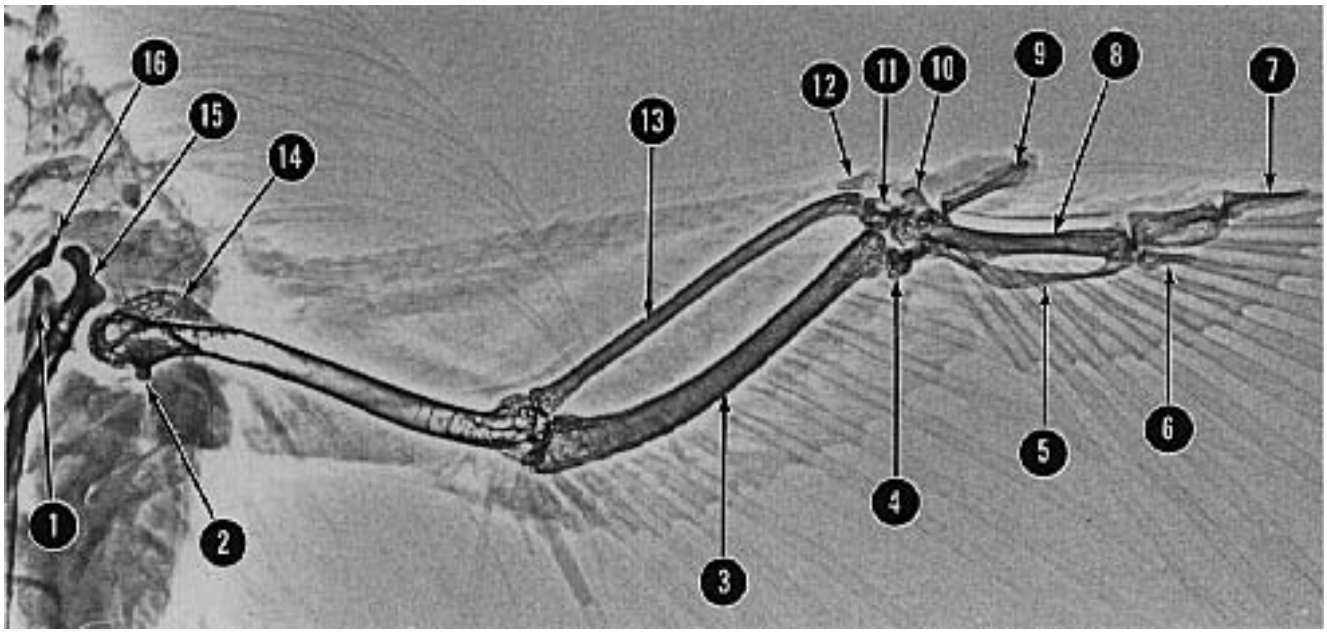

1) head of scapula
2) ventral tubercle of humerus
3) ulna
4) ulnar carpal bone
5) minor metacarpal bone
6) minor digit (consisting of one phalanx)
7) major digit (consisting of two phalanges)
8) major metacarpal bone
9) alular digit
10) extensor process of alular meta carpal bone
11) radial carpal bone
12) sesamoid bone in tendon of tensor propatagialis
13) radius
14) pectoral crest of humerus
15) shoulder extremity of coracoid bone
16) shoulder extremity of clavicle

FIG 12.30 Ventrodorsal xeroradiograph of the wing of a normal Bobwhite Quail (courtesy of Bonnie J. Smith and Stephen A. Smith).

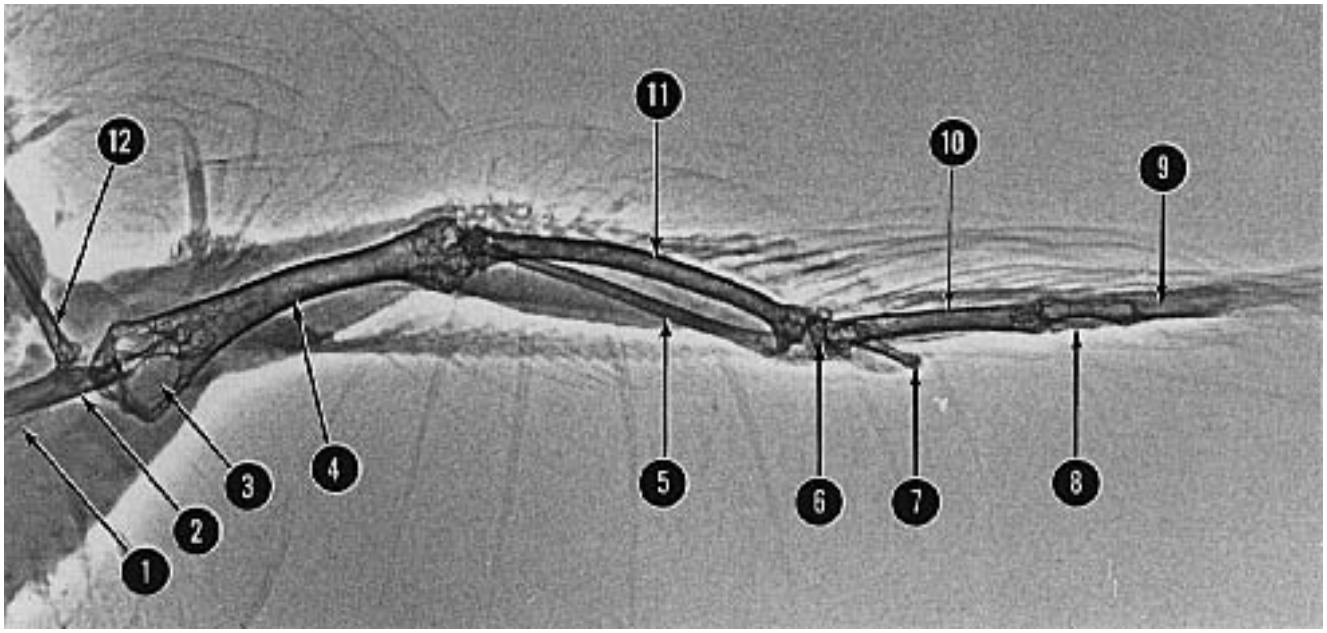

1) clavicle
2) shoulder extremity of coracoid bone
3) pneumatic foramen of humerus (point of entry of clavicular air sac)
4) humerus
5) radius
6) superimposed radial and ulnar carpal bones
7) alular digit
8) minor digit
9) distal phalanx of major digit
10) superimposed major and minor metacarpal bones
11) ulna
12) scapula

FIG 12.31 Craniocaudal xeroradiograph of the wing of a normal Bobwhite Quail (courtesy of Bonnie J. Smith and Stephen A. Smith).

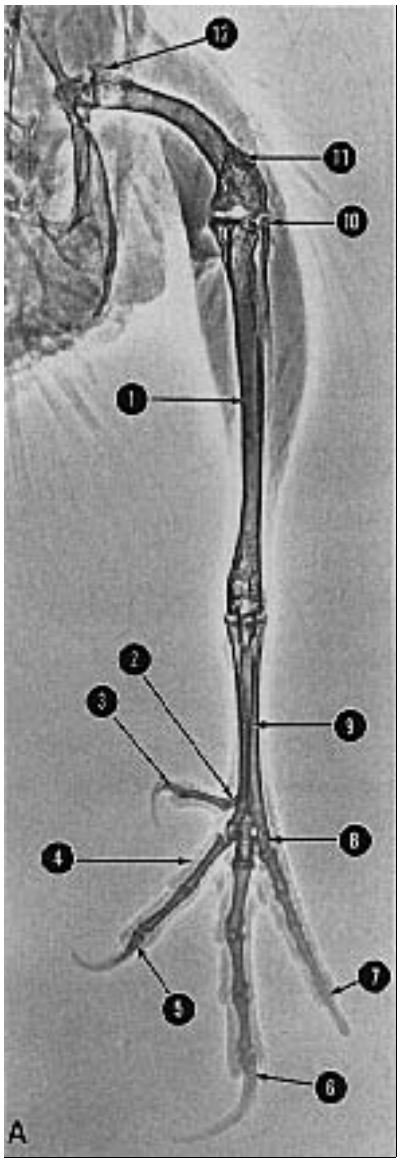

1) tibiotarsus
2) metatarsal bone I
3) distal phalanx of digit I
4) podotheca
5) distal phalanx of digit II
6) distal phalanx of digit III
7) distal phalanx of digit IV
8) tarsometatarsal trochlea for digit IV
9) tarsometatarsus
10) fibula
11) patella
12) greater trochanter of femur

FIG 12.32 Craniocaudal xeroradiograph of the pelvic limb of a normal Bobwhite Quail (courtesy of Bonnie J. Smith and Stephen A. Smith).

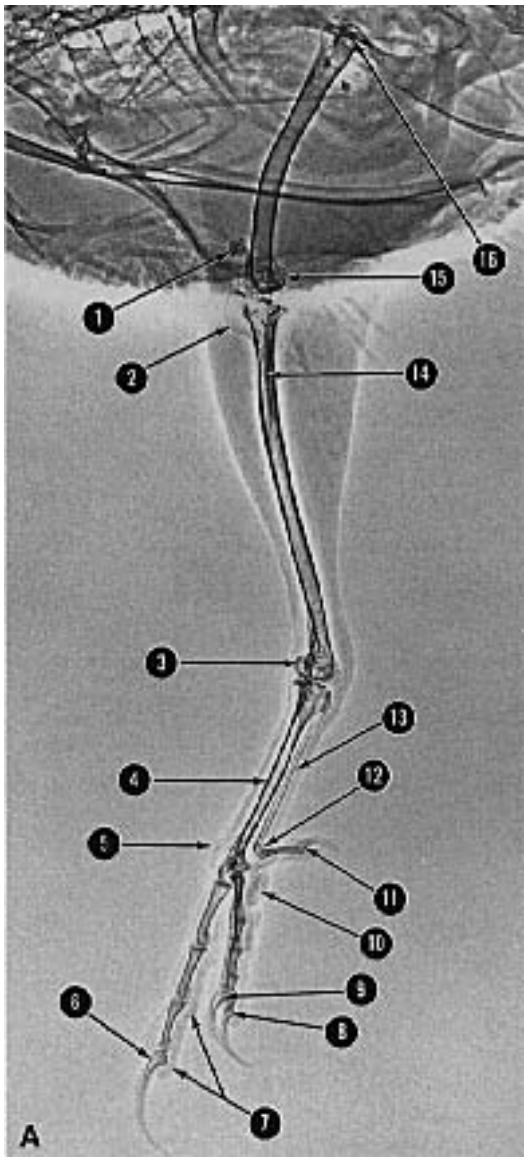

1) patella
2) cnemial crest of tibiotarsus
3) condyles of tibiotarsus
4) tarsometatarsus
5) podotheca
6) distal (fourth) phalanx of digit III (note horny nail covering bony core)
7) digital pads
8) distal (fifth) phalanx of digit IV
9) distal (third) phalanx of digit II
10) metatarsal pad
11) distal (second) phalanx of digit I
12) metatarsal bone I
13) mineralized tendons of digital flexor muscles
14) fibula, superimposed on body of tibiotarsus
15) condyles of femur
16) head of femur within acetabulum

FIG 12.33 Mediolateral xeroradiograph of the pelvic limb of a normal Bobwhite Quail (courtesy of Bonnie J. Smith and Stephen A. Smith).

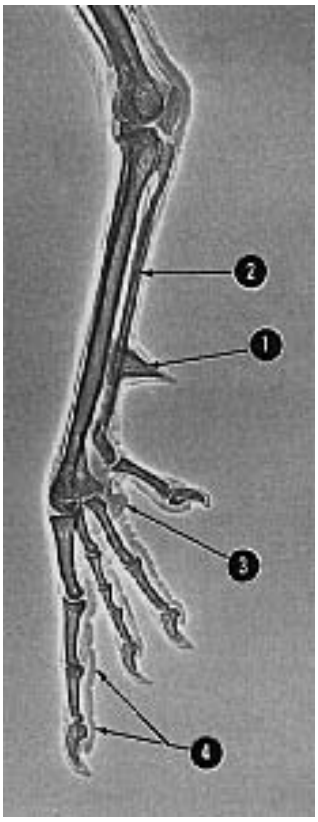

FIG 12.34 Mediolateral xeroradiograph of the pes of a peacock. 1) the calcarial process is the osseous core of the metatarsal spur or calcar. Note the horny sheath covering the process. 2) Note also the mineralization of the digital flexor tendons as well as the 3) well-developed metatarsal and 4) digital pads in this ground-dwelling bird (courtesy of Bonnie J. Smith and Stephen A. Smith).

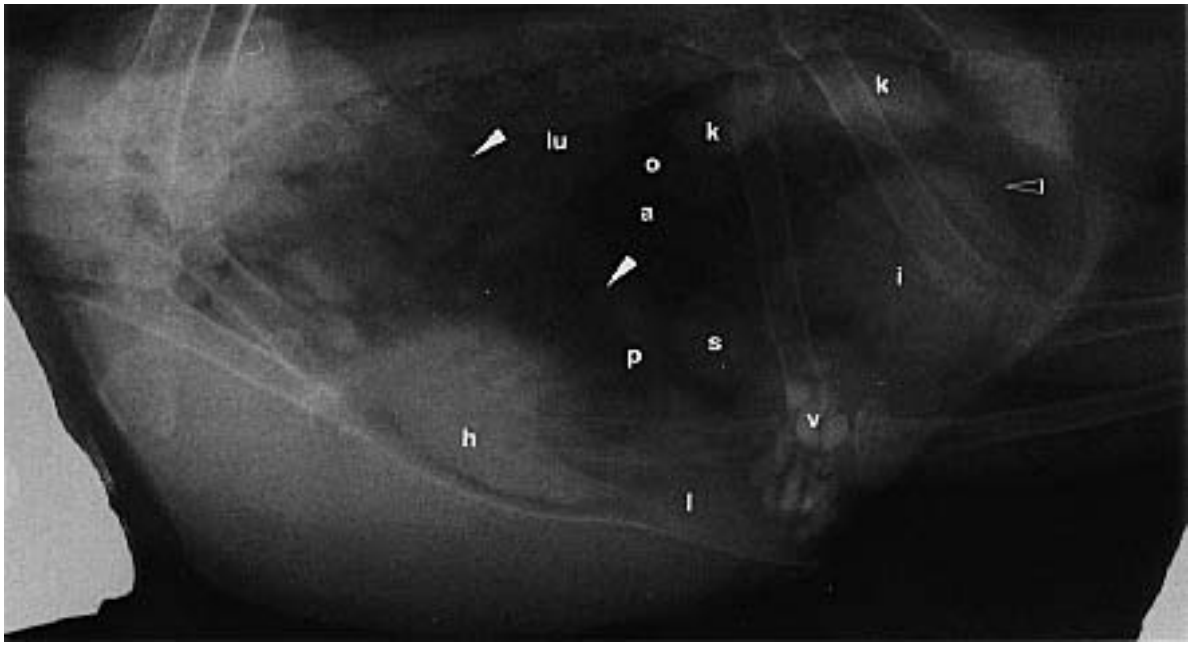

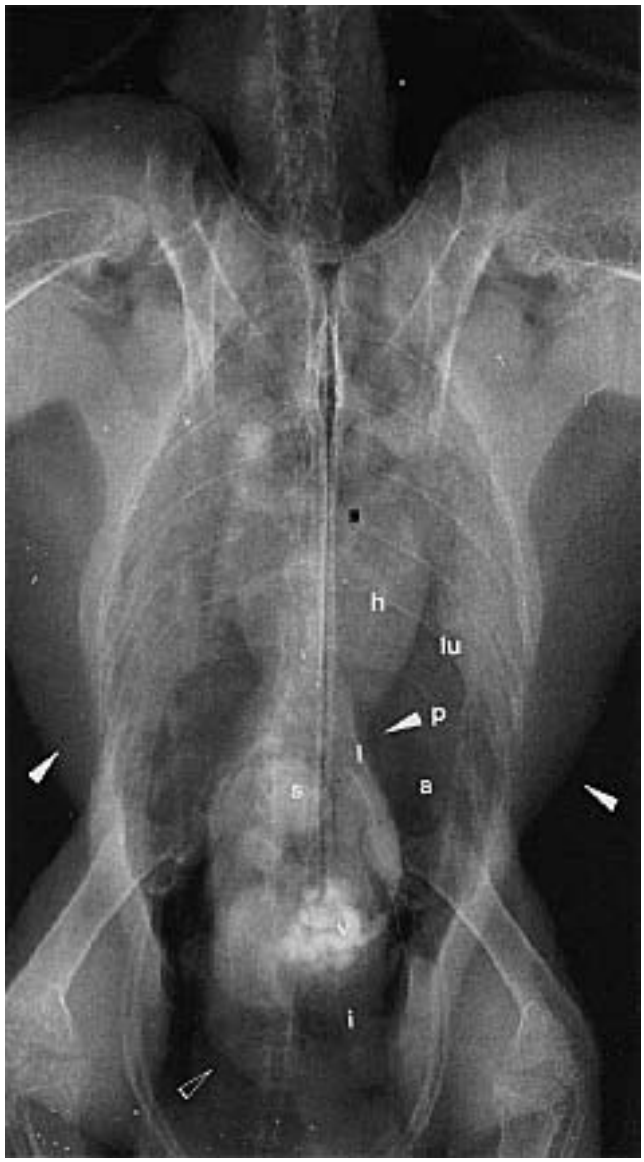

FIG 12.35 Low contrast radiographs of a Hyacinth Macaw demonstrating soft tissue structures: heart (h), spleen (s), liver (l), lung (lu), kidneys (k), proventriculus (p), ventriculus (v), ovary (o), intestines (i), contiguous area of the caudal thoracic and abdominal air sacs (a), body musculature (arrow) and right abdominal air sac (open arrow) (courtesy of Marjorie McMillan).

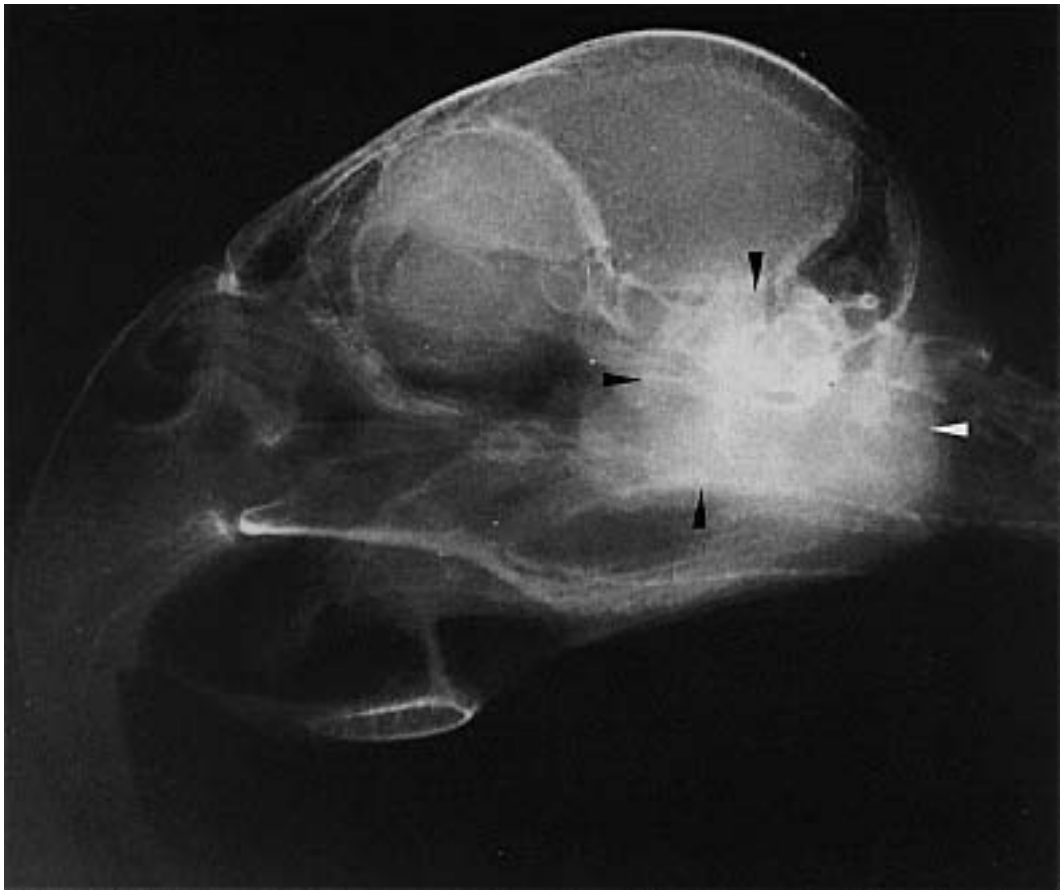

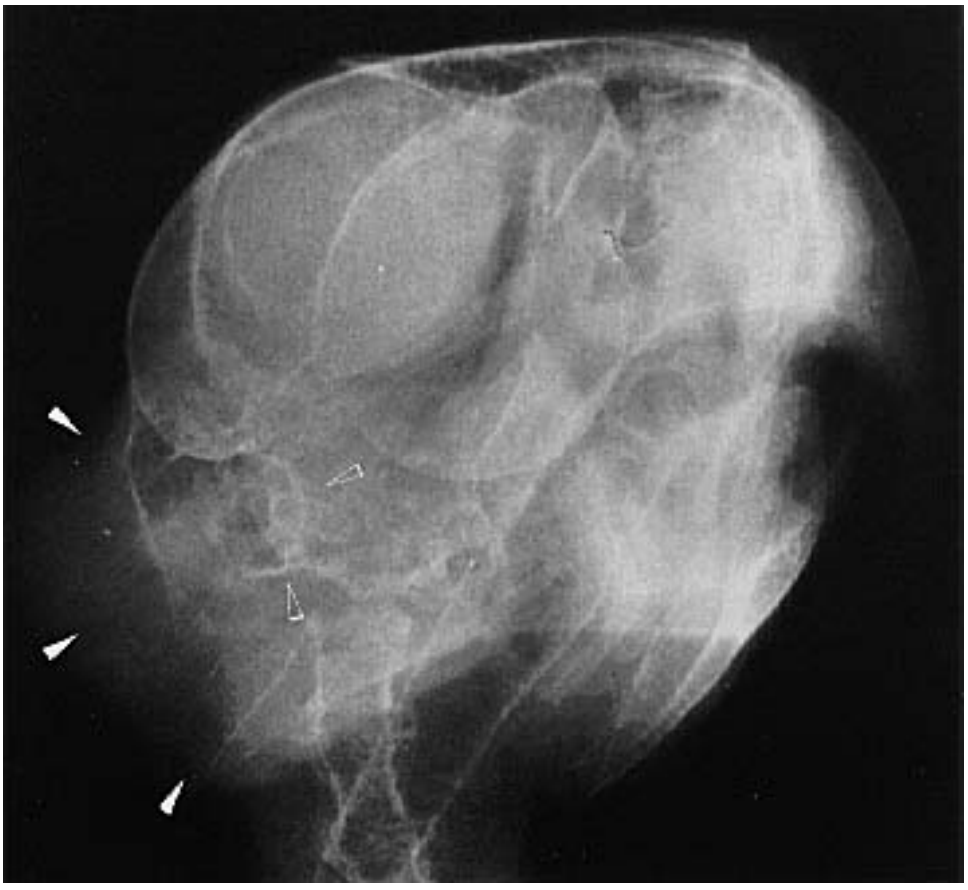

FIG 12.36 A six-year-old Amazon parrot was presented with firm bilateral swelling surrounding the auditory meatus (arrows). The masses were solid and attached. **a)** Surgical biopsy of the mass indicated chronic fibrosing cellulitis. **b)** The mass is easily visualized on an oblique view of the head (arrows). The tympanic area can also be visualized (open arrows). The masses resolved when the bird was changed from an all-seed to a formulated diet.

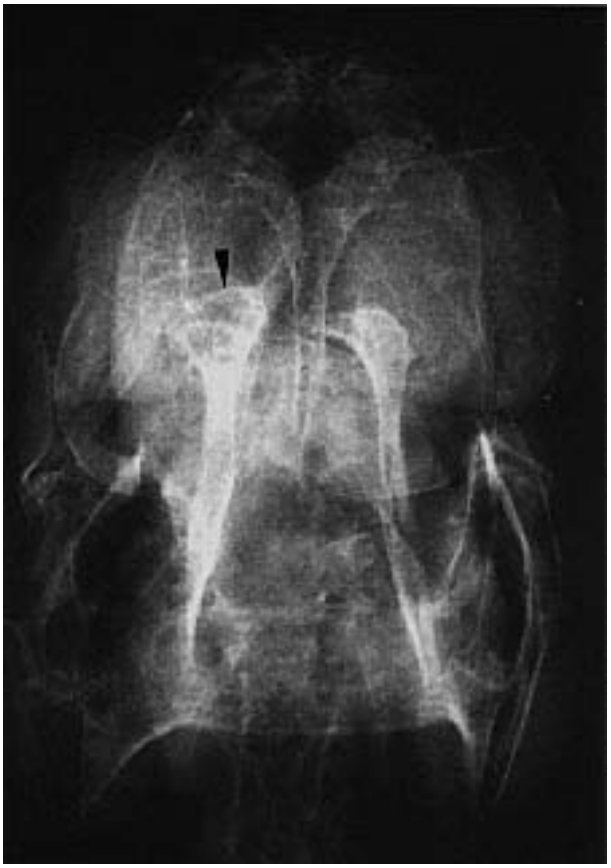

FIG 12.37 Alexandrian Parakeet with lateral deviation of the maxillae. The deformity had been present since hatching. The parents of this bird produced a defective neonate every four to six chicks, suggesting that the problem was genetic in origin. Rostrocaudal radiograph showing dorsal displacement of the right palatine bone (arrow). Ventrodorsal radiograph showing lysis of the right palatine bone (arrow).

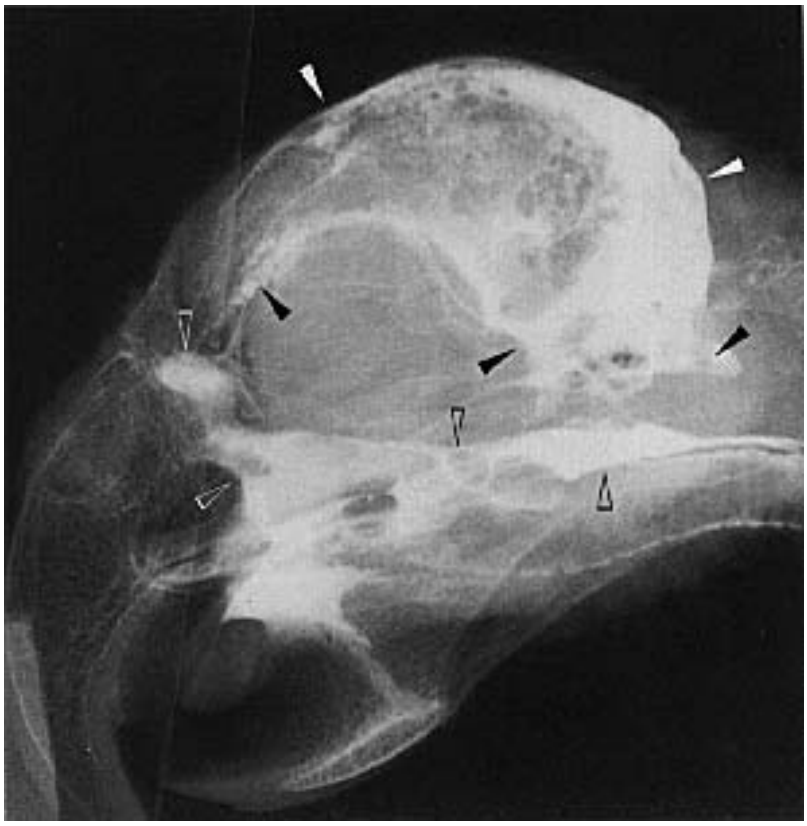

FIG 12.38 Lateral positive contrast air sacculography demonstrating the extent of the cephalic air sac in a mature Blue-fronted Amazon Parrot. The cephalic portion (arrow) of the cervicocephalic air sac connects to the caudal aspect of the infraorbital sinus (open arrow) (courtesy of Marjorie McMillan).

FIG 12.39 Lateral view of a rhinogram performed on a normal Bare-eyed Cockatoo showing the flow of contrast medium from the nasal cavity (open arrows) through the choanae at the level of the palate and into the nasopharynx and oral cavity (open arrow). Other structures include the mandible (m), zygomatic arch (z), ceratobranchial bone of hyoid (c) and tracheal tube (t) (courtesy of Elizabeth Watson).

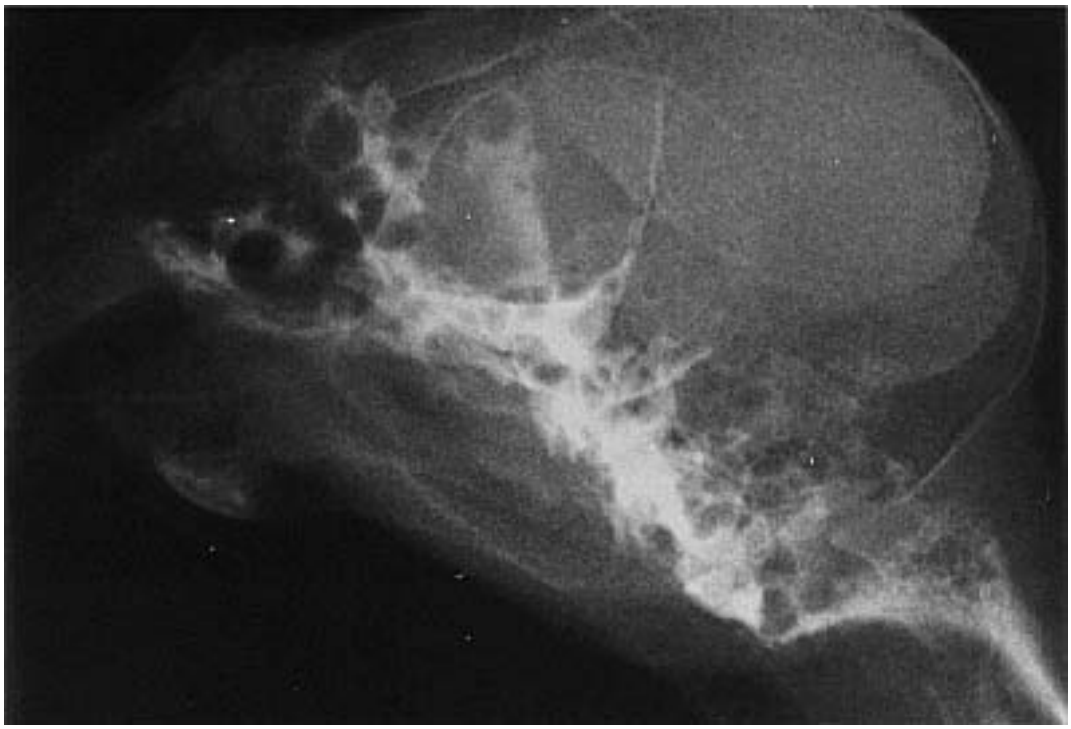

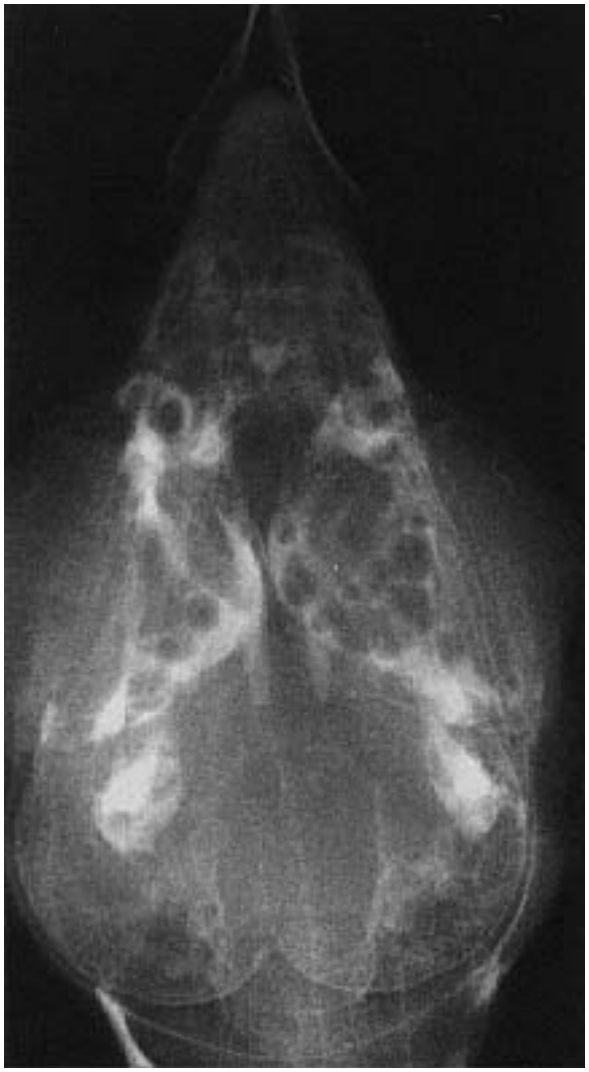

FIG 12.40 Positive contrast sinography in an adult cockatiel showing drainage and interconnections of the infraorbital sinuses (courtesy of Marjorie McMillan).

FIG 12.41 Positive contrast sinography in a mynah bird showing minimal drainage of contrast medium in comparison to Psittaciformes. Additionally, there is not communication between the infraorbital sinuses, and contrast medium injected into the right infraorbital sinus remains localized (courtesy of Marjorie McMillan).

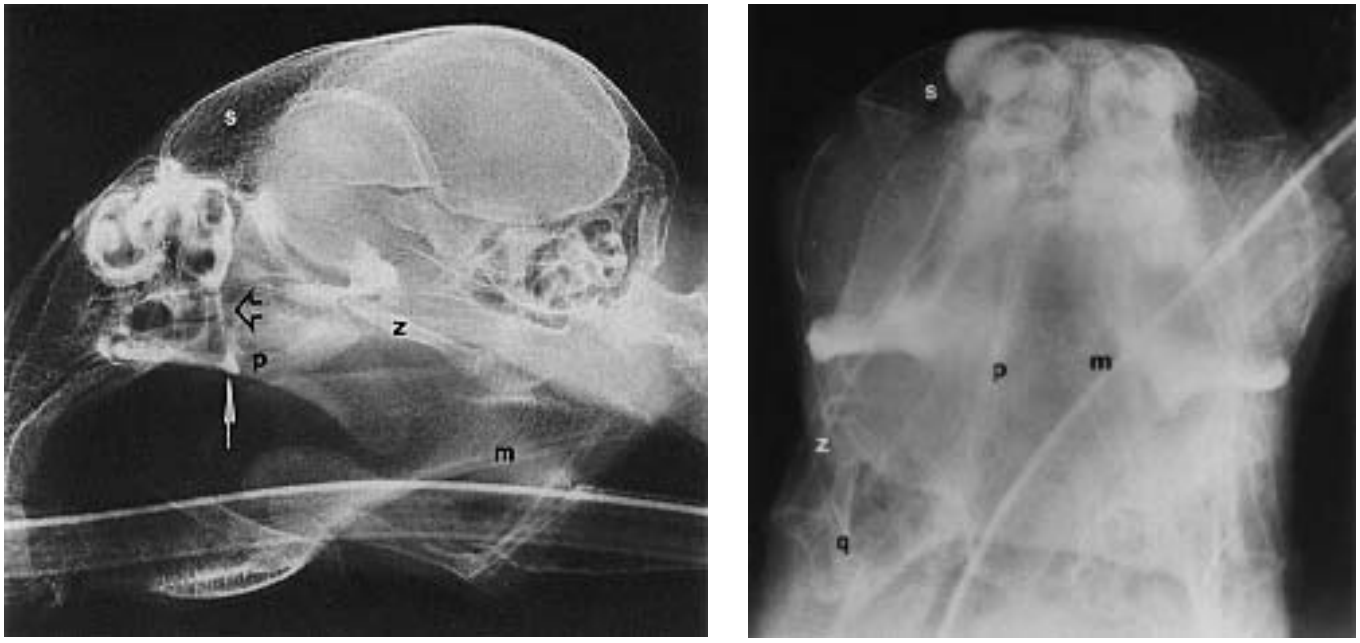

FIG 12.42 A four-month-old African Grey Parrot was presented with a life-long history of persistent serous to mucopurulent nasal discharge. Antibiotic therapy would change the discharge from mucopurulent to serous but would not resolve the problem. On physical examination, it was noted that fluid introduced into the nostrils would not exit through the oral cavity. Lateral view of rhinogram indicating that contrast medium moved ventrally through the nasal cavity (open arrow) and stopped abruptly at the level of the palate (closed arrow). Endoscopy indicated a persistent membrane covering the choana. Rostrocaudal radiograph following infusion of contrast medium into the right nostril showing communication between the infraorbital sinuses. Note that the contrast medium does not properly pass into the oral cavity in this bird. Other structures of interest include the palatine bone (p), zygomatic arch (z), mandible (m), quadrate (q) and the periorbital diverticulum of the infraorbital sinus (s) (courtesy of Elizabeth Watson).

FIG 12.43 A four-year-old Umbrella Cockatoo was presented with a long history of bilateral oculonasal discharge. Fluid flushed into the nostrils failed to enter the oropharynx. A lateral rhinogram indicated that contrast medium moved through the nasal cavity (open arrows) and stopped abruptly at the level of the palatine (closed arrows) (courtesy of Elizabeth Watson).

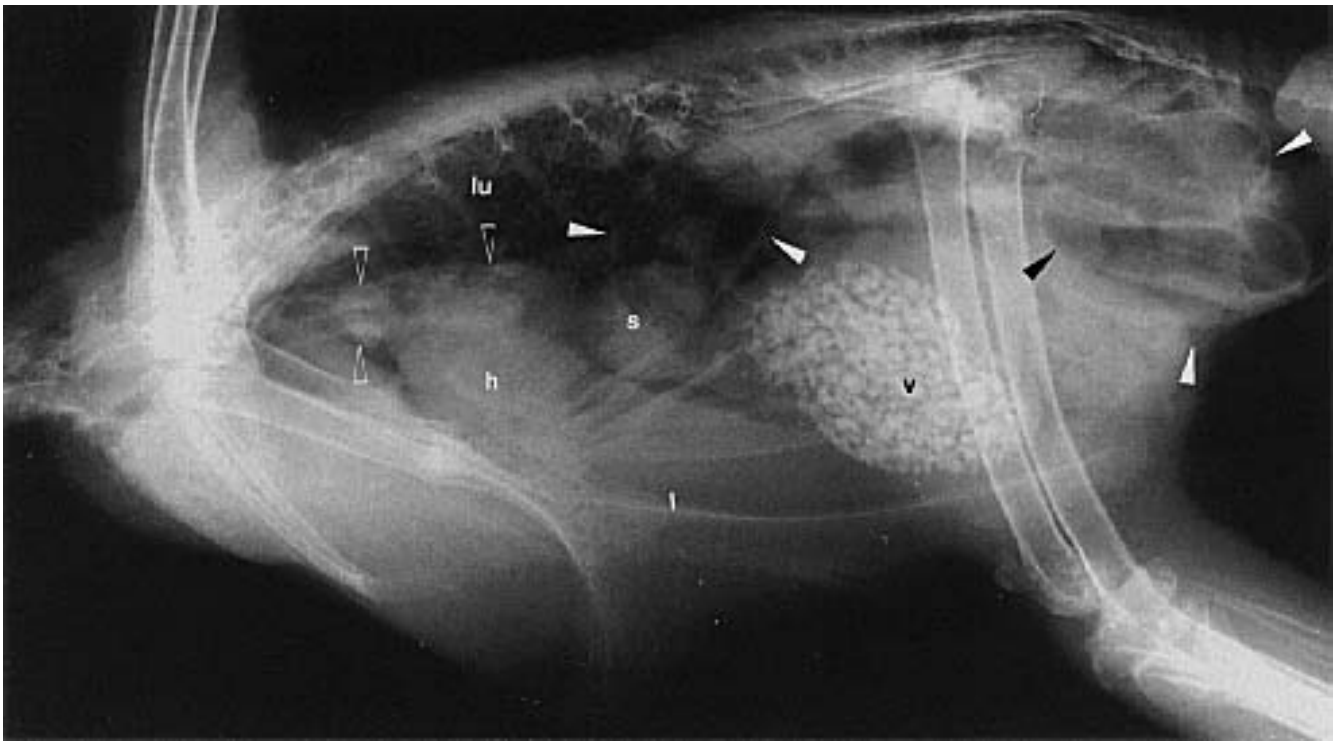

FIG 12.44 An adult male Satyr Tragopan Pheasant was presented with an acute onset of dyspnea and depression. Abnormal clinicopathologic findings include PCV=23, SGOT=490, LDH=671. Radiographs indicate gaseous distension of the gastrointestinal tract (arrows) causing cranial displacement of other abdominal organs. Increased densities were noted in the syringeal area (open arrows), and the spleen (s) was enlarged. The bird did not respond to supportive care. Necropsy findings included pericarditis and granulomatous pneumonia and tracheitis. Heart (h), liver (l), lung (lu), ventriculus containing grit (v).

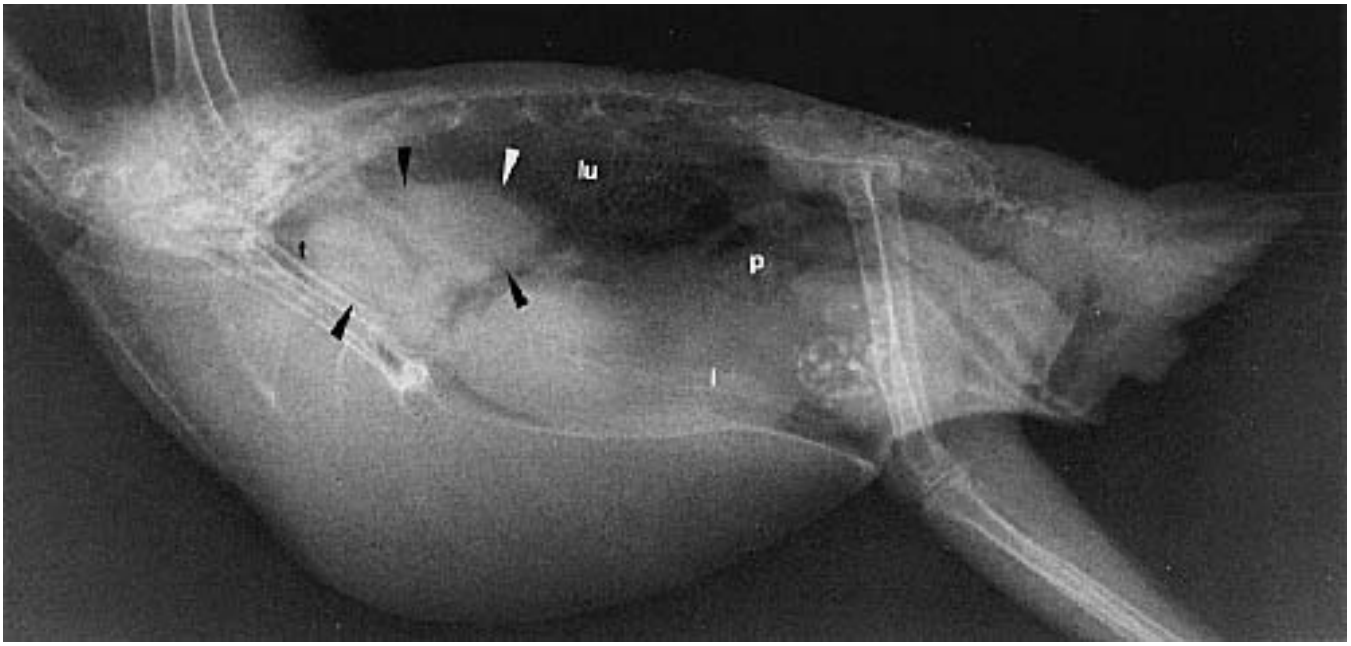

FIG 12.45 A two-year-old male cockatiel was presented for evaluation of a voice change and progressive dyspnea. A lateral radiograph showed a large, lobular, soft-tissue mass surrounding the distal trachea (arrows) that extended into the lung (lu) and displaced the trachea (t) ventrally. The liver (l) is also enlarged and is displacing the gas-filled proventriculus (p) dorsally. The histologic diagnosis was thyroid adenocarcinoma (courtesy of Marjorie McMillan).

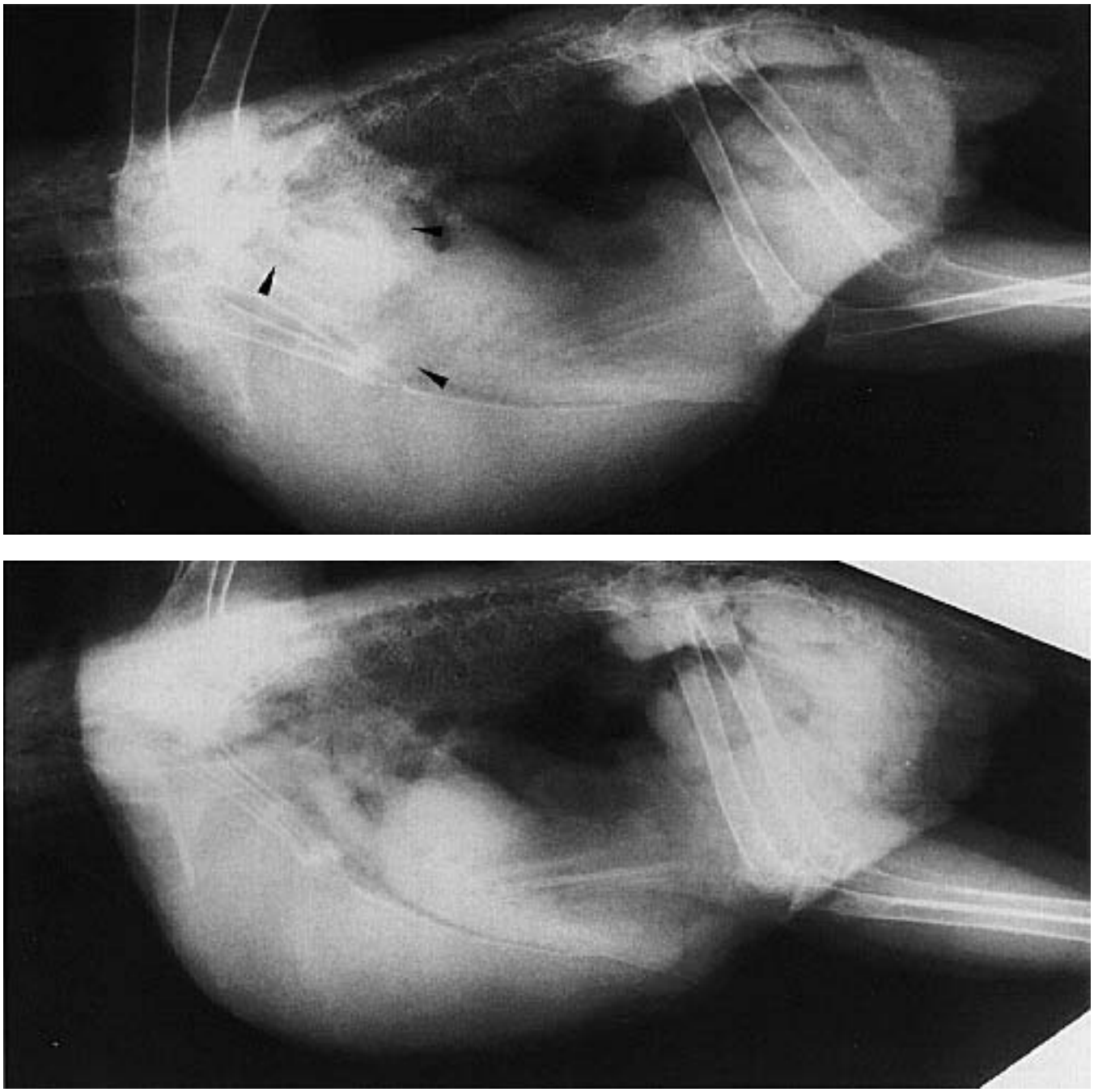

FIG 12.46 A Red-lored Amazon Parrot was presented with coughing and a voice change. Initial radiographs showed a large, soft-tissue mass (arrows) ventral to the trachea and syrinx. Radiograph taken 11 months after treatment with antifungal agents demonstrates resolution of the mass (courtesy of Marjorie McMillan).

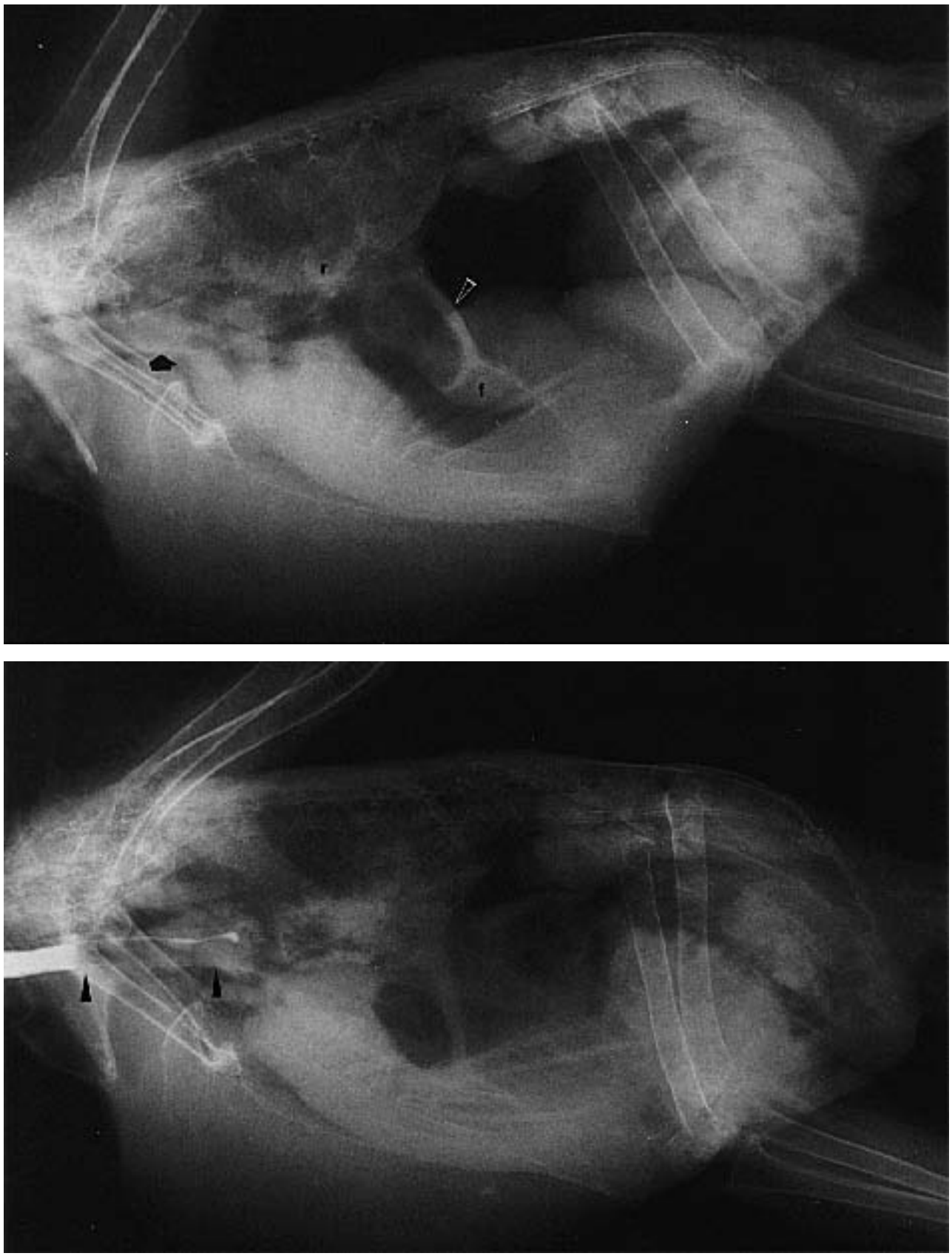

FIG 12.47 **a)** Lateral radiograph of a mature Blue-fronted Amazon with dyspnea. Abnormal findings included increased parabronchial densities (ring shadows -r), hyperinflation of the air sacs and thickening of the contiguous wall of the cranial and caudal thoracic air sacs (open arrow). The ventral separation of the contiguous wall of these air sacs forms a distinguishable fork (f) with the cranial thoracic air sac coursing cranially and the caudal thoracic air sac coursing caudoventrally. An increased soft tissue density in the trachea suggests a mass (arrow). **b)** Positive contrast study of the trachea using an oil-based contrast medium. The medium is passing dorsally across an intratracheal mass (arrows) (courtesy of Marjorie McMillan).

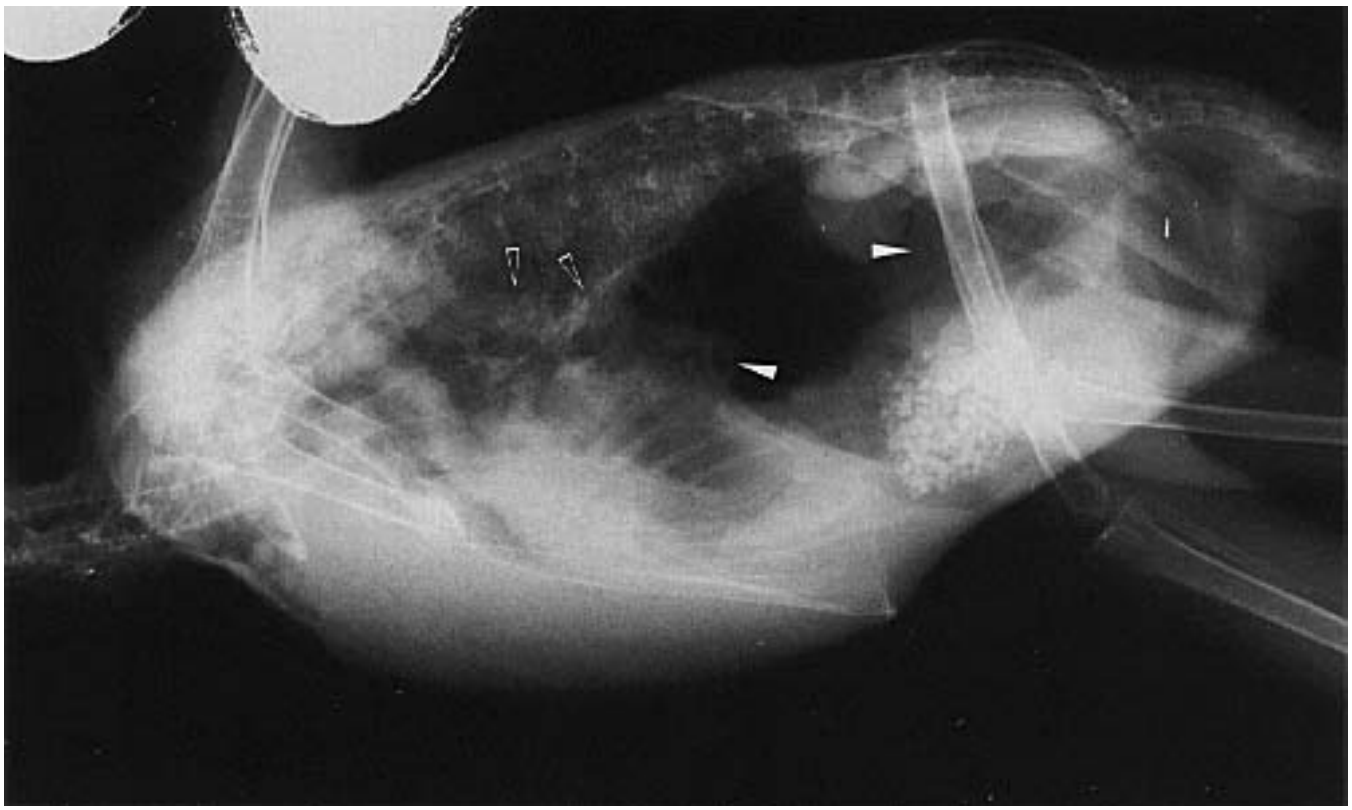

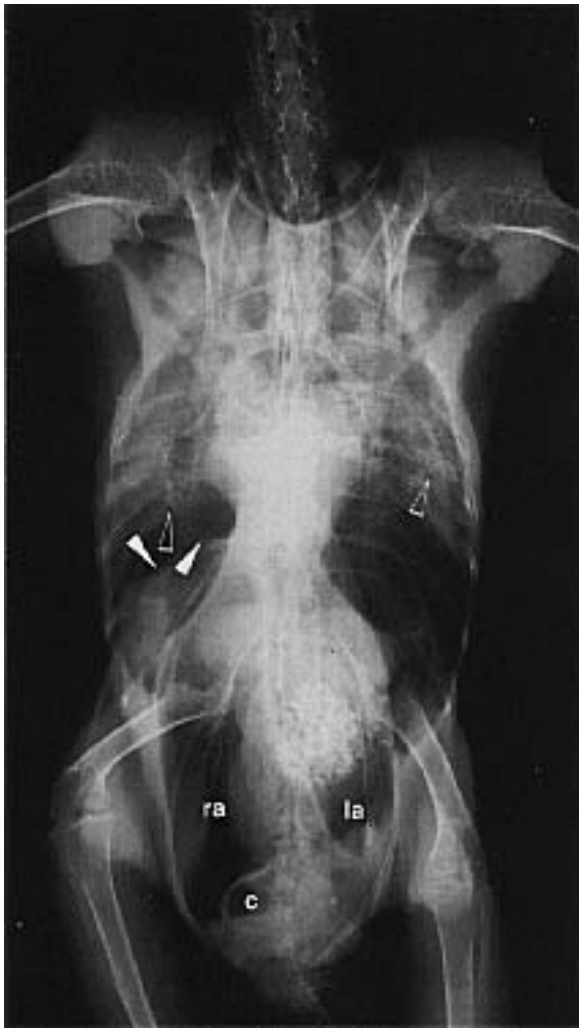

FIG 12.48 An adult Blue-crowned Amazon Parrot was presented with nasal discharge and dyspnea. The increased parabronchial densities (open arrows) in the mid and caudal portions of the lung are suggestive of pneumonia. Several thickened air sac walls are visible (arrows). The intestines (i) are filled with gas secondary to aerophagia caused by severe dyspnea. The right abdominal (ra) and left abdominal (la) air sac areas are clearly visible. The cloacal wall (c) is also evident.

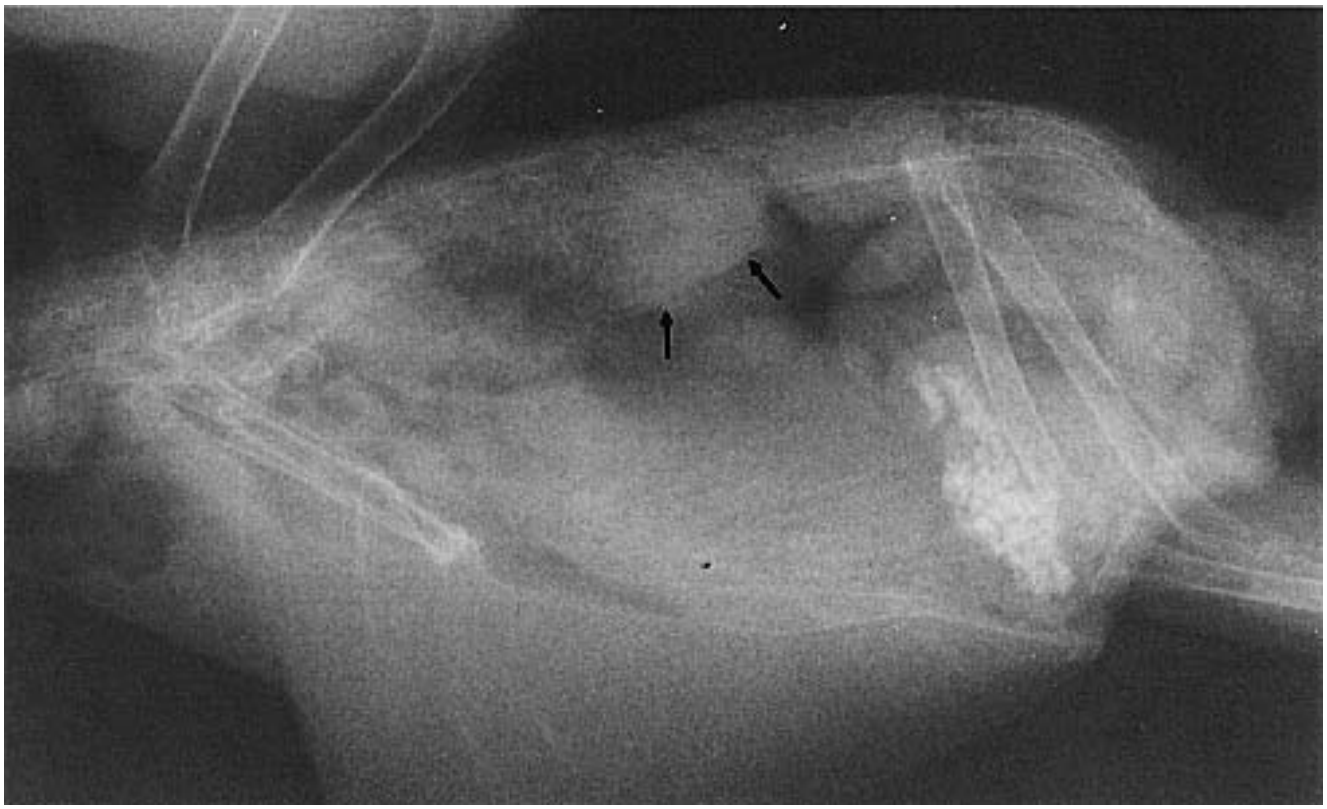

FIG 12.49 A four-year-old lovebird with a round cell carcinoma of the wing and secondary metastasis to the lung (arrows) (courtesy of Marjorie McMillan).

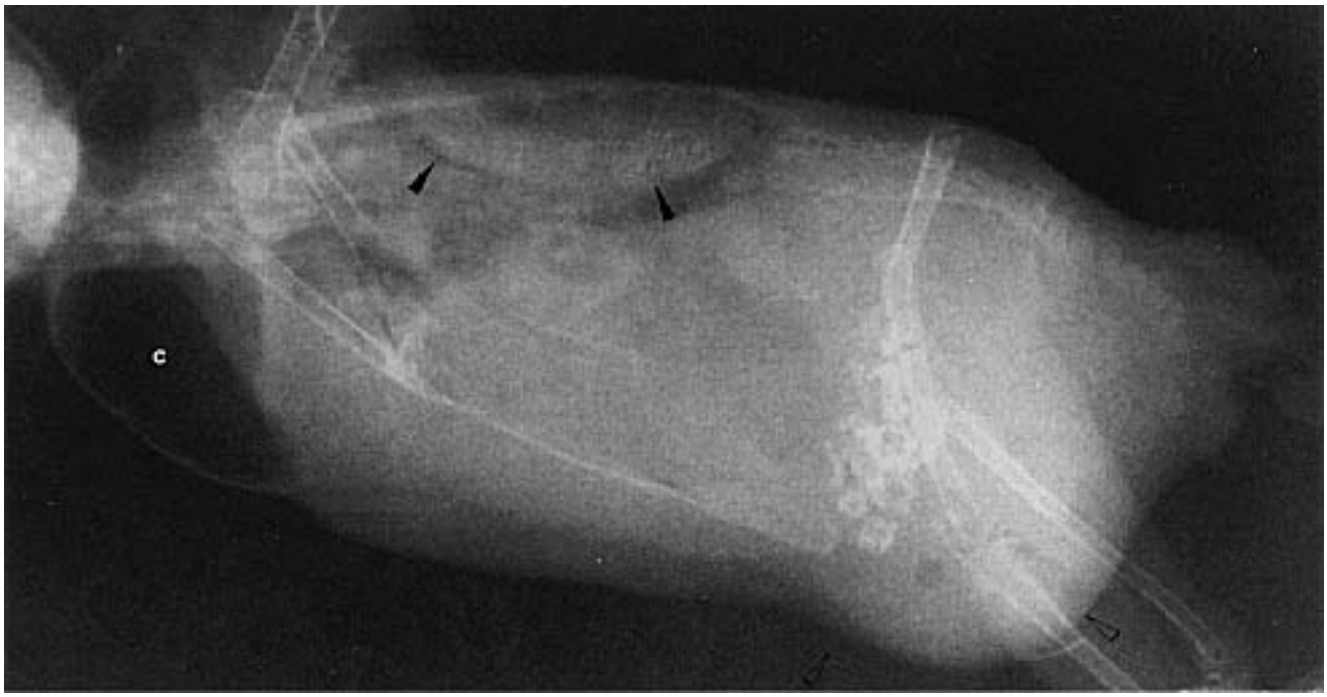

FIG 12.50 A five-year-old male budgerigar was presented for lethargy and dyspnea. Lateral radiographs indicate an air-filled crop (c) secondary to aerophagia. There is a uniform increase in the parabronchial pattern (arrows) and obliteration of the abdominal air sac space due to bulging of the abdominal wall (open arrow). The homogenous appearance of the abdomen is due to a combination of effusion and a mass. The pulmonary pattern is consistent with edema, which responded to diuretic therapy (courtesy of Marjorie McMillan).

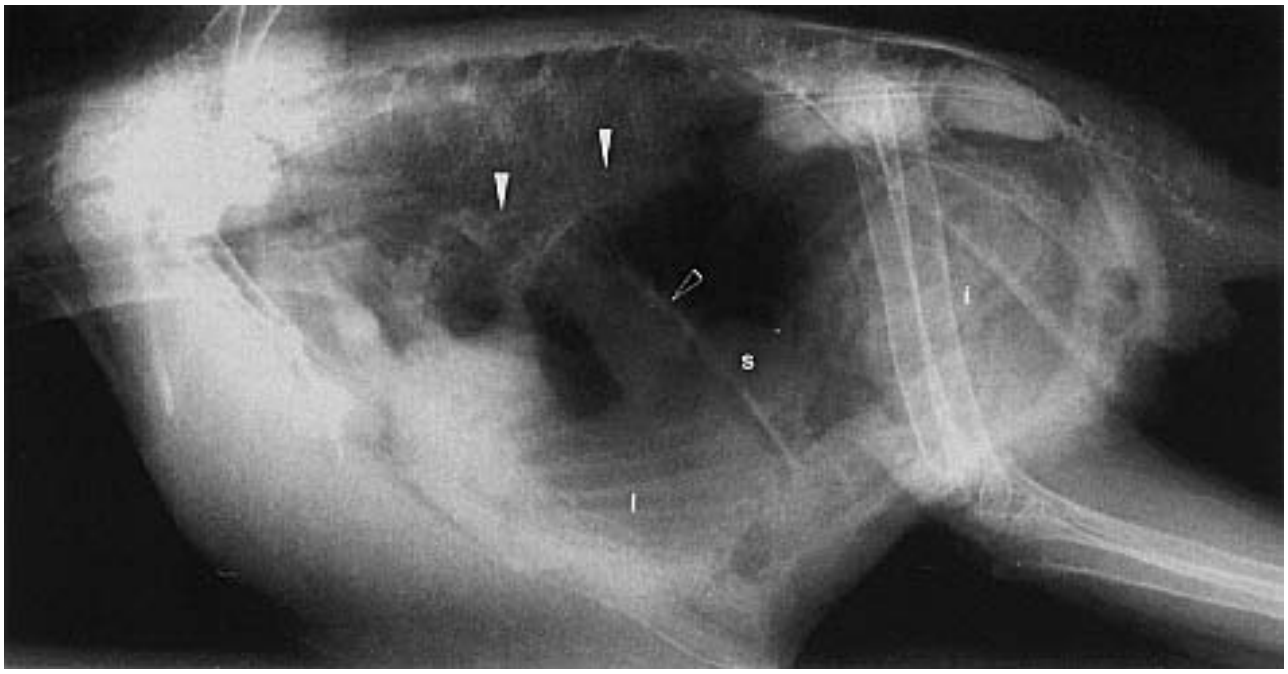

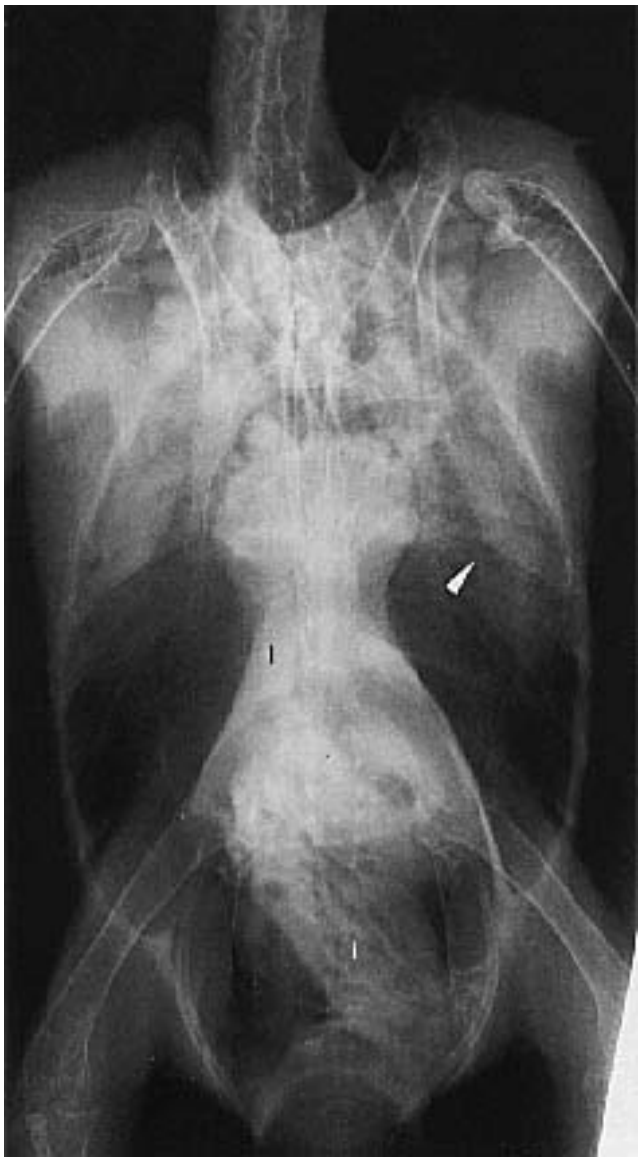

FIG 12.51 A four-month-old Double Yellow-headed Amazon Parrot was presented with a bilateral, purulent nasal discharge and dyspnea. Radiographs indicated parabronchial ring shadows (arrow) consistent with pneumonia. Hyperinflation of the thoracic and abdominal air sacs and thickening of the air sac membranes are characteristic of air sacculitis (open arrows). Note the barrel shape of the body in the VD radiograph indicative of dyspnea. Cultures from the trachea were positive for *Klebsiella* sp., and the bird responded to antibiotics. Liver (l), intestines (i) and spleen (s).

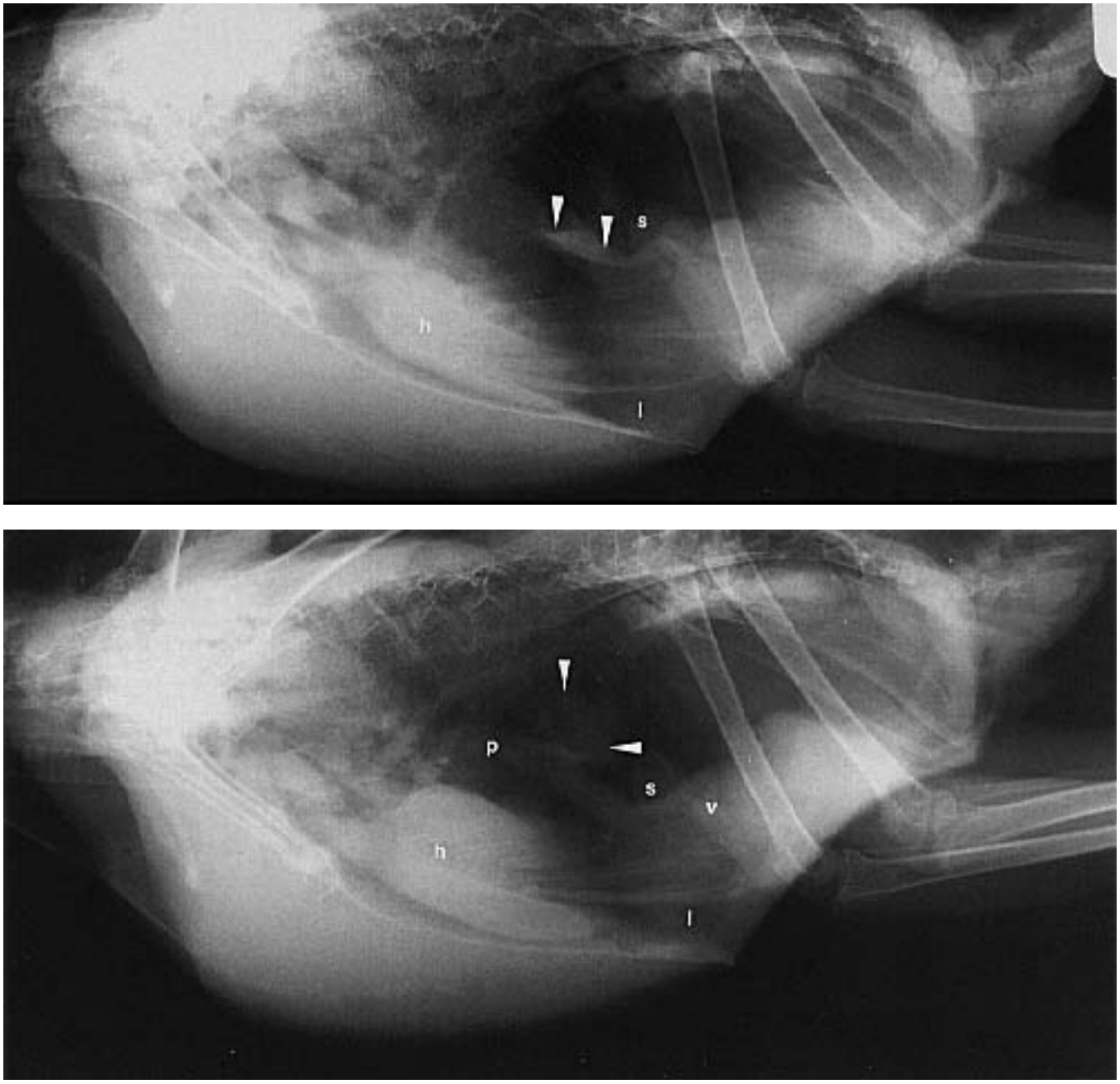

FIG 12.52 A ten-year-old Green-winged Macaw was presented with exercise intolerance. Initial radiographs (top) indicated thickening or edema of the air sacs. Radiographs one month after the initiation of antibiotic therapy indicate a decrease in the soft tissue opacity of the air sacs. However, the presence of residual thickening (arrow) would warrant continuation of therapy. Spleen (s), proventriculus (p), ventriculus (v), heart (h), liver (l) (courtesy of Marjorie McMillan).

FIG 12.53 An African Grey Parrot with a soft tissue opacity in the left cranial and caudal thoracic air sacs (courtesy of Marjorie McMillan).

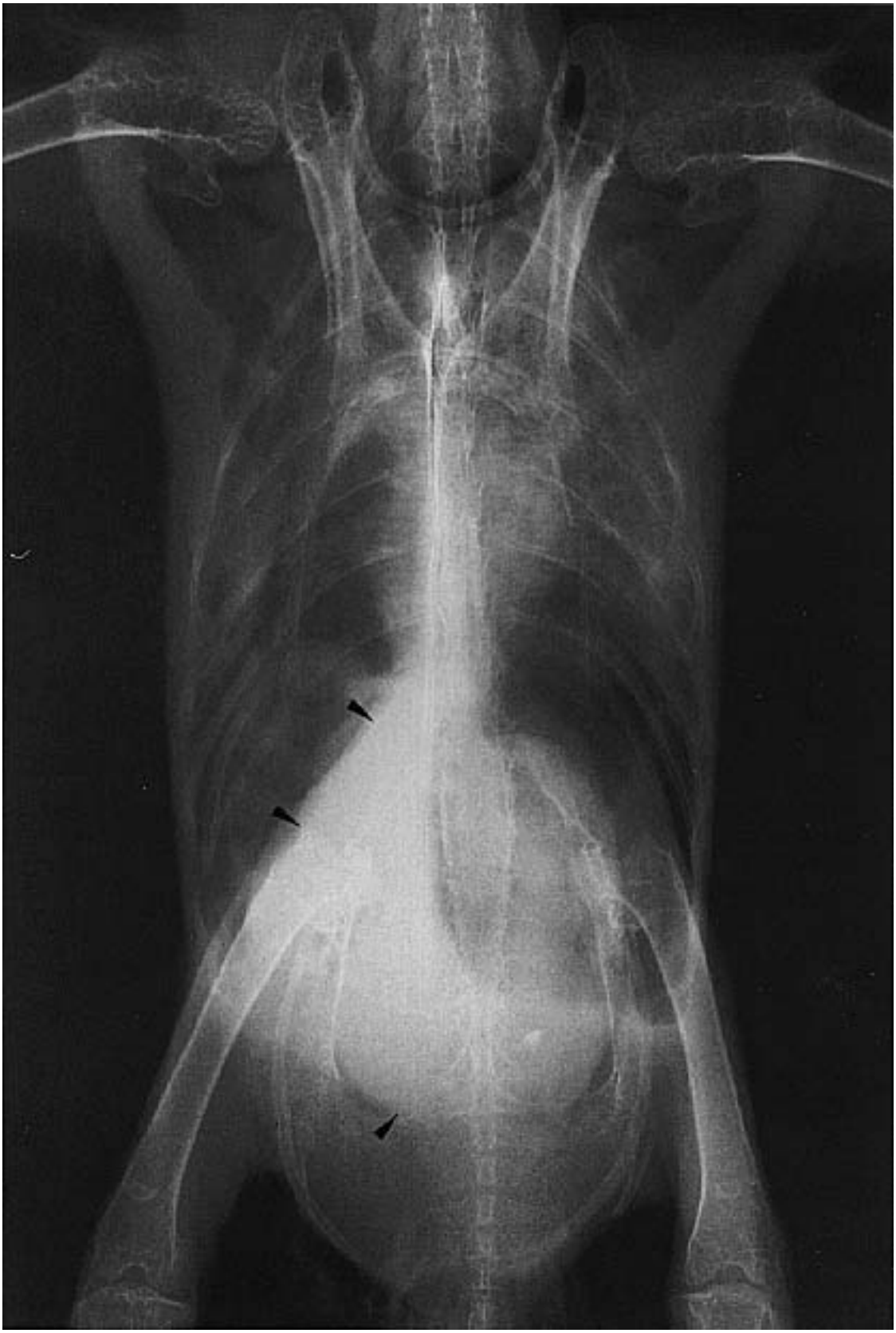

FIG 12.54 A Blue-fronted Amazon Parrot with a soft tissue plaque in the right abdominal air sac (arrows) (courtesy of Marjorie McMillan).

FIG 12.55 Excretory urogram in an African Grey Parrot. The radiographs were taken 30 seconds after the injection of contrast medium. The kidneys (open arrows) and ureters (arrows) are opacified. Note the rim of air that is normally present dorsal to the kidneys (courtesy of ME Krautwald).

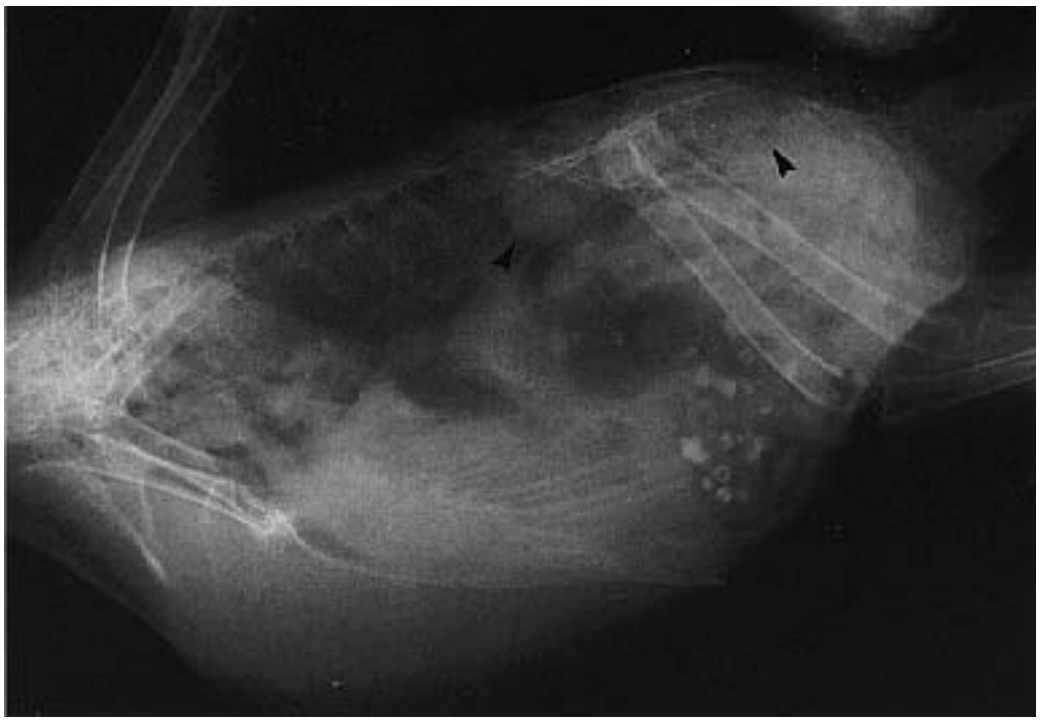

FIG 12.56 A Blue-crowned Amazon Parrot with nephromegaly (arrows). The diminished serosal detail in the coelomic cavity was caused by hemorrhage from the diseased kidney. The pathologic diagnosis was glomerulonephropathy, infarction and arteritis (courtesy of Marjorie McMillan).

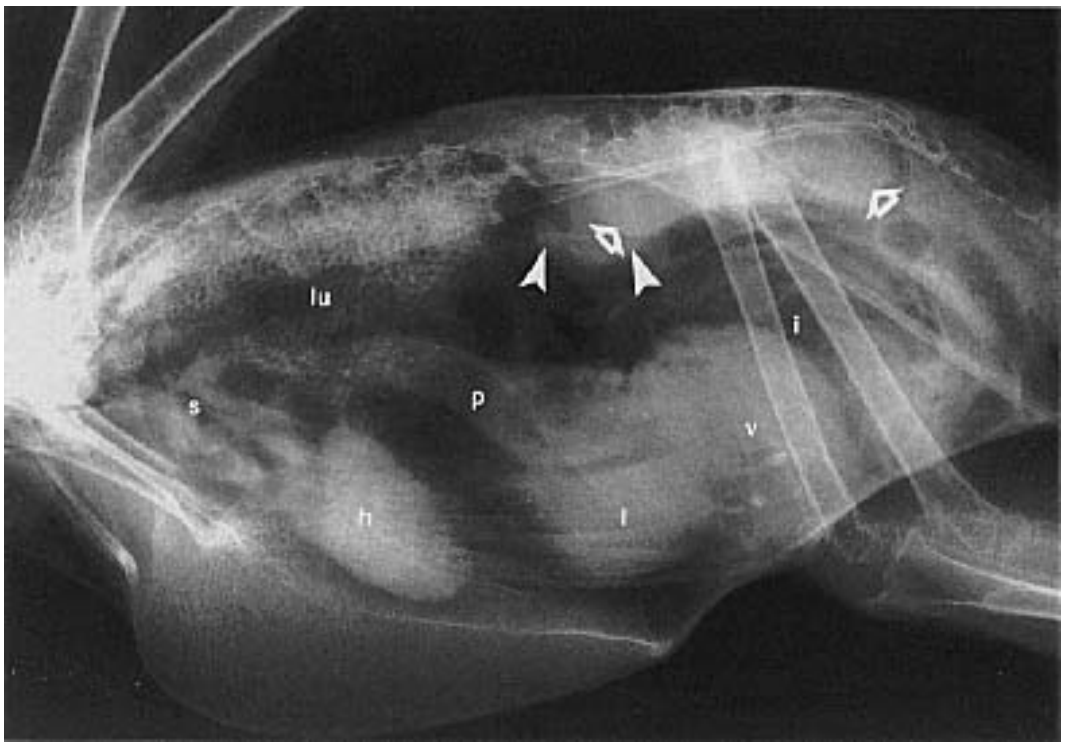

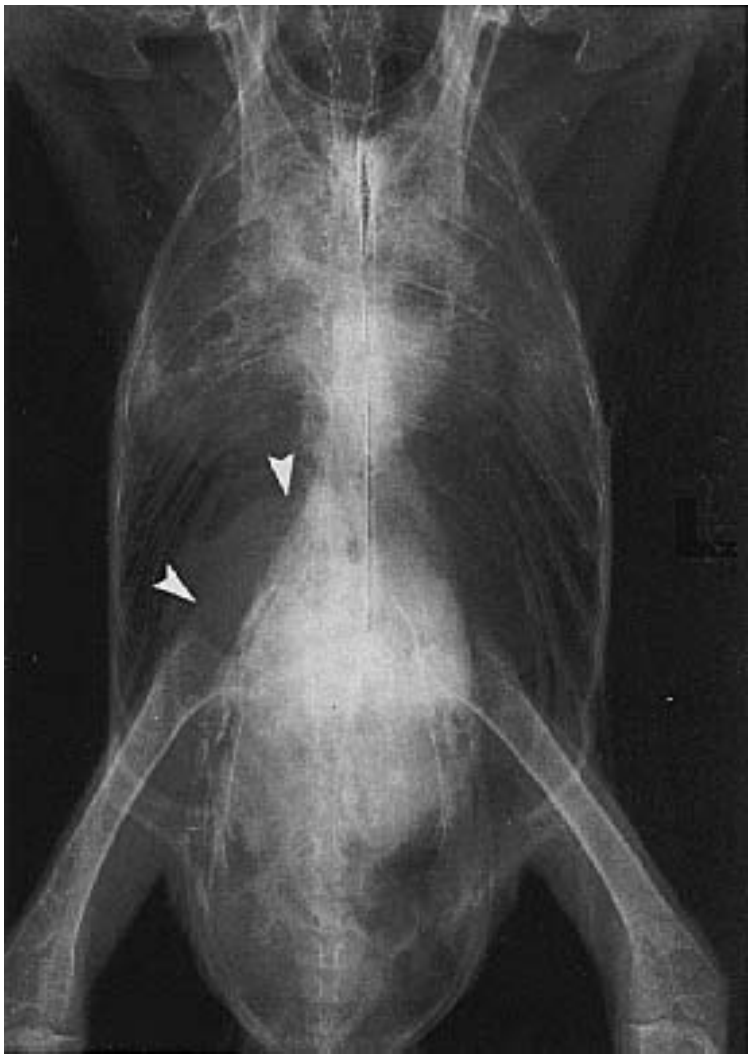

FIG 12.57 Sulphur-crested Cockatoo with nephromegaly (open arrows) and a perirenal granuloma (arrow) caused by aspergillosis. The severe air sac distension is causing the liver (l) to appear reduced in size. Other structures that are easy to identify include the heart (h), syrinx (s), lung (lu), proventriculus (p), ventriculus (v) and intestines (i) (courtesy of Marjorie McMillan).

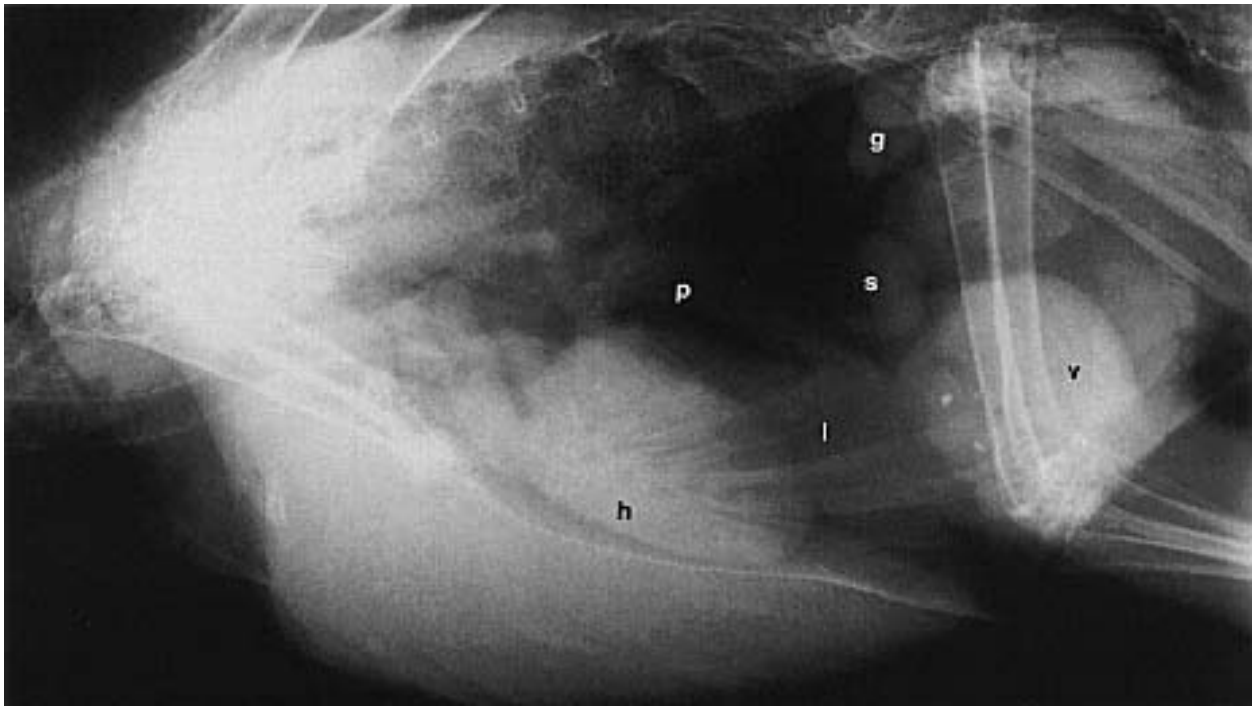

FIG 12.58 A two-year-old Blue and Gold Macaw was presented with anorexia and mild dyspnea. Increased lung sounds were noted by auscultation. Radiographs indicated microhepatia and splenomegaly. It is common for the liver to be smaller than expected in macaws and some larger cockatoos. The importance of a small liver in these birds has not been defined. Heart (h), liver (l), spleen (s), syrinx (s), proventriculus (p), ventriculus (v), gonad (g).

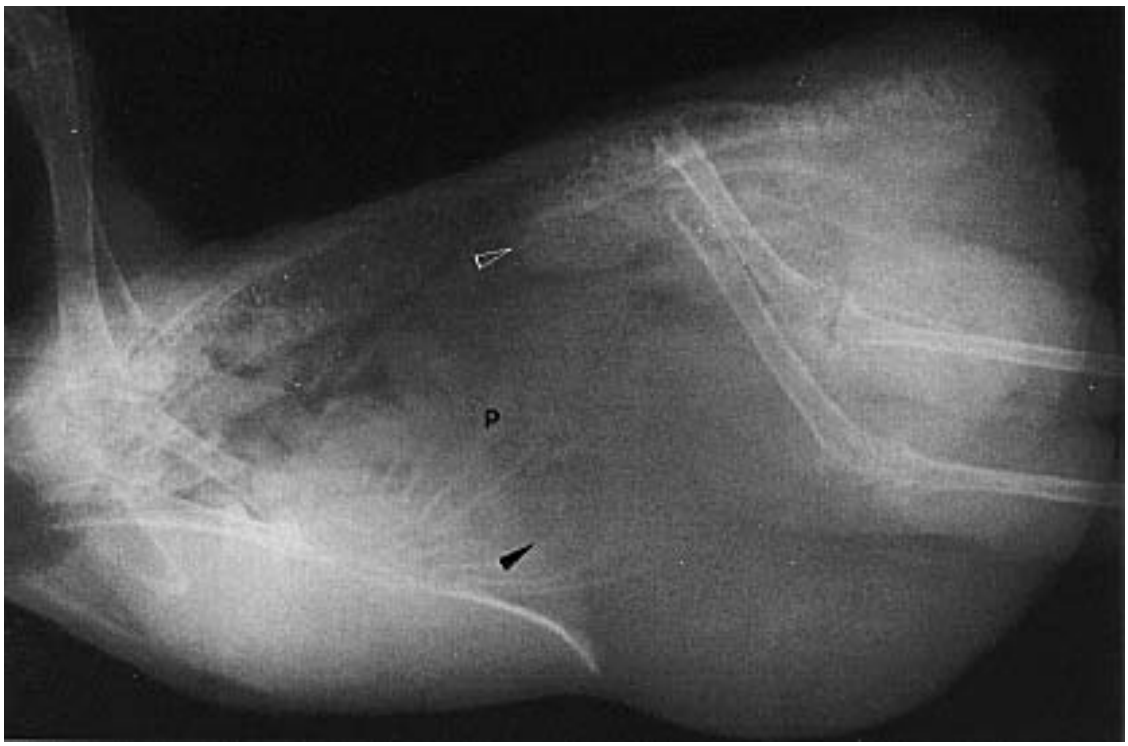

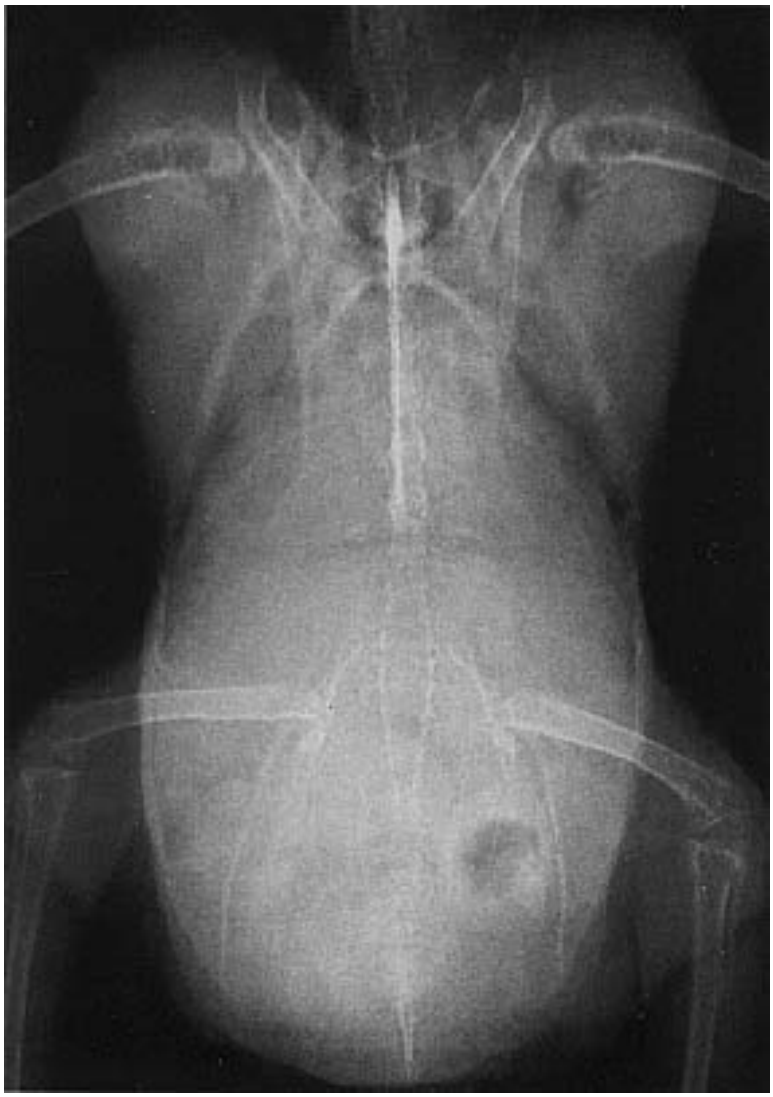

FIG 12.59 An eight-week-old Sulphur-crested Cockatoo with nephromegaly (open arrows) and massive hepatomegaly (arrows) caused by lipidosis. Note that the normal air sac triangle above the proventriculus is obliterated and the proventriculus (partially gas-filled) is being displaced cranially (courtesy of Marjorie McMillan).

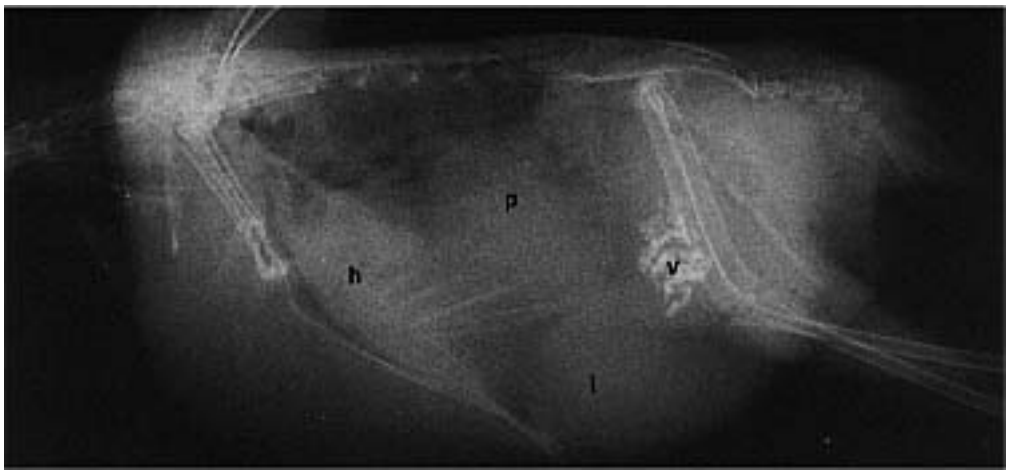

FIG 12.60 An adult male cockatiel was presented with weakness, a distended abdomen and harsh, moist respiratory sounds. Radiographs indicated massive hepatomegaly (l) with cranial displacement of the heart (h), dorsal displacement of the proventriculus (p) and caudodorsal displacement of the ventriculus (v). A mild diffuse parabronchial pattern secondary to edema was also present. Histopathology indicated severe, chronic active hepatitis and cirrhosis (courtesy of Marjorie McMillan).

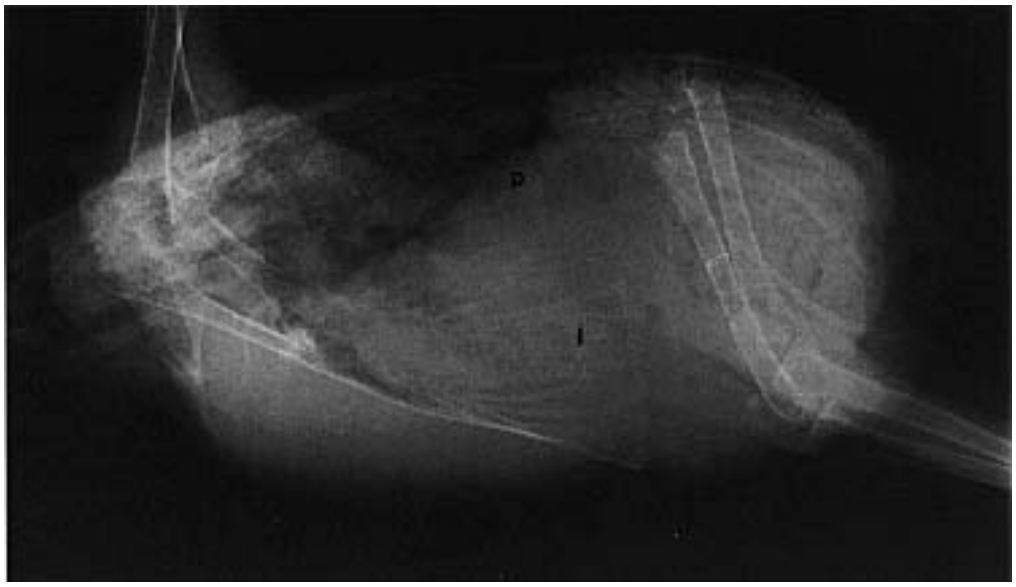

FIG 12.61 A ten-week-old Blue-fronted Amazon Parrot with a palpable abdominal mass was presented for anorexia and lethargy. Abnormal clinicopathologic findings included WBC=20,000 (4% bands), AST=12,420, LDH=8,000. Radiographs indicated hepatomegaly (l) with dorsal displacement of the proventriculus (p). Ultrasound confirmed the liver enlargement. *Chlamydia* sp. was detected in the bird's excrement using an antigen capture ELISA, and the bird responded to therapy with doxycycline.

FIG 12.62 A two-year-old Blue and Gold Macaw was presented with lethargy, anorexia and abdominal distension. Radiographs indicated a massive splenomegaly (arrow) and nephromegaly (curved arrow) caused by *Chlamydia* sp. The enlarged spleen is displacing the proventriculus (p) and ventriculus (v) ventrally and the liver (l) cranially (courtesy of Marjorie McMillan, reprinted with permission of Comp Cont Ed 8:1986).

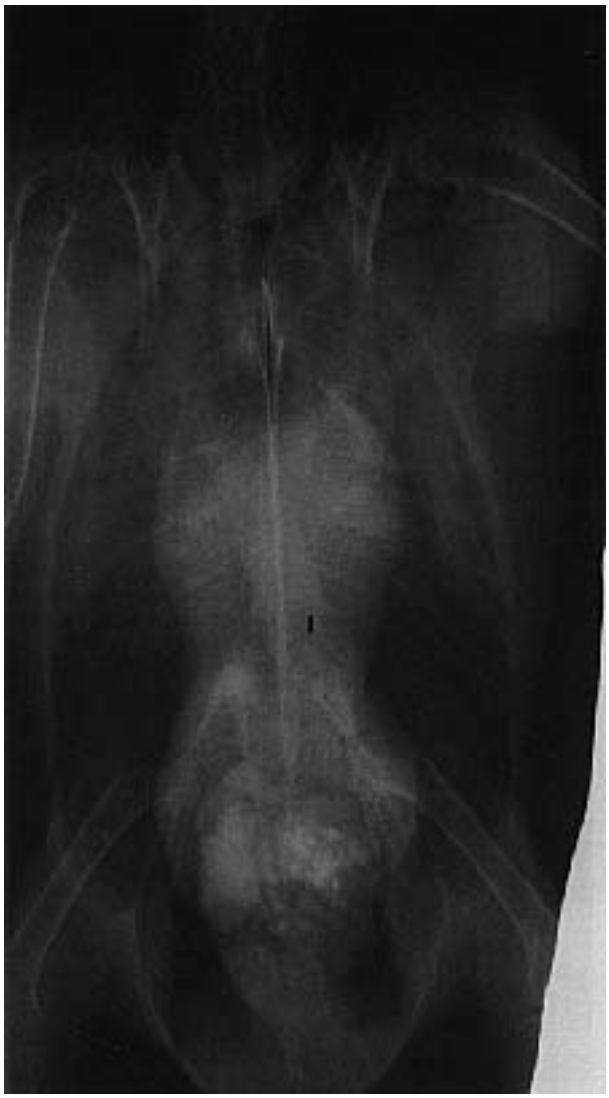

FIG 12.63 A Blue-fronted Amazon Parrot was presented with lethargy and exercise intolerance, intermittent episodes of panting and syncope. VD radiographs indicated a biatrial enlargement and a decrease in the cardiohepatic waist caused by cardiomegaly. Liver (l) (courtesy of Marjorie McMillan).

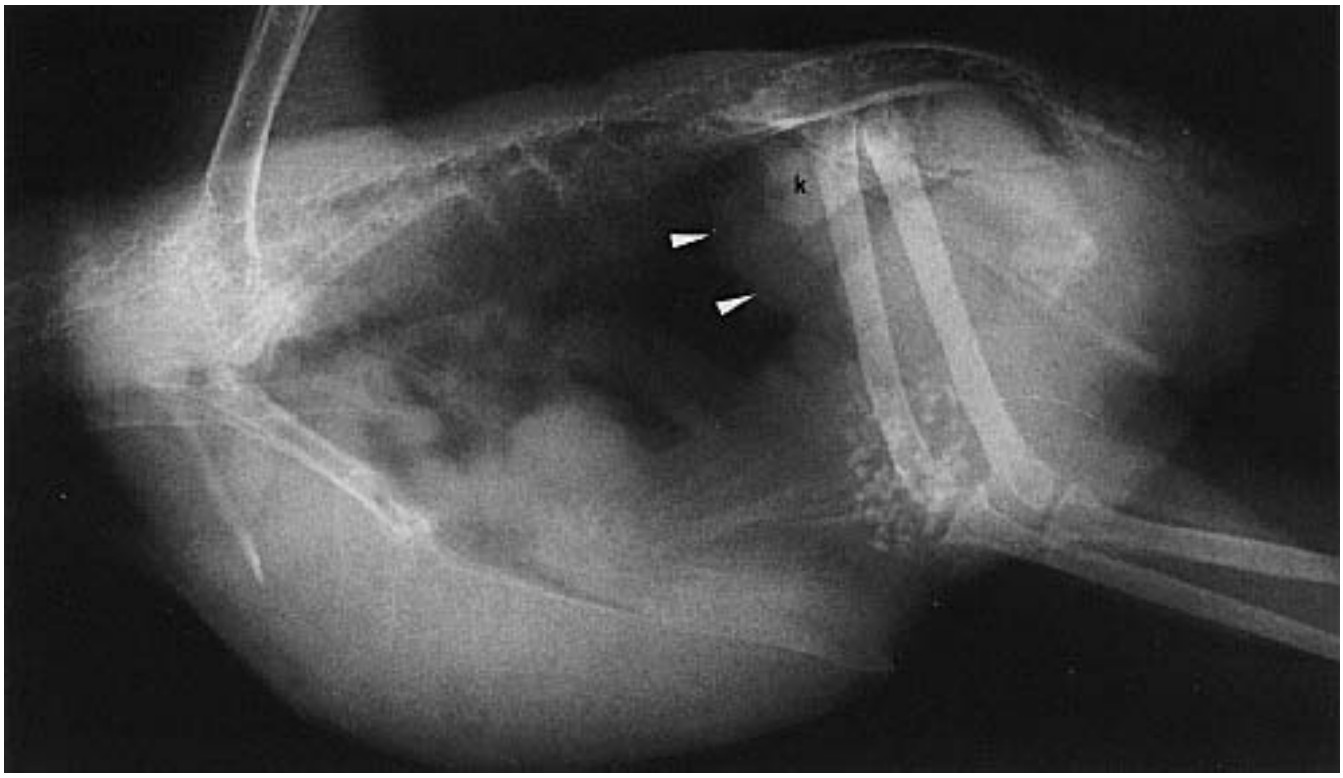

FIG 12.64 Lateral radiograph of a Double Yellow-headed Amazon Parrot with an active ovary (arrow). Note the "grape-like" cluster of follicles cranioventral to the kidneys (k) (courtesy of Marjorie McMillan).

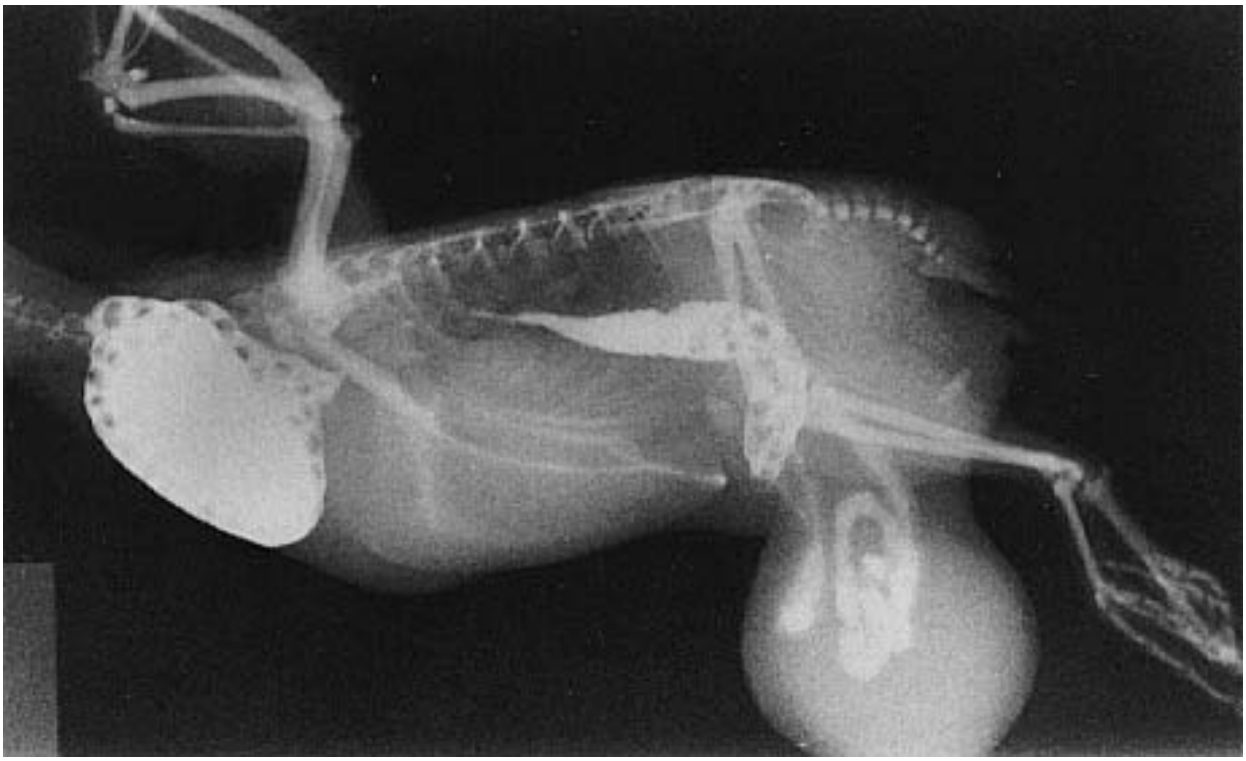

FIG 12.65 A female budgerigar was presented for evaluation of a ventral abdominal mass. A barium contrast study indicated that the mass was herniated intestines. Note also the increased density of the skeleton (polyostotic hyperostosis). Herniation and polyostotic hyperostosis are characteristic of hyperestrogenism (courtesy of Marjorie McMillan).

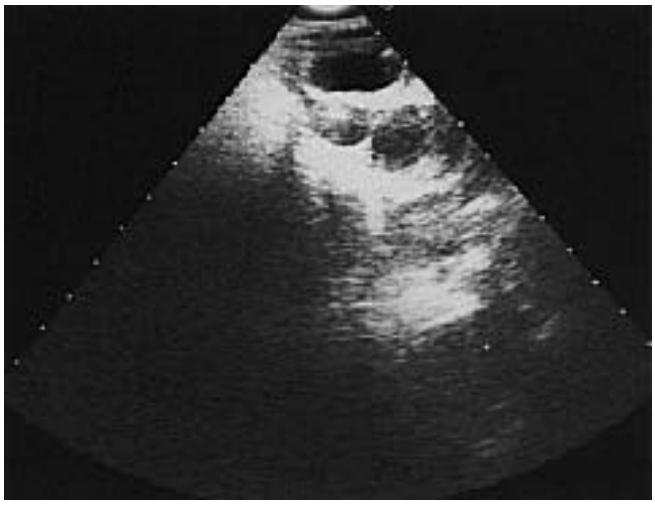

FIG 12.66 Radiographs of an egg-bound cockatiel suggest the presence of one large abnormally shaped egg and one smaller incompletely formed egg. Ultrasound indicated the presence of four eggs (courtesy of Marjorie McMillan).

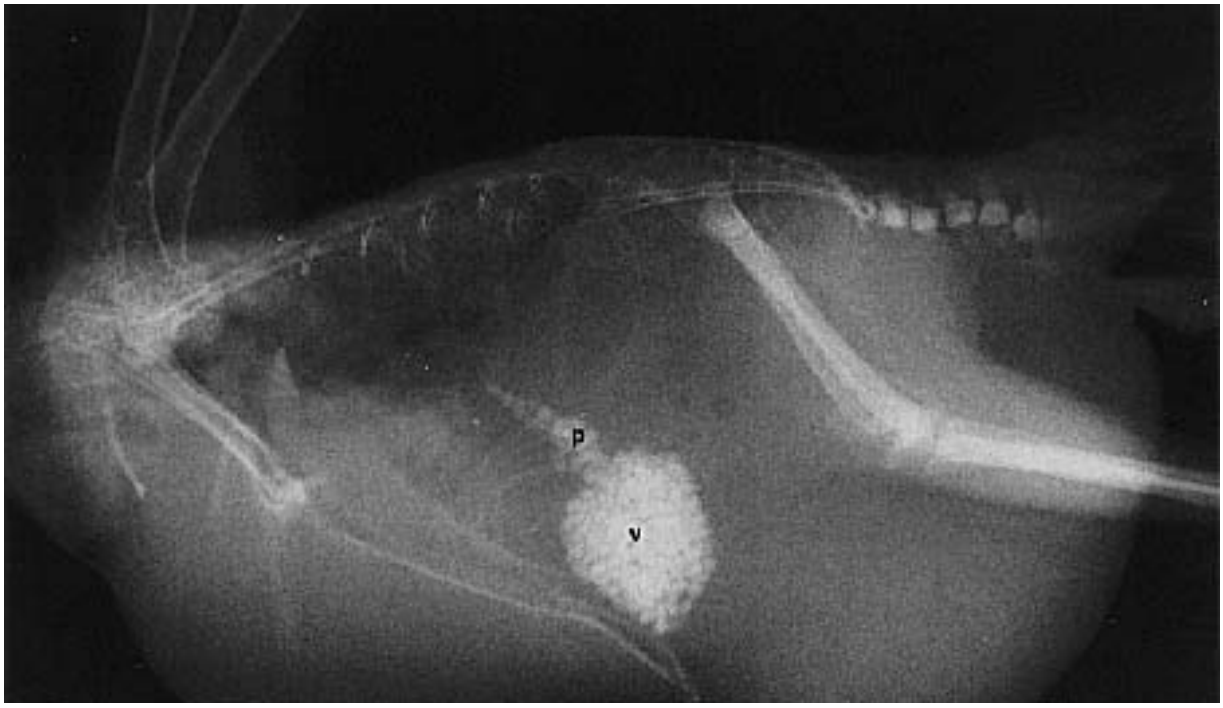

FIG 12.67 A mature cockatiel hen was presented for dyspnea and a swollen abdomen. Radiographs indicated a fluid-filled abdomen with cranial displacement of the ventriculus (v) and proventriculus (p), both of which are impacted with grit. Abdominocentesis was consistent with an exudative effusion, and the diagnosis was egg-related peritonitis. The cranial displacement of the abdominal viscera indicates that the fluid is present in the intestinal peritoneal cavity (courtesy of Marjorie McMillan).

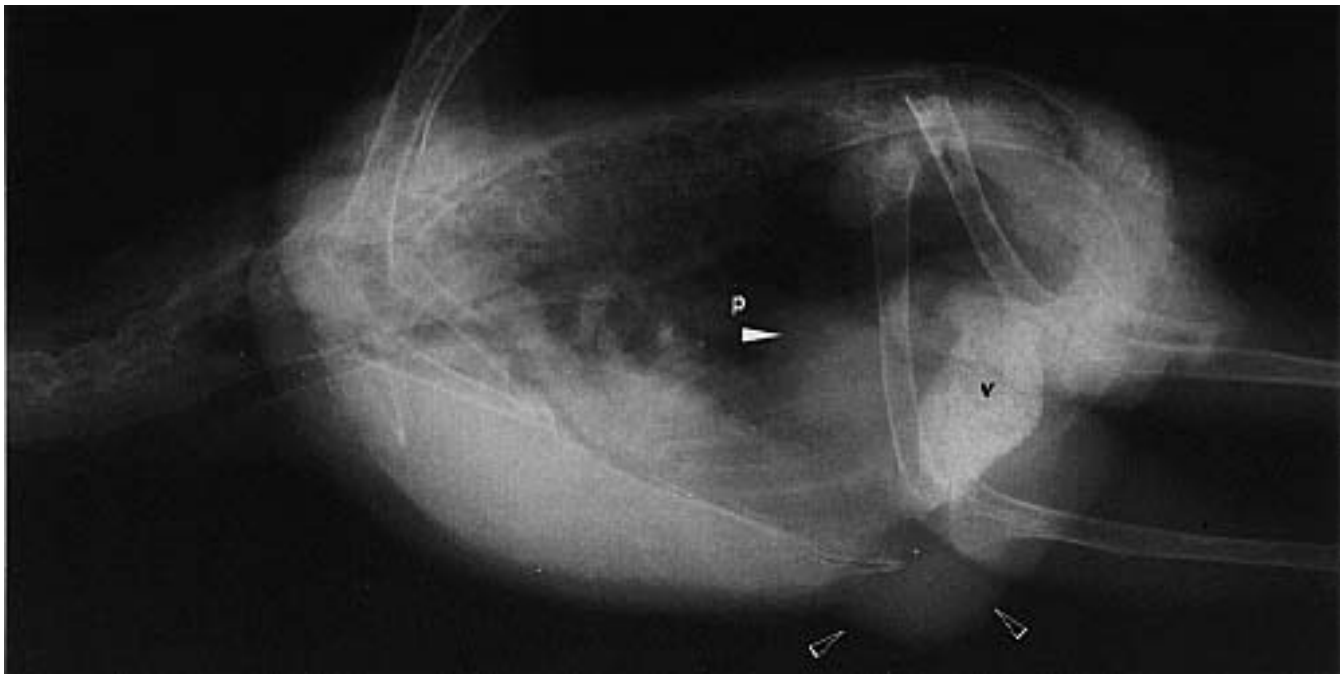

FIG 12.68 A 35-year-old Yellow-headed Amazon Parrot was presented with a firm ventral midline mass. Radiographs indicated rounding of the liver lobes and hepatomegaly (arrows). The mass was visible as a soft tissue opacity at the caudal edge of the sternum (open arrow). An exploratory laparotomy revealed a herniated liver. Proventriculus (p), ventriculus (v) (courtesy of Marjorie McMillan).

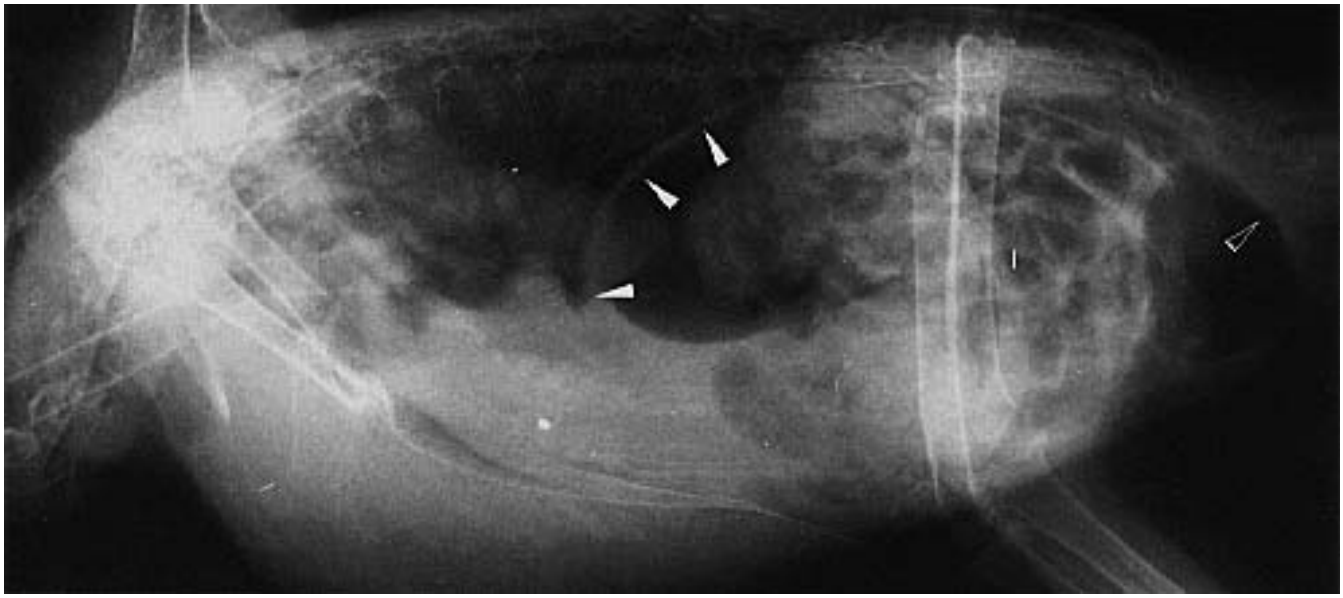

FIG 12.69 A Blue and Gold Macaw was presented with severe dyspnea including a tail bob. The bird was sneezing and had both ocular and nasal discharges. The only abnormal clinicopathologic finding was WBC=18,000. Radiographic changes included gaseous distension of the intestines (i), thickening of the contiguous membrane of the caudal thoracic and abdominal air sac (open arrow). The client was a heavy smoker, and the lesions resolved over a three-month period when the client quit smoking and the bird received daily exposure to fresh air and sunlight.

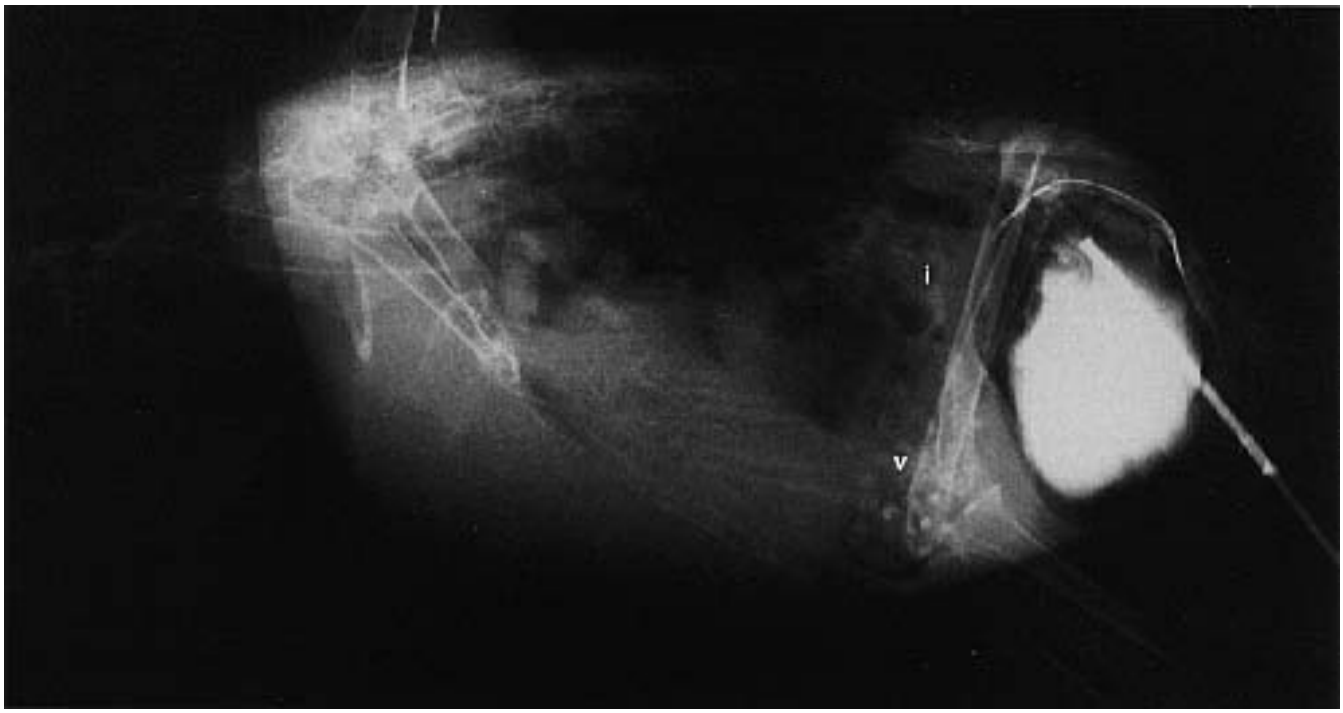

FIG 12.70 Contrast medium was injected into the gaseous distended cloaca of an Amazon parrot with severe dyspnea. Note the cranial displacement of the intestines (i) and ventriculus (v).

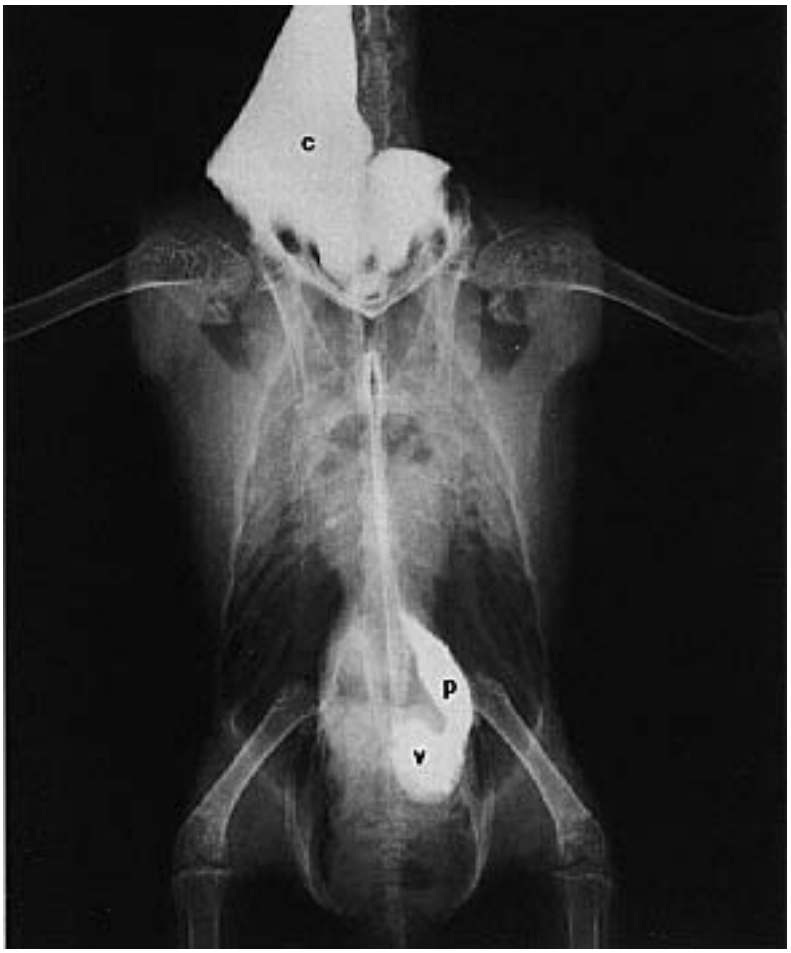

FIG 12.71 Radiographs of an adult African Grey Parrot ten minutes after administering barium sulfate. Crop (c), thoracic esophagus (arrow), proventriculus (p), ventriculus (v) (courtesy of ME Krautwald).

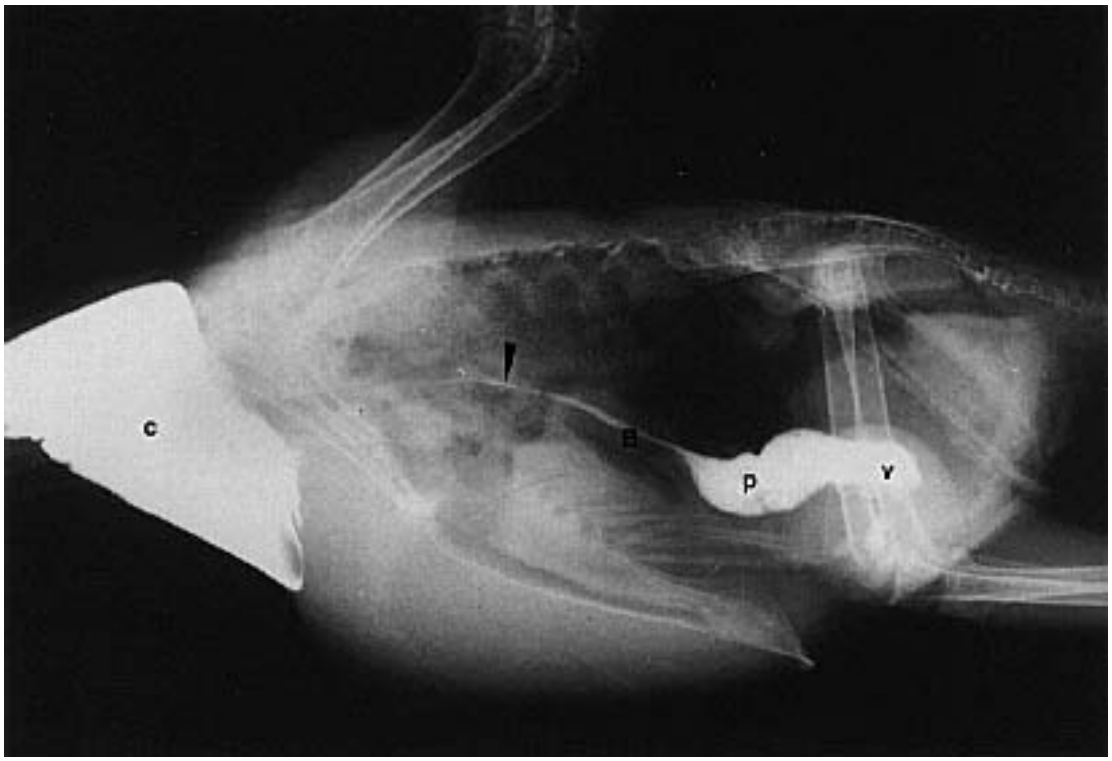

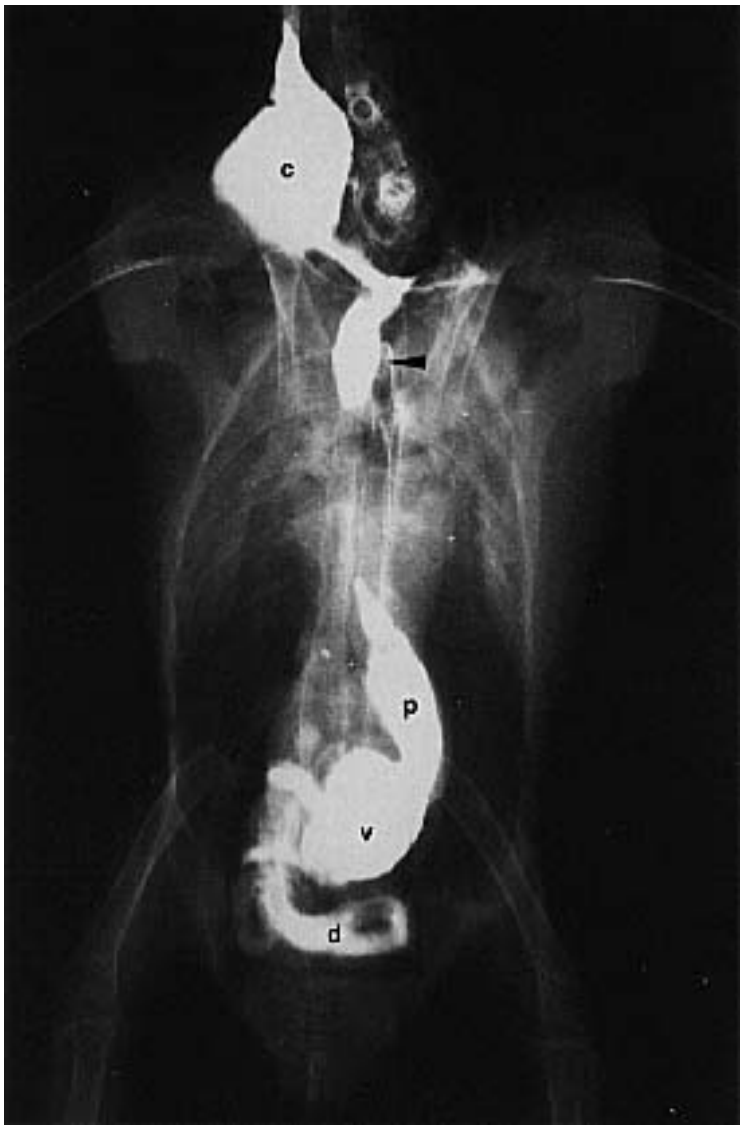

FIG 12.72 An Amazon parrot 20 minutes after barium sulfate administration. Crop (c), thoracic esophagus (arrow), proventriculus with filling defects (p), ventriculus (v), duodenum (d), ilium and jejunum (open arrow).

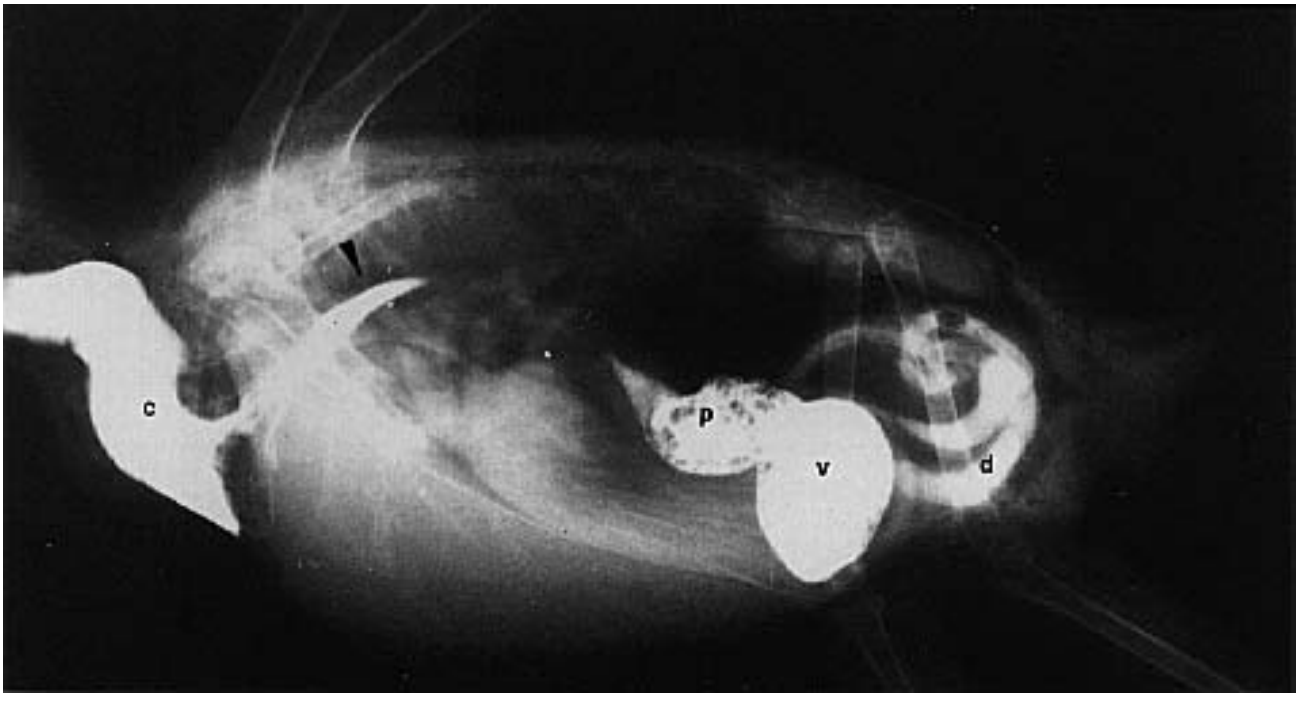

FIG 12.73 Radiographs of an adult African Grey Parrot 60 minutes after administering barium sulfate. Crop (c), thoracic esophagus (arrow), proventriculus (p), ventriculus (v), duodenum (d), intestines (i), colon (open arrow) (courtesy of ME Krautwald).

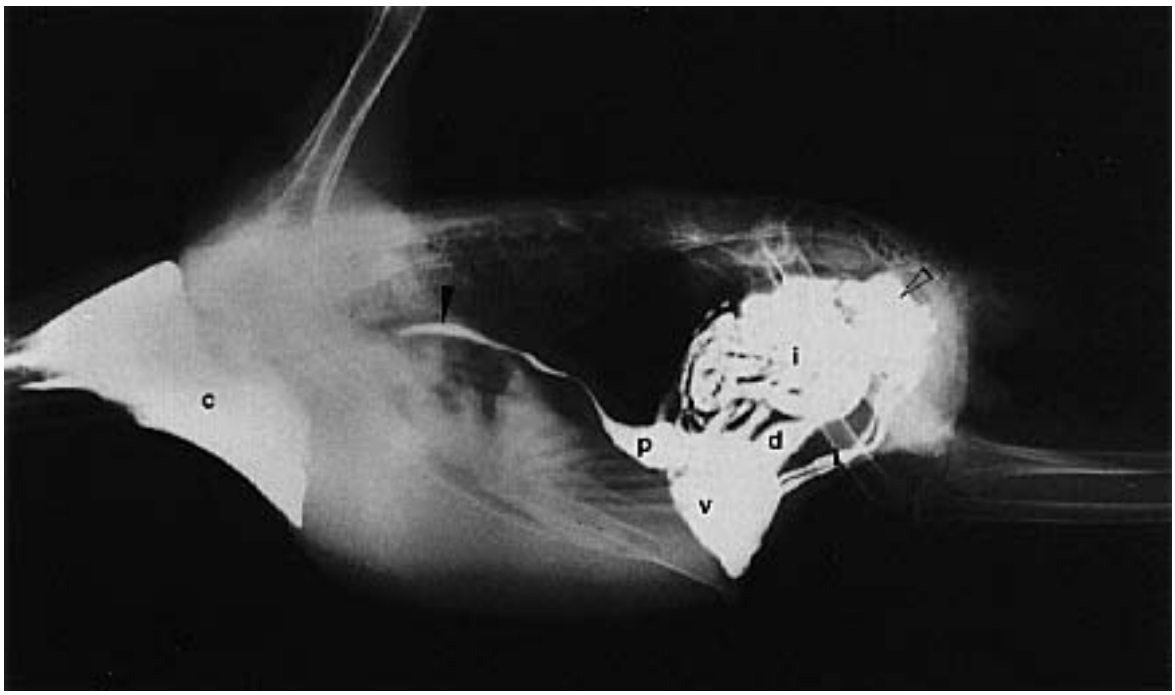

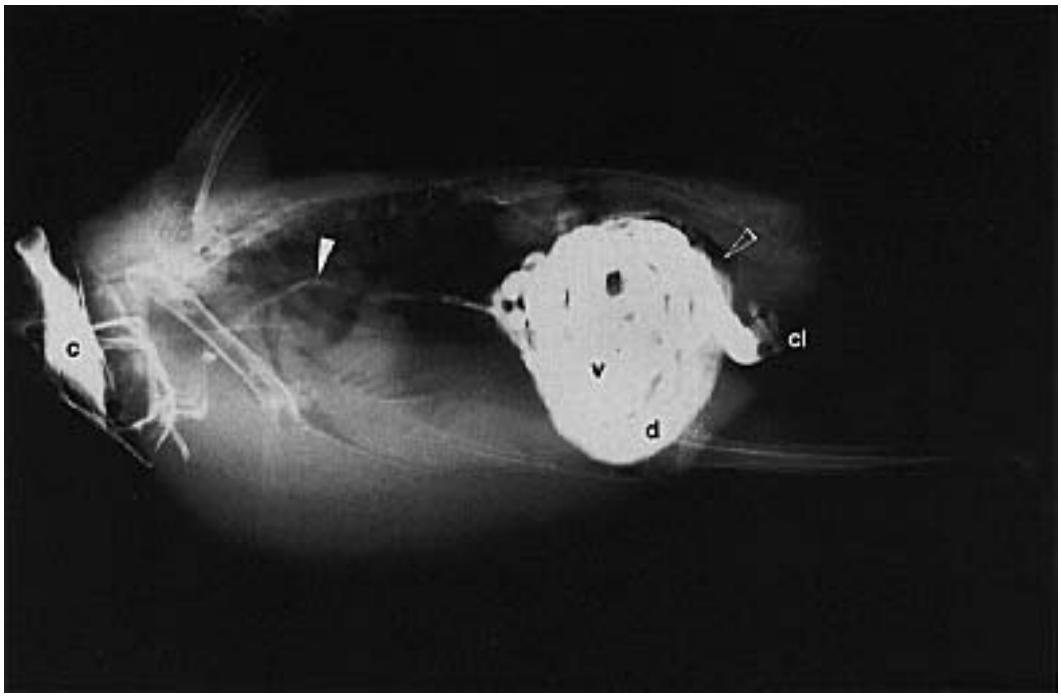

FIG 12.74 Radiographs of an adult pigeon 20 minutes after administration of barium. Note the crop (c) is composed of two lateral compartments. Thoracic esophagus (arrow), proventriculus (p), duodenum (d), colon (open arrow), cloaca (cl) (courtesy of ME Krautwald).

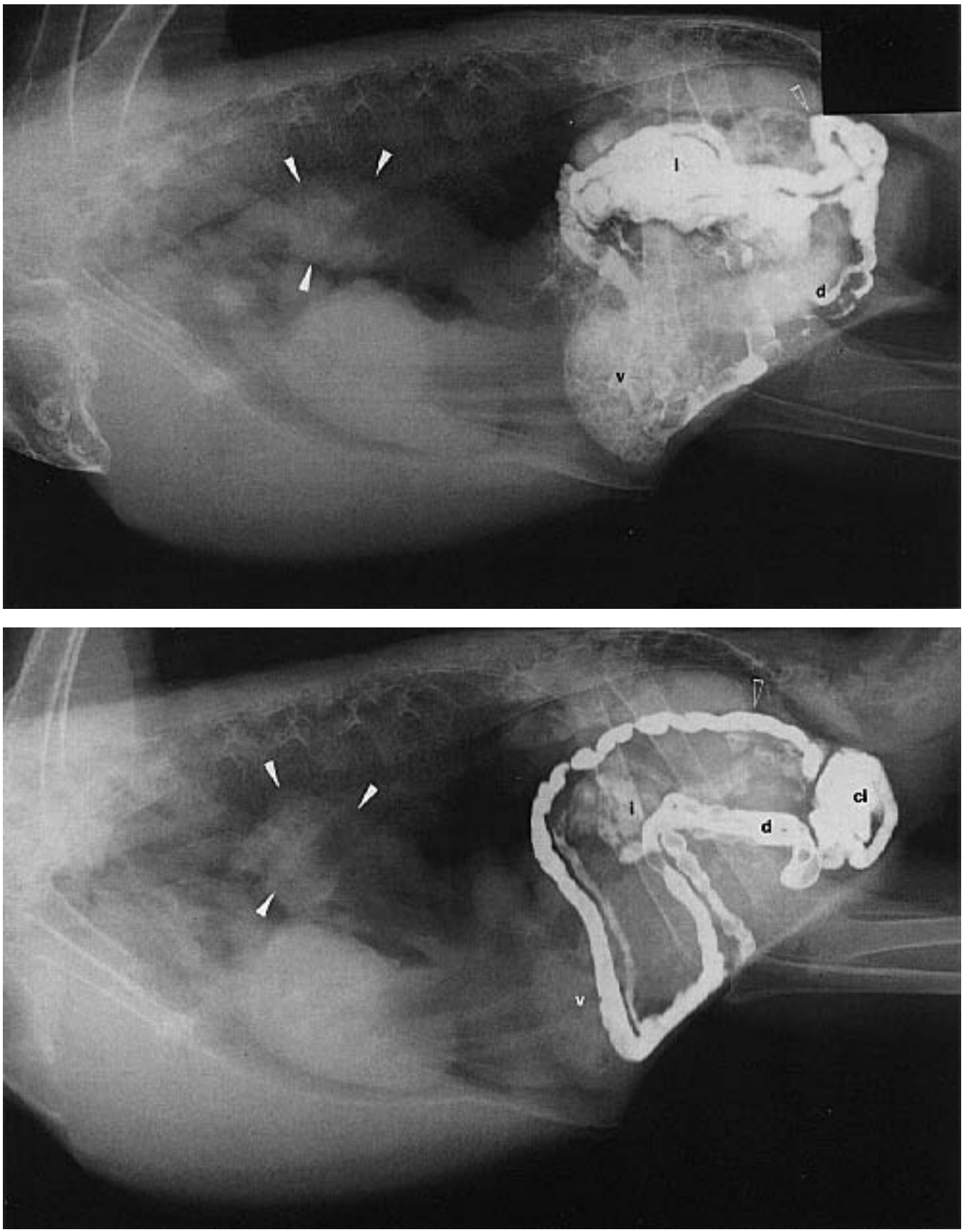

FIG 12.75 An adult Amazon parrot was presented with a history of dyspnea and weight loss. A mass (arrow) was identified in the dorsocranial thorax. Barium contrast radiography indicated that the mass was associated with the thoracic esophagus. Radiograph **a)** was taken 45 minutes and radiograph **b)** was taken 2 hours after barium administration. Contrast medium can be seen in the ventriculus (v), ascending and descending colon (d), jejunum and ileum (i), colon (open arrow) and cloaca (c).

FIG 12.76 Two-week-old pigeon. The gastrointestinal tract of neonates stays distended with food, making the delineation of abdominal structures difficult. Note the large joint spaces characteristic of developing bones in birds (arrows) (courtesy of ME Krautwald).

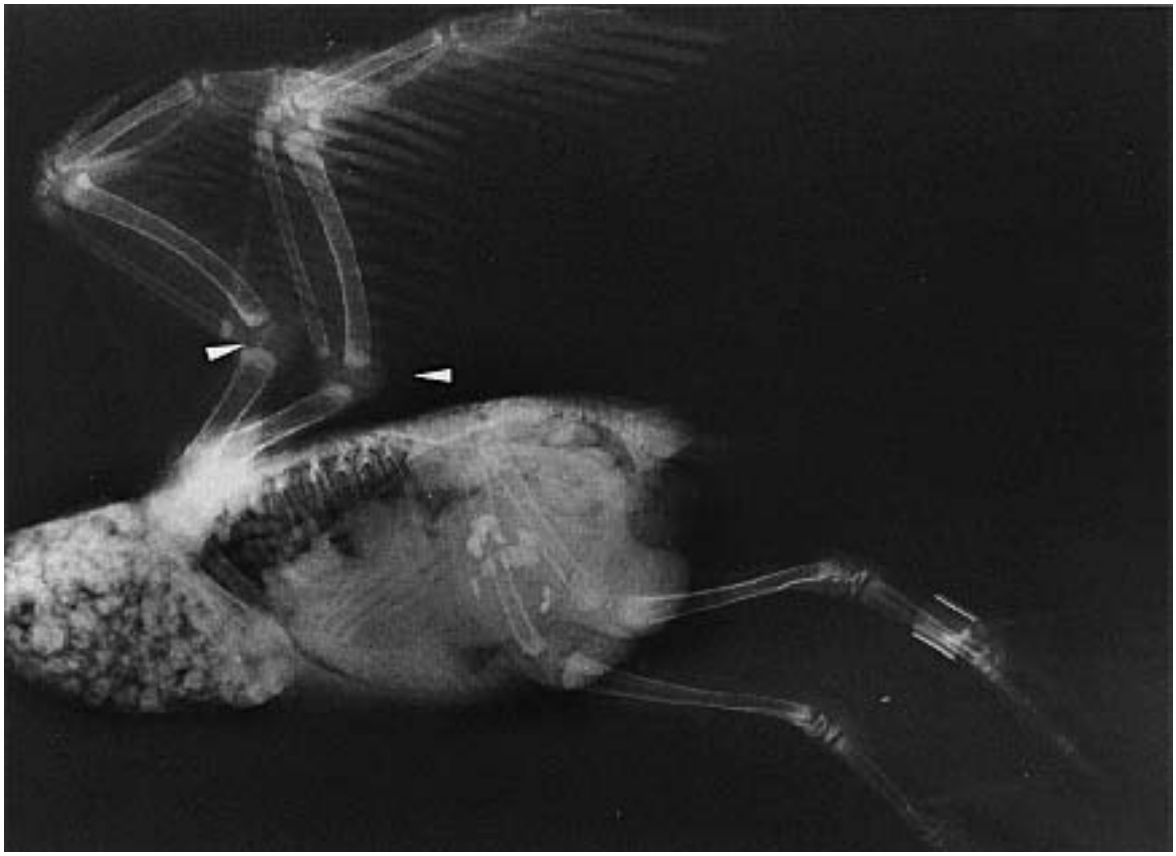

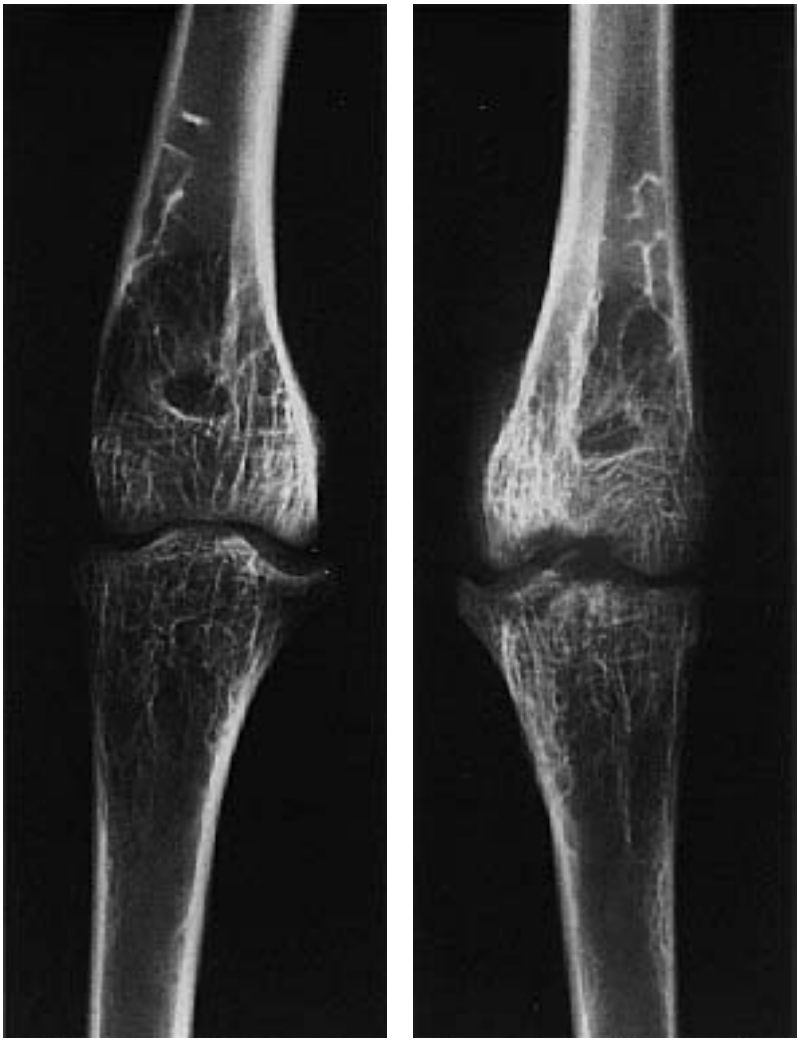

FIG 12.77 An adult swan was presented with intermittent lameness. The tibiotarsal joint was hot, firm and swollen. Radiographs indicated joint enlargement, subchondral bone lysis and erosion of the intercondylar space. These lesions were suggestive of septic arthritis. Radiograph of the normal leg for comparison.

FIG 12.78 A fledgling Golden Eagle was presented with an inability to stand and a decreased range of motion in both pelvic limbs. The bird had been equipped with a radiotransmitter and released from a hack tower several weeks before presentation. The bird was not being monitored and was found hanging upside down from a tree limb with the transmitter entangling the legs. Radiographs indicated necrosis of both femoral heads. EMGs indicated denervation of both pelvic limbs. The bird was euthanatized.

Continued from page 260

nal effusion or organomegaly, ultrasound may be used to characterize lesions (Figure 12.66).[14,19,20] Most studies can be performed without anesthesia. Patients may be held or secured with a plexiglass restraining device. Many birds that are minimally restrained in an upright position are extremely tolerant of the procedure. Feathers may be parted or removed, and a water-soluble, acoustic coupling gel is used to improve the transducer contact with the skin.

A 7.5 MHz end-fire mechanical sector scanner or phased array scanner is best in most birds, but 5.0 MHz and 10 MHz transducers may also be used. Higher frequency scanners provide less tissue penetration but finer resolution and are most useful in smaller species. Linear array transducers can also be used, but because of their shape, they do not conform well to the patient's body.

If the patient is in dorsal recumbency, the transducer is placed just caudal to the sternum and the beam is angled cranially. The liver has a uniform, slightly granular, echogenic pattern and is easily recognized (Figure 12.61). The right and left hepatic veins can be identified as anechoic channels on the dorsomedial aspect of the liver. A uniform, hyperechoic, hepatic parenchyma has been described in birds with fatty liver degeneration and hepatic lymphoma.[16] Discrete hyperechoic masses throughout the liver may represent granulomas, abscesses or neoplasms.

Hepatomegaly should be suspected if the liver can be detected caudal to the sternum. Ultrasound is of little value in detecting acute or chronic hepatitis, and it is difficult to differentiate between cirrhosis and necrosis. Granulomas and neoplasms typically appear as focal hyperechoic walls with an echoic center. Hematomas and subcapsular bleeding will appear hypoechoic.

The liver may be used as a window to visualize the cardiac silhouette. Pericardial effusion and enlargement of cardiac chambers and valvular abnormalities can be detected in larger species. Pulmonary masses such as large granulomas have been defined using ultrasonography. A lateral approach can be used for visualization of the spleen, which is normally hyperechoic in comparison to the liver and is difficult to define unless enlarged.[16]

Ultrasonographic visualization of the kidneys and gonads is not possible due to the presence of the air sacs, although large ovarian follicles can occasionally be defined. Ultrasound can be used to differentiate between soft-shelled eggs and egg-related peritonitis. Poorly mineralized eggs are often oval with a hyperechoic rim surrounding a hypoechoic content. With egg-related peritonitis, there is a heterogeneous hyperechoic appearance to the coelomic cavity (Figure 12.66). Effusion due to other processes is often anechoic or hypoechoic.

The presence of ingesta or gas will obscure portions of the gastrointestinal tract. Differentiation of the proventriculus, ventriculus and cloaca can be enhanced by administering water.

Ultrasound-guided biopsy can be used to collect diagnostic samples from the liver. The patient must be sedated or anesthetized. A variety of needles may be used for the biopsy. In larger species a 22 ga Westcott needle is used to obtain specimens for cytology, histology and culture. Spinal needles and 25 ga hypodermic needles may be used, but may be difficult to localize with the ultrasound beam and often yield only enough material for cytology.

Nuclear Scintigraphy

The potential value of nuclear medicine studies in avian patients remains unexplored. The usefulness of musculoskeletal scintigraphy in other species is well recognized.[9] Three-phase bone scans allow evaluation of the blood supply, soft tissue component and skeleton and are especially useful in occult lesions or abnormalities that are undetectable on survey radiographs. Unexplained abnormalities of the extremities, especially following trauma, would be most suitable for bone scintigraphy. Evaluation of the extent of osteomyelitis, joint disease, vascular compromise, impaired fracture healing and less commonly, bone neoplasia, is enhanced by nuclear medicine studies.

Technetium-99m(^{99m}Tc) is the isotope most frequently used because of its short half-life (six hours) and ideal energy range (140KeV). For bone scanning, the radiopharmaceutical most commonly used is ^{99m}Tc methylene diphosphonate (MDP). A whole body scan of most birds is easily obtained because the entire patient can rest on the head of the gamma camera.

Patients must be kept motionless, so sedation or anesthesia is necessary. One millicurie of radioisotope is administered intravenously, and dynamic images are obtained immediately for the vascular

phase, and within the first 15 minutes for the soft tissue phase. Delayed static images are taken within three to four hours for the bone phase.

Computed Tomography

Computed tomography (CT) is superior to other modalities except magnetic resonance imaging for evaluation of head trauma and abnormalities involving the brain and spinal cord; however, the lack of availability and high cost often prevent the use of computed tomography in birds. Patients must be anesthetized to prevent any motion during the scan. Technical factors are inadequately studied in birds; however, slice section thickness ranging from 2 mm to 5 mm non-overlapping with varying window settings have been described for body scans.[8,17] The value of CT in avian diagnostic radiology remains relatively uninvestigated, but characterization of lesions with CT should prove as valuable as in other species.

References and Suggested Reading

1. **Blackmore DK, Cooper JE:** Diseases of the reproductive system. *In* Petrak ML (ed): Diseases of Cage and Aviary Birds 2nd ed. Philadelphia, Lea and Febiger, 1982, pp 458-467.
2. **Bush M, et al:** The healing of avian fractures: A histologic xeroradiographic study. J Am Anim Hosp Assoc 12(6):768-773, 1976.
3. **Curry TS, et al:** Christensen's Physics of Diagnostic Radiology. Philadelphia, Lea and Febiger, 1990.
4. **Evans S:** Avian Radiography. *In* Thrall DE (ed): Textbook of Veterinary Diagnostic Radiology. Philadelphia, WB Saunders, Co, 1986.
5. **Hendee WR, et al:** Radiologic Physics, Equipment and Quality Control. Chicago, Mosby Yearbook Medical Publishers Inc, 1977.
6. **Krautwald ME:** Radiographic examination of the urinary tract in birds with organic iodinated contrast media. Proc Assoc Avian Vet, 1987, pp 177-193.
7. **Krautwald ME, et al:** Atlas of Radiographic Anatomy and Diagnosis of Cage Birds. Berlin, Paul Parey, 1992.
8. **Krautwald ME:** Radiology of the respiratory tract and use of computed tomography in psittacines. Proc Assoc Avian Vet, 1992, pp 366-373.
9. **Lamb CR:** Bone scintigraphy in small animals. J Am Vet Med Assoc 191(12):1616-1621, 1987.
10. **McMillan MC:** Avian radiology. *In* Petrak, ML (ed): Diseases of Cage and Aviary Birds 2nd ed. Philadelphia, Lea and Febiger, 1982, pp 329-360.
11. **McMillan MC:** Avian gastrointestinal radiology. Comp Cont Educ Pract Vet 5(4):55-60,1983.
12. **McMillan MC:** Radiology of avian respiratory diseases. Comp Contin Educ Pract Vet 8(8):551-558, 1986.
13. **McMillan MC:** Radiographic diagnosis of avian abdominal disorders. Comp Cont Educ Pract Vet 8(9):616-632, 1986.
14. **McMillan MC:** Imaging of avian urogenital disorders. J Assoc Avian Vet 2(2):74-82, 1988.
15. **Morgan JP:** Systematic radiographic interpretation of skeletal diseases in small animals. Vet Clin No Am 4(4):611-626, 1974.
16. **Newell SM, et al:** Diagnosis and treatment of lymphocytic leukemia and malignant lymphoma in a pekin duck. J Assoc Avian Vet 5(2):83-86, 1991.
17. **Orosz SE, Toal RL:** Tomographic anatomy of the golden eagle (*Aquila crysaetos*). J Zoo and Wildl Med 23(1):39-46, 1992.
18. **Paul-Murphy JR, et al:** Psittacine skull radiography. Vet Rad 31(3):125-131, 1990.
19. **Peterson ME, et al:** Ultrasonic imaging in diagnosis of an abdominal mass in a pigeon. Mod Vet Pract, pp 825-826, 1983.
20. **Riedel U:** Ultrasonography in birds. Proc First Conf Europ Assoc Avian Vet, 1991, pp 190-198.
21. **Schlumberger HJ:** Polyostotic hyperostosis in the female parakeet. Am J Pathol 35(1):1-23, 1959.
22. **Storm J, Greenwood AG:** Fluoroscopic investigation of the avian gastrointestinal tract. Proc Europ Conf Avian Med Surg, 1993, pp 170-177.
23. **Stauber E, et al:** Polyostotic hyperostosis associated with oviductal tumor in a cockatiel. J Am Vet Med Assoc 196(6):939-940, 1990.
24. **Squire LF, et al:** Exercises in Diagnostic Radiology Volume 3 Bone. Philadelphia, WB Saunders Co, 1972.
25. **Ticer JW:** Veterinary Practice. Philadelphia, WB Saunders Co, 1984.
26. **Walker M, Goble D:** Barium sulfate bronchography in horses. Vet Rad 21(2):85-90, 1980.
27. **Walsh MT, Mays MC:** Clinical manifestations of cervicocephalic air sacs of psittacines. Comp Cont Educ Pract Vet 6(9):783-792, 1984.
28. **Watters JW:** Development of a technique chart for the veterinarian. Comp Cont Educ Pract Vet 11(7):568-571, 1980.
29. **Wortman JA:** Film/screen combinations for fine detail radiography. Vet Med Report 3(1):80-86, 1991.
30. **Rübel GA, et al:** Atlas of Diagnostic Radiology of Exotic Pets. Philadelphia, W.B. Saunders Co., 1991.